SOUTHERN CALIFORNIA
EDISON®
An EDISON INTERNATIONAL® Company

A. Edward Scherer
Manager of
Nuclear Regulatory Affairs

December 2, 2004

U.S. Nuclear Regulatory Commission
Attn: Document Control Desk
Washington, DC 20555-0001

Subject: **Docket Nos. 50-361 and 50-362**
Additional Information Supporting the Third Ten-Year Inservice Inspection (ISI) Interval Relief Requests ISI-3-11, Revision 1 and ISI-3-12 to Support Pressurizer Heater Sleeve Repairs
San Onofre Nuclear Generating Station, Units 2 and 3

Reference: Letter from A. E. Scherer (SCE) to the Document Control Desk (NRC) dated October 15, 2004; Docket Nos. 50-361 and 50-362 Third Ten-Year Inservice Inspection (ISI) Interval Relief Requests ISI-3-11, Revision 1 and ISI-3-12 to Support Potential Pressurizer Heater Sleeve Repairs, San Onofre Nuclear Generating Station, Units 2 and 3

Dear Sir or Madam:

This letter provides additional information as requested by the United States Nuclear Regulatory Commission (NRC) staff to support their review and approval of the Southern California Edison (SCE), San Onofre Nuclear Generating Station Units 2 and 3 Relief Requests ISI-3-11, Revision 1 and ISI-3-12, which were previously submitted by the referenced October 15, 2004, letter. The NRC staff questions and the SCE responses are provided in the enclosure.

Additionally, this letter formally requests NRC approval to use the 1998 Edition through 2000 Addenda to perform the system leak test, as discussed in the referenced October 15 letter.

P.O. Box 128
San Clemente, CA 92674-0128
949-368-7501
Fax 949-368-7575

A047

SCE continues to request expedited review and approval of these relief requests to support reaching MODE 4 in the Unit 3 Cycle 13 Refueling Outage, which is currently planned for December 25, 2004.

Should you have any questions, please contact Mr. Jack Rainsberry at (949) 368-7420.

Sincerely,

Enclosure:

cc: B. S. Mallett, Regional Administrator, NRC Region IV
B. M. Pham, NRC Project Manager, San Onofre Units 2 and 3
C. C. Osterholtz, NRC Senior Resident Inspector, San Onofre Units 2 and 3

SOUTHERN CALIFORNIA EDISON
RESPONSE TO NRC STAFF
REQUEST FOR ADDITIONAL INFORMATION
SUPPORTING RELIEF REQUESTS ISI-3-11 AND ISI-3-12
PRESSURIZER HEATER SLEEVE REPAIR
SAN ONOFRE NUCLEAR GENERATING STATION UNITS 2 AND 3

Additional Information Supporting Relief Requests ISI-3-11 And ISI-3-12

General Question

NRC Question 1:

The replacement half-nozzle is attached to the Alloy 52 weld pad on the outside surface of the pressurizer lower head by a new weld which serves as a new primary system pressure boundary. (1) Submit the stress analysis to demonstrate that the new weld satisfies stress criteria in ASME Code Section III, NB-3000. (2) The stress analysis should demonstrate that the replacement nozzle will not eject from the pressurizer penetration. (3) Discuss future inspection of the new weld and the sleeve, including inspection technique, frequency, and coverage. (4) Discuss whether the weld pad on the outside surface of the pressurizer lower head will be inspected as a part of the inservice inspection of the attachment weld.

SCE Response:

1) and 2) A complete evaluation of the half nozzle repair per NB-3000, including fatigue and thermal ratcheting, was performed in SCE Calculation No. M-DSC-356, Revision. 1. Based on the results of the calculation, it was concluded that the ASME Code, Section III allowable stress limits and fatigue requirements are met for a 40-year service life. Nozzle ejection will not occur based on the results of this calculation.

The Purpose and Background section (pages 8 through 10) and the Summary of Results section (pages 11 through 13) of calculation No. M-DSC-356, Revision 1 are provided in Attachment 1.

3) After the repair of the Alloy 600, 82, and 182 pressure boundary components of the pressurizer heater sleeves, SCE intends to perform system leakage tests and VT-2 inspections every refueling outage as required by ASME Code. In addition, the bottom of the pressurizer, including the surge line, the 30 heater sleeves, and the instrument nozzles will continue to be maintained as an inspection point in the "Reactor Coolant System Alloy 600 Inspection" procedure and this area will continue to be inspected per the "Boric Acid Leak Inspection" procedure. Both the "Reactor Coolant System Alloy 600 Inspection" and "Boric Acid Leak Inspection" are performed at each refueling outage. Future visual inspections will be on a best effort basis without a requirement to erect scaffolding or remove insulation from the bottom head of the pressurizer. Gaps in the insulation allow observation of the partial penetration weld and heater-to-heater sleeve fillet weld, however, the entire weld pad surface will not be inspected on a routine basis.

4) The applicable ISI requirements for the external weld pad and the new heater sleeve j-groove weld, integral to the pad, are given in ASME XI, Table IWA-2500-1, Examination Category B-P, item B15.20. A System Leakage Test and Visual, VT-2 examination is required to be performed prior to plant start up following each reactor refueling outage.

Questions Specific to NRC Review of Calculation M-DSC-402

NRC Question 2:

Sheet 1 of M-DSC-402. The licensee indicated that "Tech Spec/LCS" is not affected. (1) Confirm that LCS stands for limiting condition statement; and (2) Discuss whether the transients used in the flaw evaluation of the postulated flaw in the J-groove weld are consistent with the pressure-temperature limit curves for the reactor vessel and pressurizer in the plant technical specifications.

SCE Response:

1) LCS stands for "Licensee Controlled Specifications." This is similar to what other utilities refer to as a Technical Requirements Manual, and contains specifications relocated from the Technical Specifications when we converted to the Improved Technical Specifications. The subject modification and the results of the associated evaluations do not impact the Technical Specifications or the Licensee Controlled Specifications.

2) All transients are based on the pressurizer design specification, which contains heat-up and cool-down limits for the pressurizer that are consistent with but separate from the heat -up and cool-down limits for the reactor vessel. The pressurizer heat-up and cool-down limits are controlled by the pressurizer design specification; they are not part of the technical specifications.

NRC Question 3:

Page 10. The licensee concluded that the final flaw depth for both uphill and downhill locations are acceptable for a 40-year design life. Clarify when is the starting point of the 40-year design life.

SCE Response:

The starting point is the present time, (i.e., the time the modification is implemented).

Additional Information Supporting Relief Requests ISI-3-11 And ISI-3-12

NRC Question 4:

Page 11. Item 8. Confirm that cooldown transient with flooding is the same as "pressurizer in-surge" transient.

SCE Response:

The cooldown transient with flooding is the same as a pressurizer in-surge transient. This transient, and the other transients included in the analysis, can be found in Section 5 of the calculation.

NRC Question 5:

Page 15. Item 3. Discuss the safety margin used in calculating stress intensity factors in Item 3.

SCE Response:

The discussion under Item 3 is a restatement of the procedures given in Article A-5300 of Appendix A to Section XI. The calculation of K_I in determining the allowable flaw depth is based on all applied stresses (pressure and thermal) and residual weld stresses. There is no structural factor applied to the calculation of K_I. However, a factor of $10^{1/2}$ for normal/upset conditions, and $2^{1/2}$ for emergency/faulted conditions, is applied to the fracture toughness value as given by Eq. 4-4 of the calculation. These flaw evaluation acceptance criteria are in accordance with IWB-3612 and are analytically equivalent to applying the structural factors as direct multiplying factors on K_I.

NRC Question 6:

Page 16. Equation 4-9. (1) Clarify whether the stress intensity factor expression shown in Equation 4-9 is the equation used in the flaw evaluation because the expression in Equation 4-9 seems simplistic to be applicable to the complex geometry of the postulated flaw in the J-groove weld. (2) The licensee stated that the stress intensity factor is calculated by the BIGIF program, which is an EPRI program published in 1978. The staff is not clear as to how the stress intensity factor due to applied stresses is calculated in the program (e.g., by closed-form method or computer modeling). The licensee needs to explain in detail how the stress intensity factor of the final flaw size is calculated to satisfy IWB-3600. (3) Submit Reference 8, "BIGIFBFracture Mechanics Code for Structures," Manual 2, User's Guide, EPRI NP-838.

SCE Response:

1) Equation 4-9 is a formula that represents the generic form for K_I. The analytical complexity of this equation is represented by the function F, which, in this calculation, is numerically determined by integrating the weight function for the flaw model with the applied general-varying stress field. The flaw geometry used in computing K_I is that of a quarter corner crack in a plate as shown in Fig. 8-1 of the calculation. Additional details of the BIGIF methods are given in Reference 8 of the calculation.

2) The BIGIF program uses the weight function or influence function method in computing K_I for complex (nonlinear varying) stress fields acting on cracked bodies. The calculation of K_I using the weight function method follows from the general equation:

$$K_I = \int_0^a h_i[x,a]\,\sigma[x]\,dx$$

where K_I is computed by the integration over the crack for a given crack face stress, $\sigma[x]$, with the weight function, $h_i[x,a]$. The weight function is a function of spatial position, x, and crack size, a, and also depends on the specified boundary conditions, component geometry, and crack front position. The weight functions for various flaw geometries are contained within BIGIF. The flaw geometries contained in the BIGIF program include both 1D and 2D flaw shapes including buried and surface elliptically shaped crack fronts. The BIGIF program accepts crack dimensions, stress distribution data, fatigue crack growth rate parameters as input for a given problem. BIGIF then performs the numerical integration to compute K_I, ΔK_I, etc. in determining the K_I versus crack depth distributions and final crack size dimensions following the flaw growth analysis. Additional program details are contained in Reference 8 of the calculation.

3) The user's manual (Reference 8) is provided as Attachment 2.

NRC Question 7:

Pages 16 and 46. The staff has reservations regarding the licensee's use of the ASME Section XI, Appendix K method in the flaw evaluation because of the following reasons. (a) The Appendix K method is based on elastic-plastic fracture mechanics which is not the same as the linear-elastic fracture mechanics specified in ASME Section XI, IWB-3600, which the licensee stated that it will use and which does not reference Appendix K. (b) The Appendix K method is developed to address the postulated flaws in the reactor vessel beltline region. The flaw geometry in the J-groove weld in pressurizer nozzles is not the same as the flaw geometry in the beltline region. The safety margins used in Appendix K method may not be applicable to the flaws in

the J-groove weld and the Appendix K safety margins are not the same as the safety margins in IWB-3600.

The staff has permitted the use of elastic-plastic fracture mechanics in analyzing the postulated flaw in the J-groove weld if the postulated flaw could not satisfy the safety margins in ASME Code Section XI IWB-3600. The licensee did not provide evidence that its postulated flaw could not meet safety margins of IWB-3600; therefore, the staff is not clear why Appendix K is used. The linear elastic fracture mechanics analysis gives more conservative results than the elastic-plastic fracture mechanics.

The licensee needs to (1) demonstrate that the elastic-plastic fracture mechanics method in Appendix K is applicable to the postulated flaw in the remnant J-groove weld, considering the above three staff concerns; and (2) explain why Appendix K is used in the flaw evaluation if the postulated flaw in the J-groove weld satisfies IWB-3600.

SCE Response:

The purpose of the Appendix K calculations was to verify the Appendix A analysis with the assumptions made on residual stress was indeed conservative.

Section 2 (pages 9 and 10) and Section 8 (pages 41 through 53) of SCE calculation M-DSC-402 provide the results and the allowable limits for the pressurizer heater sleeve J-groove weld flaw evaluation. As required by ASME Section XI, IWP 3600, an Appendix A analysis was completed with acceptable results. Additionally, an Appendix K calculation was performed to verify Appendix A analysis with the assumptions made on residual stress was indeed conservative.

1) An explanation of the purpose and basis for performing the Appendix K evaluation is given in Section 8.4.3.2 of the calculation. The Appendix K procedures are appropriate as an alternate demonstration for flaw acceptance because the analysis conditions for the pressurizer heater sleeve are consistent with the analysis scope of Appendix K:

    a) Appendix K evaluates the adequacy of fracture toughness of the material to resist fracture of a flaw. The size of the postulated flaw assumed for the pressurizer bottom head is on the order of the postulated flaw to be used in an Appendix K evaluation for fracture.

    b) The Appendix K procedures are for conditions where upper shelf behavior is expected. The pressurizer bottom head region will be at upper shelf temperatures for the design transients for normal and upset conditions under evaluation for the heater sleeve J-groove.

c) The structural factors of 1.4 on pressure and 1.0 on thermal stress are specified within Appendix K procedures. In the calculations performed for the heater sleeve J-groove, a structural factor of 3.16 on pressure and 1.0 on thermal stress were conservatively used.

2) The Appendix A calculations were completed for the postulated flaws for which it was determined that the allowable flaw size were acceptable to the structural factors of $10^{1/2}$ and $2^{1/2}$ following the flaw acceptance criteria of IWB-3612. These results are shown in Figs. 8-3 and 8-4 of the calculation. In performing these elastic calculations, some assumptions were made as to the level and extent of tensile residual stresses based on finite element stress results. Further, the combination of residual and applied stresses created unrealistically high peak stresses and the Appendix A calculations considered limiting peak stresses to the yield strength of the sleeve material. As an independent check on these analysis assumptions, the calculation for allowable flaw size was also performed following the procedures and criteria provided in Appendix K for performing an elastic-plastic evaluation. Therefore, the purpose of the Appendix K calculations was to verify the Appendix A analysis with the assumptions made on residual stress was indeed conservative.

NRC Question 8:

Page 17. Equation 4-14. Discuss why there is no safety factor applied to the stress intensity factor due to thermal stresses (K_{It}). The safety factor of 3.16 for the stress intensity factor due to pressure stresses (K_{Ip}) should be applied to K_{It} as specified in ASME Section XI, IWB-3600.

SCE Response:

Equation 4-14 was derived from the J-integral evaluation procedure given in Articles K-4210 and K-4220 of Appendix K. That evaluation equation is

$$J = 1000(K_{Ip} + K_{It})^2 / E'$$

From Article K-4220, the safety factor on pressure is 1.15 and the safety factor on thermal load is 1.0. The pressure to be used in the Appendix K procedure is the accumulation pressure, which yields an equivalent safety factor on operating pressure of 1.4 as discussed on Page 17 of calculation M-DSC-402. However, in the application of the above Appendix K equation in the calculation, a safety factor of $10^{1/2}$ or 3.16 is conservatively used on pressure.

Additional Information Supporting Relief Requests ISI-3-11 And ISI-3-12

NRC Question 9:

Page 18. The licensee stated that the BIGIF program was used to calculate the allowable and final flaw depth due to cyclic loading. (1) Discuss whether the staff has approved a relief request submitted by other licensees who used this program for their flaw evaluation. (2) Discuss how this program was benchmarked and verified to determine its accuracy.

SCE Response:

1) The BIGIF program has been used to perform Section XI type flaw evaluations for both allowable flaw size and flaw growth calculations required by Section XI procedures. The same basic approach has been used for other J-groove fracture evaluations at SONGS, namely the CEDM nozzles and instrumentation nozzles.

   A search of correspondence to show NRC review precedent for the use of the BIGIF program resulted in the following list:

   a) Letter from M.O. Medford (SCE) to J.A. Zwolinski (NRC) dated April 22, 1985; Subject: Docket No. 50-206, Transamerica Delaval Inc. (TDI) Diesel Engine Torsiographic Test Report/Evaluation of Transient Conditions, San Onofre Nuclear Generating Station, Unit 1

   b) Letter from George E. Lear (NRC) to Kenneth P. Baskin (SCE) dated January 7, 1986; Subject: Status of the Long-Term Operability Review of Transamerica Delaval, Inc. (TDI) Diesel Engines

   c) Letter from George E. Lear (NRC) to Kenneth P. Baskin (SCE) dated March 14, 1986; Subject: Draft Safety Evaluation Report on Transamerica Delaval, Inc. (TDI) Diesel Generators

   d) Letter from George E. Lear (NRC) to Kenneth P. Baskin (SCE) dated January 28, 1987; Subject: Safety Evaluation Report on the Operability/Reliability of Emergency Diesel Generators Manufactured by Transamerica Delaval, Inc. (TDI)

   e) Letter from M.O. Medford (SCE) to the Document Control Desk (NRC) dated July 15, 1988; Subject: Docket No. 50-206, Supplement to Amendment Application No. 153, San Onofre Nuclear Generating Station, Unit 1

   f) Letter from Charles M. Trammell (NRC) to Kenneth P. Baskin (SCE) dated July 22, 1988, Subject: Issuance of Amendment No. 104 to Provisional Operating License, San Onofre Nuclear Generating Station, Unit No. 1 (TAC No. 68439)

g) Letter from F. R. Nandy (SCE) to the Document Control Desk (NRC) dated January 13, 1989; Subject: Docket No. 50-206, Standby Diesel Generators, San Onofre Nuclear Generating Station, Unit 1

2) The BIGIF program was benchmarked against closed-form solutions and numerical results from finite element and boundary integral equations methods as part of the code development. Also, the analytical procedures for numerical integration associated with flaw growth calculations have been verified by test case. Approximately 30 test cases have been used to verify the program. The BIGIF program is maintained under Aptech's nuclear quality assurance program, which has been periodically audited by utilities.

NRC Question 10:

Page 38. Submit for staff review Reference 15, "Evaluation of Modified Pressurizer Heater Sleeves - SONGS Unit 2 and 3," Calculation No. AES-C-5212-1, Aptech Engineering Services.

SCE Response:

The "Purpose and Background" section (pages 8 through 10) and the "Summary of Results" section (pages 11 through 13) of SCE calculation No. M-DSC-356, Revision 1 (Aptech Engineering Services Calculation No. AES-C-5212-1) are provided in Attachment 1.

NRC Question 11:

Page 42, Section 8.2. (1) Discuss how the weld residual stresses are treated in calculating the stress intensity factor of the crack (e.g., as a primary stress or secondary stress). (2) Provide the percentage of the total stress intensity factor that is contributed by the weld residual stresses; and (3) Discuss how far into the J-groove weld would the residual stresses attenuates to zero.

SCE Response:

1) The weld residual stresses are combined with the applied stresses. In the calculation of K_I, they are considered in the same manner as the applied stresses. All stresses are effectively considered as primary stresses.

2) The value of K_I was computed for the total stress including residual stress as shown in Figures 8-3 and 8-4 of the calculation. The calculation of K_I for just the residual stress was not performed as part of the evaluation so the contribution from just the residual stress to K_I is not available.

3) The distribution of residual hoop stress at operating conditions is shown in Fig. 8-2 of the calculation. From these results, the peak tensile stresses occur mainly in the J-groove weld and the point where the tensile residual stress attenuates to zero is taken at the clad to base metal interface.

NRC Question 12:

Page 43. Item 1. (1) Discuss how the residual tensile stress attenuates with distance from the surface of the weld (i.e., show, by analysis, the attenuation per length). (2) Discuss the basis for the assumption that the tensile residual stresses are the yield strength of the weld material, which is 60 ksi. (3) Discuss the basis for the assumption that the compressive residual stresses is 50% of the yield strength. (4) The licensee stated that the alloy head base metal will be under compressive residual stress at the clad interface. Discuss how the interaction of the tensile and compressive residual stresses affects flaw propagation into the RV head base metal (i.e., how are the residual stresses considered in the fatigue flaw growth calculation.) (5) Discuss how are the residual stresses applied to the crack tip (i.e., constant loading or variable loading).

SCE Response:

1) The general distribution of residual stress is reflected in the finite element results shown in Fig. 8-2, which is taken from Reference 14. The residual stress attenuates very quickly with distance from the J-groove weld. The attenuation occurs in both the axial direction along the sleeve and the circumferential distance away from the weld.

2) It was assumed that the peak residual stress would be on the order of the yield strength of the Alloy 600 material. This basic assumption is consistent with measured residual stresses in as-welded heater sleeve mockups [J. F. Hall, et. al, "Measurement of Residual Stresses in Alloy 600 Pressurizer Penetrations," SFEN, September 12-16, 1994]. The residual hoop stress near the ID surface of the sleeve was determined to be in the range of 250 to 500 MPa (36 to 73 ksi). In this mockup, the nominal yield strength of the sleeve material was 64 ksi, which was then reamed to create a cold-worked condition. This assumption is also justified based on the finite element results of Reference 14, which are shown in Fig. 8-2 in the calculation. The finite element results indicate that the local residual plus operating hoop stress is in the range of 50 to 75 ksi at the J-groove region and within the sleeve. It is expected that the residual stress would be somewhat less than this range when the

operating stress (i.e., pressure) is subtracted from the total stress. Further, a survey of supplied sleeve material documented in Reference 14 indicated the room temperature yield strength ranged between 38 to 63.5 ksi. A 60 ksi yield value was used in the calculation and was judged to be a conservative estimate of yield strength at operating temperatures.

3) The basis for the assumption that the compressive residual stresses is 50% of the yield strength is the "Operability Assessment for CEOG Plants with Hypothetical Circumferential Flaw Indications in Pressurizer Heater Sleeves," Draft WCAP-16180, Rev. O, Westinghouse Electric (November 2003), listed as Reference 14 in calculation M-DSC-402. The finite element results in Reference 14 indicate the ratio between peak tensile and compressive hoop stresses is approximately 2-to-1.

4) The effect of residual stress would be to change the mean stress (i.e., R-ratio equal to K_{min}/K_{max}) for fatigue. Tensile residual stress would lead to a higher value of R, which in turn increase the rate of growth. Likewise, compressive residual stresses would lower the R value and subsequently decrease the rate of flaw growth. Because the postulated flaw is large relative to the depth of the clad, and the crack tip residing in the alloy steel head material would be within the compressive zone, the residual stresses were conservatively ignored in the fatigue crack growth analysis.

5) The residual stresses were not explicitly included in the fatigue crack growth analysis.

NRC Question 13:

Page 45. ASME Section XI, IWB-3613 specifies that the stress intensity factor should have a safety margin of $\sqrt{2}$ for conditions of bolt-up and pressurization not exceeding 20% of the design pressure during which the minimum temperature of the reactor coolant is not less than RTndt + 60 degrees F. (1) Discuss whether this criterion is satisfied. (2) On page 25, the licensee stated that RTndt of the reactor vessel closure head (SA-533B-1) will be less than 20 degrees F, which is based on NUREG-0577. Discuss whether there are actual material test data from the vessel fabricator to confirm the 20 degrees F.

SCE Response:

1) Yes, because the acceptance criterion used $10^{1/2}$ as the safety margin for all loads, the criterion of IWB-3613 is met.

2) There were no drop weight tests performed on the bottom head plate material for either SONGS unit. Charpy impact tests were performed at a test temperature of +10 degrees F and the NSSS vendor used the data to estimate RTNDT. The

estimated value for RT_{NDT} is +30 degrees F based on MTEB 5-2 guidance. An RT_{NDT} of + 30 degrees F does not change the results of the calculation. The pressurizer bottom head will be at upper shelf conditions for normal operating conditions if RT_{NDT} is +30 degrees F.

NRC Question 14:

Page 46. Item 3. The licensee stated that "Higher stress conditions occur when the RCS pressure is below 20% of the design pressure. Maximum stress occurs when the RCS pressure is near zero." Explain these two statements.

SCE Response:

The purpose of these statements was to indicate that the calculated stresses are highest when the maximum stress occurs during the cooldown with flooding transient. The internal pressure in the pressurizer will be below 20% of the design pressure and the maximum stress occurs when the pressurizer is at atmospheric pressure. The statements were made to demonstrate the Appendix A flaw evaluation for allowable flaw size (Figures 8-3 and 8-4) with the associated assumptions is conservative. The two statements follow from the transient information shown in Fig. 5-2 for the cooldown condition with flooding. The stress during this portion of the transient is due to a thermal gradient across the head only. These statements were made to indicate the criteria of IWB-3613 could be applicable to the cooldown transient. The point of the statements is that IWB-3613 permits a lower safety factor for flaw acceptance, and the imposition of the full safety factor of $10^{1/2}$ as was done in this calculation for this transient is very conservative.

NRC Question 15:

Page 46. The allowable depth for the postulated flaw in the J-groove weld is 1.42 and 1.52 inches for the nozzle uphill side and weld downhill side, respectively. Discuss the allowable length of the flaw. If the length of the postulated flaw is assumed to be the entire circumferential length of the J-groove weld (i.e., 360 degrees around the nozzle), then this question would be moot.

SCE Response:

The flaw plane is assumed to be axial-radial with respect to the sleeve. Single individual flaws at both the uphill and downhill locations were postulated. This is shown in Fig. 4-1 and 8-1 of the calculation. Being planar flaws, there is no dimension of the flaw that is circumferential with respect to the sleeve. This flaw orientation is the more likely orientation for a crack initiating in the sleeve and growing across the J-groove weld, and therefore the more limiting case.

NRC Question 16:

Page 47. The final flaw depth was calculated to be 1.21 inches and 1.25 inches for the uphill side and downhill side of the nozzle, respectively. (1) Discuss whether this depth will result in crack tip to be located in the pressurizer base metal. (2) Discuss the dimension of the largest size J-groove weld in terms of the distance from the weld surface to the vessel head base metal intersection.

SCE Response:

1) The initial flaw depth of 1.0 inch will place the crack tip within the head base metal. Therefore, the crack growth to any deeper depth will maintain the crack tip within the base metal.

2) The depth of the J-groove prep is about 5/16 inches for the outermost heater sleeve, and the thickness of the cladding is 7/16 inch. Thus, the J-groove prep lies entirely within the cladding. The distance between the mid-point of the weld surface to the base metal is about 0.64 inches on the uphill side of the outermost sleeve based on a clad thickness of 7/16 inches and a weld fillet radius of 3/16 inches. The corresponding distance on the downhill side is smaller. The center of the postulated corner crack is located at the intersection of the sleeve inside surface and the line representing the vessel head inside surface, as shown in Figure 8-1. The distance from the center to the base metal is less than 0.5 inches. Thus, the crack tip will be located in the base metal if a crack depth of 1 inch is postulated.

NRC Question 17:

Page 48. (1) Submit for staff review Reference 5, "Evaluation of Half-Nozzle Repair for Pressurizer and Steam Generator Instrumentation Nozzles Under Long-Term Service Conditions," Calculation No. AES-C-3247-1, Aptech Engineering Services. (2) The half-nozzle design will leave a small gap between the original nozzle and replacement nozzle in the penetration. Discuss whether this gap would be exposed to the primary coolant and the trapped coolant in the gap would lead to crevice corrosion in the penetration.

SCE Response:

The half sleeve repair leaves the sleeve bore in the base metal exposed to primary water, which could potentially result in base metal corrosion. The calculation refers to Reference 5 (AES-C-3247-1) for the evaluation of the effect of corrosion on half-nozzle repair geometry for pressurizer and steam generator instrumentation nozzles. This calculation is also applicable for the heater sleeve penetrations. The allowable

corrosion depths were calculated at two locations: (1) at the gap between the halves of the heater sleeve, and (2) in the crevice region at the nozzle-to-pad weld. The corrosion rate for borated water in contact with the alloy steel head was conservatively determined as 0.0017 in/year for the bottom head from corrosion test data applicable to SONGS as documented in BW Technologies report 51-1235153-00, "Corrosion Evaluation for Base Metal Exposure within RCS Nozzles," dated February 27, 1995. The depth of corrosion was assumed to be uniform and the extent of corrosion around the hole circumference was conservatively taken as 360 degrees. Based on this analysis, the total corrosion depth including fatigue after 40 years of service was shown to be less than the allowable corrosion depth established by the analysis.

Section 2.3 "Borated Water Corrosion Evaluation," (pages 12 and 13) and Figure 4-2 "Postulated BWC in Nozzle Repair Region" (page 27) from Aptech Engineering Services calculation No. AES-C-3724-1 (Reference 5) are provided in Attachment 3.

Attachment 1

to

SOUTHERN CALIFORNIA EDISON
RESPONSE TO NRC STAFF
REQUEST FOR ADDITIONAL INFORMATION
SUPPORTING RELIEF REQUESTS ISI-3-11 AND ISI-3-12
PRESSURIZER HEATER SLEEVE REPAIR
SAN ONOFRE NUCLEAR GENERATING STATION UNITS 2 AND 3

Pages 8 through 13 of SCE Calculation # M-DSC-356, Revision 1 (Aptech Engineering Services Calculation No. AES-C-5212-1)

Calculation No.: AES-C-5212-1 SCE No. M-DSC-356, Rev. 1 Title: Evaluation of Modified Pressurizer Heater Sleeves - SONGS Units 2 and 3	Made by:	Date: 9/17/04	Client: Southern California Edison
	Checked by: MTC	Date: 17 Sept 04	Project No.: AES 03105212-1Q
	Revision No.: 0	Document Control No.: I-1	Sheet No.: 8 of 1083

1.0 PURPOSE AND BACKGROUND

The purpose of this calculation is to perform an American Society of Mechanical Engineers (ASME) Code evaluation of the half-nozzle repair design as applied to the pressurizer (PZR) heater sleeve penetrations. There are 30 heaters that penetrate the bottom head of the PZR. The primary purpose of the heater sleeve is to form the pressure boundary between the heater elements and the PZR vessel. In the original design, the pressure boundary is the J-groove attachment weld on the inside surface of the bottom head. Figure 1-1 provides an illustration of the original weld design. The original Code of construction was the 1971 Edition Summer 1971 Addenda of ASME section III (Ref. 1).

A schematic illustration of the repair is shown in Figure 1-2 (Ref. 2). The repair constitutes the removal of the lower portion of the original sleeve by cutting at approximately the mid-wall location. A new Alloy 690 sleeve of the same dimensions is attached to the PZR bottom head. The new attachment weld is a J-groove weld at the outside surface of the PZR bottom head. The J-groove is machined on a weld pad, which is deposited on the exterior of the head as part of the weld repair procedures. When installed, a vertical gap is maintained between the original sleeve stub, which is not removed and remains in service, and the new sleeve in order to prevent interference during service conditions.

The original sleeve material is Alloy 600. There is a potential for the Alloy 600 sleeves to degrade over time by primary water stress corrosion cracking (PWSCC). In anticipation of such events, the half-nozzle repair technique has been developed. The resistance of Alloy 690 to PWSCC is superior to that of Alloy 600. As a result of the repair, the pressure boundary is moved from the original interior J-groove weld to the outside J-groove/weld pad connection between the PZR head and the Alloy 690 sleeve.

The purpose of this calculation is to perform a design analysis to ASME Section III of the repair weld geometry. This analysis is for SONGS Units 2 and 3. The scope of the analysis covers all 30-heater sleeve locations. The analysis considers the combination of pressure and thermal loads for the original design basis for a 40-year design life commencing when the actual repair is performed.

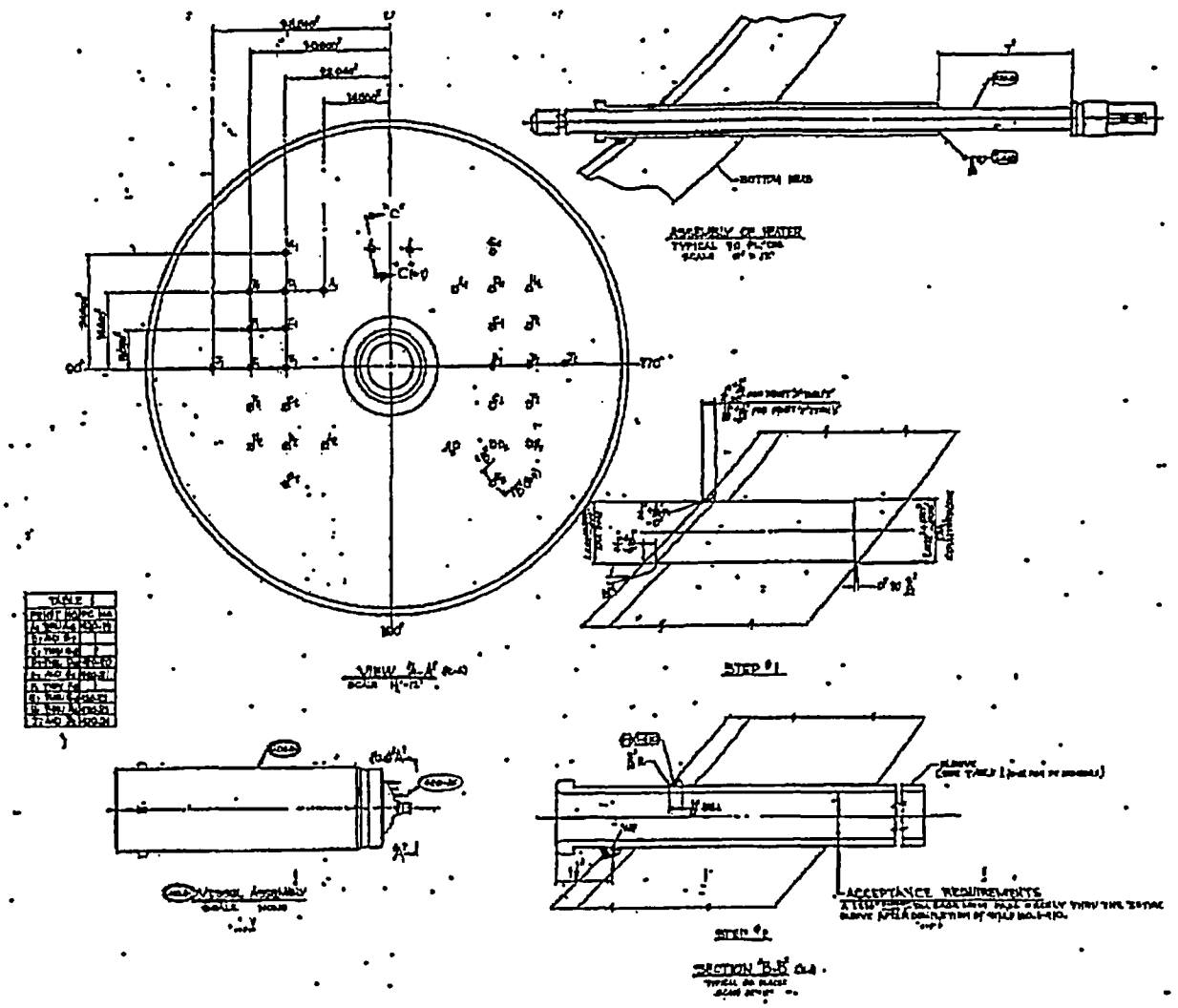

Figure 1-1 — Original J-Groove Attachment Detail for PZR Heater Sleeves.

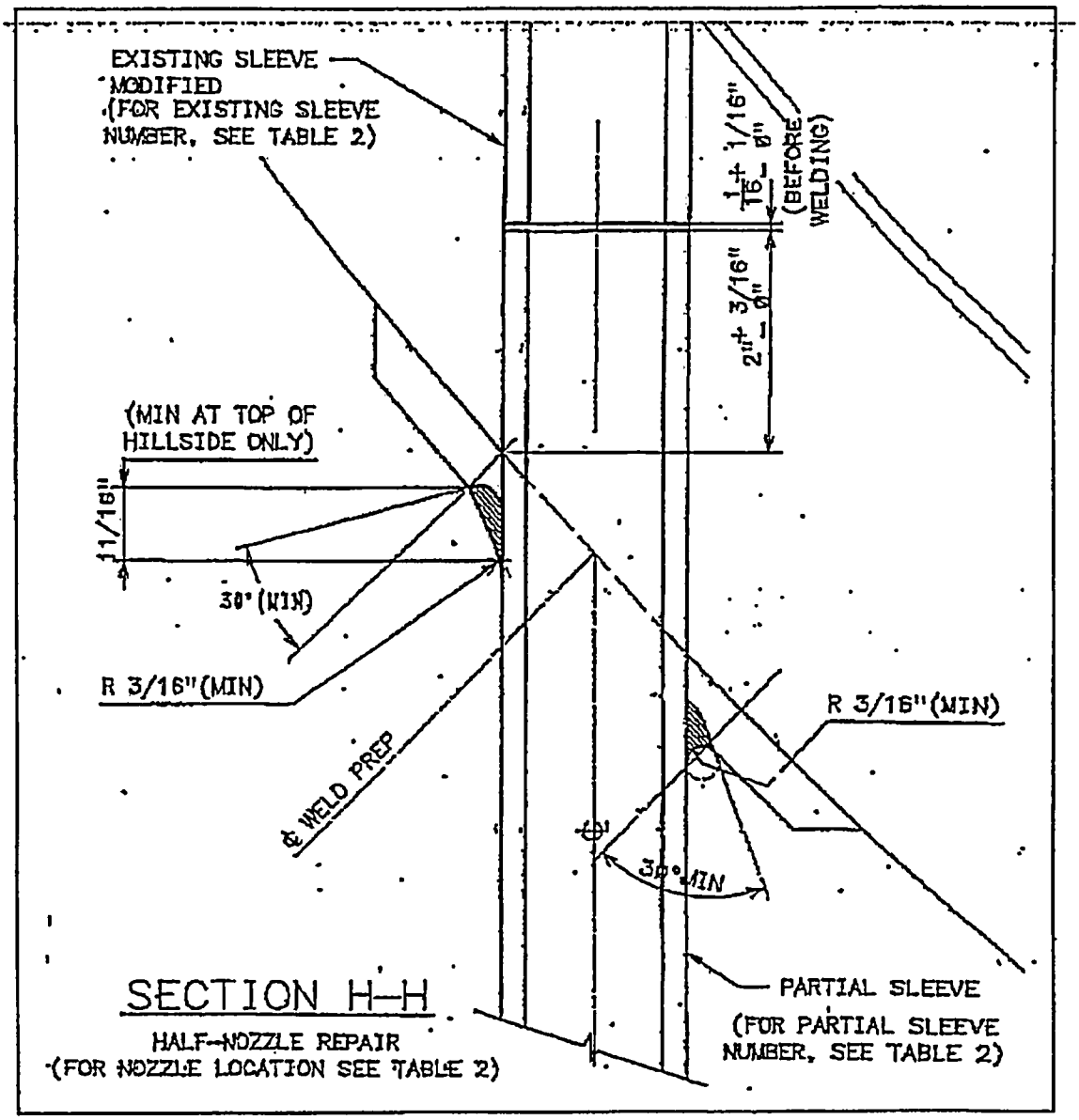

Figure 1-2 — Schematic Illustration of Half-Nozzle Repair Configuration.

2.0 SUMMARY OF RESULTS

Evaluation of SONGS half-nozzle repair for the PZR heater sleeves was completed in accordance with the 1989 Edition of ASME Section III, Division 1, Subsection NB-3200 (Ref. 3). The outermost sleeve (52 degree intersection angle with the PZR bottom spherical head) was evaluated as a bounding case for all heater sleeves in the SONGS pressurizers. Nine analysis sections of the J-groove repair weld were evaluated to Code requirements for general and local membrane, primary plus secondary stress limits for maximum stress range, and fatigue usage. These regions are the sleeve near the attachment weld, the attachment weld throat, and the weld pad near the attachment. These three sections were evaluated at three locations around the sleeve circumference, specifically the 0 degree or downhill side, the 90 degree side and the 180 degree or uphill side.

The evaluations were completed with a combination of finite element analyses performed with the ANSYS computer code, and closed form calculations following Code rules. The NOZ computer code was used to compute the stress ranges and fatigue usage. The NOZ computer code was validated for use in this calculation as discussed in Section 8.1.

As described above, a total of nine sections through various planes of the sleeve and weld were evaluated to ASME Section III design rules. Additional details of the analysis are given in the appendices. Appendix A gives a summary of heat transfer coefficient calculations. Appendix B gives a summary listing of the finite element analysis cases for mechanical (pressure) and thermal transient cases used in the evaluation. Appendix C provides the output from the NOZ program for the evaluation of each nozzle location. Appendix D contains the input listings for the ANSYS computer model cases for pressure, heat transfer, and thermal stress analysis solutions for the three dimensional PZR bottom head model.

2.1 Stress Limit Results

The code evaluation per NB-3200 of ASME Section III was performed at nine critical locations in the half-nozzle repair design. All calculated stresses meet the ASME Code stress limits, as summarized and noted in Table 2-1. All evaluated regions of the half-nozzle repair met the general and local membrane, and primary plus secondary stress limits of NB-3222.2 of $3S_m$ at all nozzle regions except for the uphill side weld section at the outside surface. The ratio of P_L+P_B+Q to $3S_m$ was highest at that location (Analysis Section 8) with a value of 1.21. Analysis of the uphill weld to the rules of NB-3222.2 indicated that the stress limits for $P_L+P_B+Q^*$ (excluding thermal bending) are satisfied as noted in Table 2-1.

Table 2-1 – Stress Summary

	Allowable Stress Ratio			
	Primary Stress		Primary + Secondary	
	P_m	$P_L + P_B$	$P_L + P_B + Q$	Location[1]
Design	0.69	0.82	—	Uphill Sleeve ID
Normal and Upset[2]	—	—	0.89	Uphill Weld OD
Emergency	0.52	0.62	—	Uphill Weld OD
Test	0.79	0.81	—	Uphill Sleeve ID

Notes: 1) Location listed is for the section that gives the highest stress ratio in that row.
2) Stress limit is for primary plus secondary excluding thermal bending.

The thermal ratchet evaluation of NB-3222.5 was required because the limits on stress range with thermal bending included were not satisfied for the uphill weld outside surface. The allowable thermal stress range from NB-3222.5 for preventing thermal ratcheting was evaluated and shown to exceed the calculated thermal stress range at this location. Therefore, the stress limits on maximum stress range for normal and upset conditions have been satisfied.

2.2 Fatigue Evaluation Results

The calculated fatigue usage factors for the nine half-nozzle repair locations (both inside and outside surfaces) were all less than the allowable limit of 1.0. The highest fatigue usage was computed for the weld throat on the uphill side on the outside surface. The computed usage factor at this location is U = 0.038. Therefore, the fatigue usage for the heater sleeve repair is acceptable to ASME Code requirements for a 40-year design life for the repair.

2.3 Conclusions

It is concluded that, based on the design loading conditions at the PZR bottom head, the half-nozzle repair satisfies the ASME Code Section III allowable stress and fatigue requirements for a 40-year design life. This includes the requirements for all design conditions, maximum stress range allowable stress limits for normal and upset conditions (including thermal ratchet limits, and fatigue usage factor), emergency conditions, and testing conditions.

Attachment 2

to

SOUTHERN CALIFORNIA EDISON
RESPONSE TO NRC STAFF
REQUEST FOR ADDITIONAL INFORMATION
SUPPORTING RELIEF REQUESTS ISI-3-11 AND ISI-3-12
PRESSURIZER HEATER SLEEVE REPAIR
SAN ONOFRE NUCLEAR GENERATING STATION UNITS 2 AND 3

Reference 8, The BIGIF Users Manual

BIGIF
Fracture Mechanics Code for Structures

User's Guide
Manual 2

NP-838
Research Project 700-1

Key Phase Report, August 1978

Prepared by

FAILURE ANALYSIS ASSOCIATES
750 Welch Road, Suite 116
Palo Alto, California 94304

Principal Investigators
Russell C. Cipolla
Philip M. Besuner
Dale C. Peters

Prepared for

Electric Power Research Institute
3412 Hillview Avenue
Palo Alto, California 94304

EPRI Project Manager
Floyd Gelhaus
Nuclear Power Division

LEGAL NOTICE

ABSTRACT

The fracture mechanics approach to structural reliability accepts that some flaws will be present but that conditions can be established to assure that flaws do not grow to an unacceptable size during the life of the structure. Fracture mechanics life prediction requires calculation of crack-tip stress intensity factors to quantify both stable crack growth and the conditions for unstable fracture in complex geometries under complex loading conditions which lead to high stress gradients. The BIGIF computer code has been developed to perform accurately and inexpensively these life predictions for a wide range of two- and three-dimensional elastic stress fields, and crack and structural geometries, given that the elastic stress for the uncracked structure is available from another independent source.

This user's guide, the second of three manuals documenting BIGIF, provides detailed input instructions and problem modeling tips for utilizing the BIGIF program. The first manual provides a general description of BIGIF and the influence function method which is its basis, while the third manual is a programmer's guide.

TABLE OF CONTENTS

SECTION	TITLE	PAGE NUMBER
1.0	INTRODUCTION	1-1
1.1	Background and Scope	1-1
1.2	Program Applications	1-2
1.3	Required Program Input	1-3
1.4	Program Documentation	1-4
2.0	ANALYSIS METHODOLOGY AND PROBLEM MODELING	2-1
2.1	Fracture Mechanics Background	2-1
2.2	Key Definitions in LEFM	2-3
2.3	Calculation of K by the IF Method	2-6
2.4	Crack Growth Rate Representation	2-8
2.5	Fatigue Cycle Spectrum Description	2-12
3.0	DATA INPUT DESCRIPTION	3-1
3.1	General Coding Description	3-1
3.2	Card A - Title Card	3-3
3.3	Card B - Problem Control Card	3-3
3.4	Card Series C - Geometry Data	3-8
3.4.1	Card C1 - Initial Crack Dimensions	3-8
3.4.2	Card C2 - Body Dimensions and Crack Position	3-8
3.4.3	Card Series C3 - Variable Thickness Data (NTH = 1)	3-9
3.5	Card Series D - Materials Properties Data	3-9
3.5.1	Card D1 - Material Toughness and Equational Parameter Card	3-9
3.5.2	Card D2 - Crack Growth Rate Data	3-10
3.6	Card E - Transient Cycle Spectrum	3-15
3.6.1	Card E1 - Transient Description Card	3-15
3.6.2	Cards E2A, E2B, and E2C - Cycle Definition Cards	3-18
3.7	Card F - Job Termination Card	3-22
4.0	FLAW MODEL LIBRARY	4-1
4.1	Library Description	4-1
4.2	Special Cases ($100 \leq IFI \leq 199$)	4-4
4.2.1	Center Cracked Infinite Plate in Tension (IFI = 101)	4-4
4.2.2	Edge Cracked Infinite Plate in Tension (IFI = 102)	4-7
4.3	Two-Dimensional Flaw Model Library ($200 \leq IFI \leq 299$)	4.7
4.3.1	Center Cracked Plate for Modes, I, II, or III (IFI = 201, 202, 203)	4.7
4.3.2	Edge Cracked Plate for Modes I, II, or III (IFI = 204, 205, 206)	4-9

SECTION	TITLE	PAGE NUMBER
4.4	Three-Dimensional Flaw Model Library (300 ≤ IFI ≤ 399)	4-14
4.4.1	Nozzle Blend Radius Corner Crack (IFI = 300)	4-14
4.4.2	Buried Circular Crack (IFI = 301)	4-18
4.4.3	Circular Surface and Corner Crack (IFI = 302, 303)	4-18
4.4.4	Buried Elliptical Crack (IFI = 304)	4-21
4.4.5	Elliptical Surface and Corner Cracks (IFI = 305, 306)	4-25
5.0	GENERAL GUIDELINES FOR PROGRAM USAGE, INPUT, AND TROUBLESHOOTING	5-1
5.1	Guidelines for Problem Modeling	5-1
5.1.1	Failure Analysis	5-1
5.1.2	Failure Prevention Analysis	5-2
5.2	Tips for Data Input	5-3
5.3	Program Output and Diagnostics	5-4
5.4	Common Errors and Troubleshooting	5-5
6.0	ADVANCED PROBLEM MODELING TIPS AND TECHNIQUES	6-1
6.1	LEFM Background Information	6-1
6.2	Through-Cracks in Unnotched and Notched Structures	6-2
6.3	Part-Through Cracks and Leak-Before-Break	6-6
6.4	Effect of Welding on Residual Life	6-8
6.5	Fatigue Analysis Involving Once-in-a-Lifetime Maximum Stress Condition	6-9
6.6	Flaw Evaluations According to ASME Code Section XI, Appendix A	6-11
6.7	Effect of the Crack on Structural Stiffness	6-13
6.8	Relative Estimates in Fracture Mechanics	6-14
7.0	EXAMPLE PROBLEMS	7-1
7.1	Introduction	7-1
7.2	Example 1 - Simple Edge Crack in an Unnotched Infinite Plate Under Tension	7-1
7.2.1	Problem Scope	7-1
7.2.2	Problem Statement	7-2
7.2.3	Problem Solution and Answers to (1) and (2) Above	7-5
7.3	Example 2 - Through-Cracks in Notched Structures	7-6
7.3.1	Problem Statement	7-6
7.3.2	Problem Solution	7-10
7.4	Example 3 - Fatigue Analysis of a Weld Crack	7-14
7.4.1	Problem Statement	7-14
7.4.2	Problem Solution	7-15
7.5	Example 4 - Pressure Vessel Nozzle Corner Crack Under Two Loading Transients	7-19
7.5.1	Problem Statement	7-19
7.5.2	Problem Solution	7-22
	APPENDIX A - BIGIF INPUT DESCRIPTION	A-1

SECTION	TITLE	PAGE NUMBER
	APPENDIX B - SAMPLE DATA INPUT CODING FORMS	B-1
	APPENDIX C - PROBLEM OUTPUT FOR EXAMPLE ANALYSES	C-1
	APPENDIX D - CONVERSION FACTORS FOR LEFM UNITS	D-1

ILLUSTRATIONS

Figure		Page
2.1	Review of Linear Elastic Fracture Mechanics	2-5
2.2	Schematic of Fatigue Crack Growth Data Representation	2-10
2.3	Schematic Showing Five Cyclic Stress Intensity Factor Parameters	2-13
3.1	Paris Rule Equational Form for IDADN=1	3-11
3.2	Forman's Rule Equational Form at R=0 (IDADN=3)	3-12
3.3	Forman's Rule Equational Form, R=RRATIO(1) (IDADN=4)	3-13
3.4	Paris Rule Single Tabular Form (IDADN=2)	3-14
3.5	Forman's Rule Single Tabular Input, (IDADN=5)	3-16
3.6	Forman's Rule Multi-Tabular Input (IDADN=6)	3-17
3.7	Schematic Showing a Transient Cycle Spectrum Breakdown	3-19
4.1	Definition of Global and Local Coordinate Systems	4-5
4.2	Optimum Method for Mapping the Nozzle Uncracked Stress Field Onto the Semicircular Model Geometry	4-16
4.3	Percent Errors of Stress Intensity Factor Estimates Caused by Ignoring Certain Details of the Nozzle Geometry in Calculation of Influence Functions	4-19
6.1	Single Edge Notched Plate Containing a Crack Under Nominal Tension	6-4
6.2	Two Possible Flaw Model Representations of an Edge-Notched Plate Containing a Crack	6-5
6.3	Schematic Showing Analytical Conditions at Incipent Leaking for Assessing Leak-Before-Break	6-7
6.4	Schematic Illustrating BIGIF Input for Fatigue Analysis With Once-in-a-Lifetime Loading Condition for a Component With a Forty-Year Service Life	6-10
7.1	Schematic Representation of Example 1a, a Long Axial Surface Crack in the Bore of a Rotor	7-3
7.2	Two Examples of Through Cracks in Notches	7-8
7.3	Weld-Induced Symmetric Residual Stress, $\sigma(x)$ in an Uncracked Specimen and Resulting Stress Intensity Factor K(a) When a Center-Crack of Length 2a is Introduced	7-17
7.4	Weld Crack Propagation in a 10 Inch Wide Specimen for Three Mean Stress Distributions	7-18
7.5	Idealization of Crack in Blend Radius of a Nuclear Reactor Pressure Vessel Nozzle (IFI = 300)	7-20

ILLUSTRATIONS (Continued)

Figure		Page
7.6	A Schematic Representation of the Multiple-Load Inner Surface Stress Transient of a Pressure Vessel Feedwater Nozzle	7-21
7.7	Comparison of Results of a Worst-Case Fracture Mechanics-Based Fatigue Analysis Showing Crack Depth "a" as a Function of Usage Time (Years).	7-25

TABLES

Table		Page
3.1	Card Input Description	3-2
3.2	First Production Version Problem Size Limits	3-4
3.3	Flaw Model Library in BIGIF	3-5
3.4	Integration Point Breakup Scheme	3-7
3.5	Summary of IPLD Parameter Options for Stress Field or K Input in Card E2A	3-20
4.1	Flaw Model Library in BIGIF	4-2
4.2	IFI = 101 - Center-Cracked Infinite Plate in Tension	4-6
4.3	IFI = 102 - Edge-Cracked Semi-Infinite Plate in Tension	4-8
4.4	IFI = 201 - Center-Cracked Plate in Mode I	4-10
4.5	IFI = 202 - Center-Cracked Plate in Mode II	4-11
4.6	IFI = 203 - Center-Cracked Plate in Mode III	4-12
4.7	IFI = 204 - Edge-Cracked Plate in Mode I	4-13
4.8	IFI = 300 - Nozzle Blend Radius Circular Corner Crack	4-17
4.9	IFI = 301 - Buried Circular Crack	4-20
4.10	IFI = 302 - Circular Surface Crack	4-22
4.11	IFI = 303 - Circular Corner Crack	4-23
4.12	IFI = 304 - Buried Elliptical Crack	4-24
4.13	IFI = 305 - Elliptical Surface Crack	4-26
4.14	IFI = 306 - Elliptical Corner Crack	4-27
5.1	Problem Debugging and Troubleshooting Aid	5-7
7.1	Data Input Listing for Example 1	7-7
7.2	Comparison of Input Parameters in Example 2	7-11
7.3	Data Input Listing for Example 2	7-12
7.4	Example 2 - Numerical Results	7-13
7.5	Data Input Listing for Example 3	7-16
7.6	Data Input Listing for Example 4	7-23

NOMENCLATURE

SYMBOL	DEFINITION
a	Crack size (depth or length)
a_1, a_2, a_3, a_4	Crack dimensions for general elliptical shape
a_c	Critical flaw depth on length (size)
a_f	Final flaw size
a_i	Initial crack size
a_ℓ	Crack size at incipient leak
b	Crack origin position for nozzle corner model
c	Major axis length of the elliptical crack
C	Coefficient in fatigue crack growth relations
da/dN	Crack growth rate on a cyclic basis
da/dt	Crack growth rate on a time basis
E	Modulus of elasticity
F	Correction factor which accounts for geometry, mode of loading, and stress gradient effects on the stress intensity factor
h	Influence or weight function which is independent of loading
K	Stress intensity factor
$\bar{K}$	Local average of K at a discrete position around the crack front
ΔK	Range of applied K in the stress cycle
K_c	Critical value of applied stress intensity factor (material property)

SYMBOL	DEFINITION
K_{IC}	Critical value of K under Mode I plane strain conditions
K_{max}	Maximum applied K in the stress cycle
K_{mean}	Mean K level in the stress cycle
K_{min}	Minimum applied K in the stress cycle
K_I, K_{II}, K_{III}	Stress intensity factor for loading Modes I, II, and III
K_t	Stress concentration factor (ratio of maximum stress to nominal stress)
K_{tx}	Stress concentration factor for x-direction gradient
K_{ty}	Stress concentration factor for y-direction gradient
n	Exponent in fatigue crack growth rate relations
N	Number of applied cycles or loading blocks
N_f	Number of cycles required for failure
N_i	Number of cycles to initiate a crack
N_p	Number of cycles to propagate a crack
ν	Poisson's Ratio
ϕ	Local crack orientation in (x,y) plane (degrees)
Q	Constant coefficients in stress field equations
r	Radius of body curvature
R	Ratio of K_{min} to K_{max}
r_b	Nozzle blend corner radius
S	Dimensionless scale factors

SYMBOL	DEFINITION
σ, σ_o	Applied uniform stress
$\Delta\sigma$	Cyclic stress range
$\sigma_{ij}(x,y)$	General varying stress distribution acting on the crack plane
σ_{zz}	Applied uniform stress in z-direction
$\sigma_{zz}(x,y)$	General varying normal stress component acting on the crack plane
$t(x)$	Body thickness variation; thickness direction is parallel to the crack front in two-dimensional crack geometry models
U	Strain energy
w	Body width
x	Global x coordinate
x'	Local x coordinate for crack
x_c	Global x coordinate for crack center
y	Global y coordinate
y'	Local y coordinate for crack
y_c	Global y coordinate for crack center
z	Global z coordinate always normal to crack plane

Note: Computer variable names are defined at appropriate locations in the text and appendices and are listed in the BIGIF Programmer's Manual.

1.0 INTRODUCTION

1.1 Background and Scope

This manual provides the details and input instructions necessary to use BIGIF, a computer program which performs engineering fracture mechanics, residual life, and residual strength computations. BIGIF utilizes input material crack growth rates and numerically integrates over the crack tip stress intensity factor field which is calculated by BIGIF for the specified crack and component geometries, and the applied load and stress fields. BIGIF thus calculates the number of loading cycles or the loading time to grow a specified initial "crack-like" imperfection through a specified component geometry and stress field to a final dimension.

The name BIGIF is an acronym for Boundary-Integral-equation-Generated-Influence-Functions. The key feature of BIGIF, and the influence function method which is its basis, is its ability to account, accurately and efficiently, for the crack-caused redistribution of stress fields with high stress gradients. The BIGIF program has an expandable library of flaw models from which the user can select from among eleven different crack geometries, under general stress gradients, varying from simple crack problem solutions available in the literature to more complicated crack geometries where extensive prior numerical analysis was performed to obtain the general three-dimensional solutions now stored in BIGIF.

All fracture mechanics analyses depend on estimates of the stress distribution "near" the crack tip. Most present theory assumes that the net

section stress cycle is elastic, and under this condition, the theory asserts that the rate of crack propagation and the onset of "rapid fracture" under cyclic and steady loading are functions of only one stress parameter. The parameter is the stress intensity factor, K. It is important to note that the stress intensity factor should not be confused with stress intensities (i.e., the maximum principal stress difference) used in the ASME Code Section III design procedure (1-1). Here, K is a quantity which defines the magnitude, or singularity strength, of the "near crack tip" stress distribution. Additional discussion of fracture mechanics principles can be found in later sections.

1.2 Program Applications

The influence function methodology utilized in BIGIF was initially applied in the gas turbine industry, particularly to disk bores, rim slots, and other rotating components in jet engines. For such problems, the fatigue initiation and propagation of flaws in the presence of stress risers such as inclusions, notches, and holes are of primary concern. Similar applications exist in the steam turbine generator systems of power generating plants.

BIGIF has also been successfully applied to problems involving welded structures, where both nominally applied service stresses and residual weld stresses are present, such as pressure vessels and nozzles. It is intended that BIGIF also be utilized in performing flaw evaluations to meet the requirements of Appendix A of Section XI (1-2) of the ASME Code, especially when the application of the Code procedure, such as by use of the computer

program FACET (1-3), is inadequate. The application of BIGIF to flaw problems is discussed in Sections 6.0 and 7.0

1.3 Required Program Input

The BIGIF program requires two types of input (1) material property data derived from experiments, and (2) "uncracked" stress distributions along the plane that is or might be cracked for the various loading conditions. To define these inputs, the user may utilize the results from mechanical behavior tests and/or analytical or numerical stress analyses. A significant amount of mechanical behavior data already exists in the literature and adequate stress input is often available from calculations performed during design or in-service evaluation. The mechanical behavior data must

(1) Express crack propagation rate (da/dN or da/dt) as a function of ΔK or K_{max}, respectively, taking into account mean stress effects ($R = K_{min}/K_{max}$), loading frequency, and environmental conditions and

(2) Predict the critical K level (fracture toughness K_c or K_{IC}) required for unstable or brittle fracture.

A solution technique (i.e., flaw model) must be chosen with which BIGIF can compute K for the growing crack as a function of the input stress field and geometry. For each flaw model available in BIGIF (see Section 4.0), the required input is the "uncracked" stress distribution in the region of the

crack (i.e., the stress solution at the crack plane or locus but without the crack present in the stress model). BIGIF accounts for the crack's disturbance of the uncracked stress field in the model geometry. Typical design stress analysis, such as required by Section III (1-1) for nuclear components, would be a good starting point to determine the uncracked stress field. However, more detailed stress analysis may be required to enable sufficient definition in regions of concern. If detailed stress analysis has not been performed, conservative approximations can be utilized to bound the fracture computations and a detailed analysis can later be introduced, if necessary, to refine the fracture analysis.

1.4 Program Documentation

Besides this User's Manual, there are two additional manuals which document the BIGIF program. The first manual (1-4) is a general introduction which presents the theoretical background and major applications of the program. It also contains some numerical details of the algorithm. The third manual (1-5) is a programmer's guide which provides a program source code description, detailed flowcharts showing the program logic, data flow, numerical form of the functions, and a source listing of BIGIF.

REFERENCES

1-1 ASME Boiler and Pressure Vessel Code, Section III, 1977 Edition, Summer Addenda.

1-2 ASME Boiler and Pressure Vessel Code, Section XI, 1977 Edition, Summer Addenda.

1-3 Cipolla, R. C., "Computerized Method to Perform the Flaw Evaluation Procedure as Specified in the ASME Code, Section XI, Appendix A, Part I: General Description," EPRI RP-217-1 and RP-700-1 Technical Report FAA-76-2-1(I), Revised December 1977.

1-4 Besuner, P. M., Peters, D. C., and Cipolla, R. C., "BIGIF: A Computer Program Which Performs Engineering Fracture Mechanics Computations for Structures Under Complex Stress Gradients and Cyclic Load Spectra, Introduction and Theoretical Background (Manual 1 of 3)," Technical Report FAA-78-1-3(1), EPRI RP-700-1, December 1977.

1-5 Peters, D. C., Besuner, P. M., Sorenson, K. G. and Cipolla, R. C., "BIGIF: A Computer Program Which Performs Engineering Fracture Mechanics Computations for Structures Under Complex Stress Gradients and Cyclic Load Spectra, Program Description (Manual 3 of 3)," Technical Report FAA-78-1-3(3), EPRI RP-700-1, March 1978.

2.0 ANALYSIS METHODOLOGY AND PROBLEM MODELING

2.1 Fracture Mechanics Background

The traditional approach to structural life prediction has been the alternating-stress-versus-cycles (S-N) technique. Initially smooth or notched test specimens are polished so that all surface defects are removed. These specimens are tested to failure (which can be defined as crack initiation or fracture of the specimen) and the resulting cyclic lives for various alternating stresses serve as a basis for the design of a component against fatigue failure. For example, in the ASME Code design procedure (1-1) the S-N approach is used to establish usage factors for the component. However, the principles of linear elastic fracture mechanics have been adopted recently by the Code to (1) assure adequate material toughness for the reactor pressure vessel at the start of life, and (2) provide flaw evaluation procedures for defects found during service so that rules for flaw acceptability and component operation without repair could be established.

Linear elastic fracture mechanics (LEFM) application, assuming valid laboratory data, stress analysis, and stress intensity factor solutions are available, has three major advantages over the S-N technique of life prediction. Specifically, LEFM:

(1) Accounts for initial crack-like defects,

(2) Allows generation of a family of S-N curves from one specimen (exclusive of natural fatigue life "scatter"); that is, nominal load or stress distribution is essentially eliminated as a test variable, and

(3) Allows the lives of other component or crack geometries to be predicted from the results of the one tested; thus, eliminating geometry as a test variable.

In order to obtain these valuable advantages, extra experimental and analytical efforts must be performed as part of LEFM analysis. For example:

(1) Fatigue crack growth rate laboratory data are required for actual operating conditions since present theory does not account for the effects of many variables. These include temperature, time at load, environment (e.g., corrosion), material composition and microstructure, and (to a lesser extent) complicated load interaction effects (e.g., overload). These items must therefore be considered test variables.

(2) Surface or maximum stress estimates may not be sufficient. An estimate of internal stress must often be made to enable calculation of K.

(3) An "initial" or reference crack configuration must be specified. Most LEFM life prediction algorithms predict infinite life from crack-free structures.

There are other less obvious advantages of LEFM that become apparent after a few typical structural applications. Examples are:

(1) Often, a structural detail like a weld bead or rim slot has an extremely high or unestimable stress concentration factor (say, $K_t > 4$). The detail can often be modeled as a crack to obtain

useful lower bounds on fatigue life and other performance parameters. This is especially true if the highest stresses are extremely local.

(2) Probabilistic systems can be created which account for the occasional presence of a true fatigue crack or crack-like defect. The engineer is no longer restricted to representing flawed structures with mathematical models of flawless structures.

(3) LEFM accounts for the important physical size effect of the structural detail or notch. Crack propagation data shows that for a given initial crack, concentrated stress and nominal stress, the larger the notch the lower the fatigue crack growth life to failure. Since LEFM accounts for the notch's decaying stress field, it can predict this life decrease.

(4) LEFM data interpretation allows a formulation of a simple cumulative damage hypothesis (used in BIGIF) in which the crack growth rates for each cycle in a loading block are summed to calculate the growth rate per block. This damage hypothesis replaces Miner's rule (2-6) and appears to do a good job handling certain failure modes involving both low cycle (LCF) and high cycle fatigue (HCF) in the absence of significant overloads.

2.2 Key Definitions in LEFM

The fracture mechanics equations effectively link three parameters--the defect size, the fracture toughness or subcritical crack growth rate, and the applied stress, so that if any two of these are known, the third

can be quantified. The stress distribution for any arbitrary mode of loading and shape of body and crack can be quite difficult to determine; however near the tip of the crack, essentially one of three things can occur; the faces can be pulled apart (Mode I) or sheared perpendicular or parallel to the leading edge of the crack (Modes II or III). These three load modes are shown schematically in Fig. 2.1a. The crack opening mode or Mode I is generally regarded as the most damaging of the three modes. The character of the near-crack-tip stress distribution is illustrated in Fig. 2.1b. The stress intensity factor, K, defines the magnitude of stress distribution and is calculated from the relation

$$K = \sigma F\sqrt{\pi a}, \quad \sigma < \sigma_y \tag{2.1}$$

where σ is the applied stress, σ_y is the yield strength, $\underline{a}$ is the crack length, and F is a correction factor that depends on the flaw and structural geometry, the mode of loading, stress gradients, and the structural displacement constraints. For the case of a center-cracked, infinitely wide plate under uniform tensile stress, α is unity.

When the value of K reaches a critical value, K_c, fracture will occur in an unstable manner. Thus, the critical flaw size, a_c, can be determined by rearranging Eq. (2.1) to yield

$$a_c = \frac{1}{\pi}\left(\frac{K_c}{F\sigma}\right)^2 \tag{2.2}$$

For the assessment of a fatigue failure mode, fracture mechanics assumes that the flaw of initial size, a_i, can grow to some final size, a_f, under the action of cyclic loading during the lifetime of the structure.

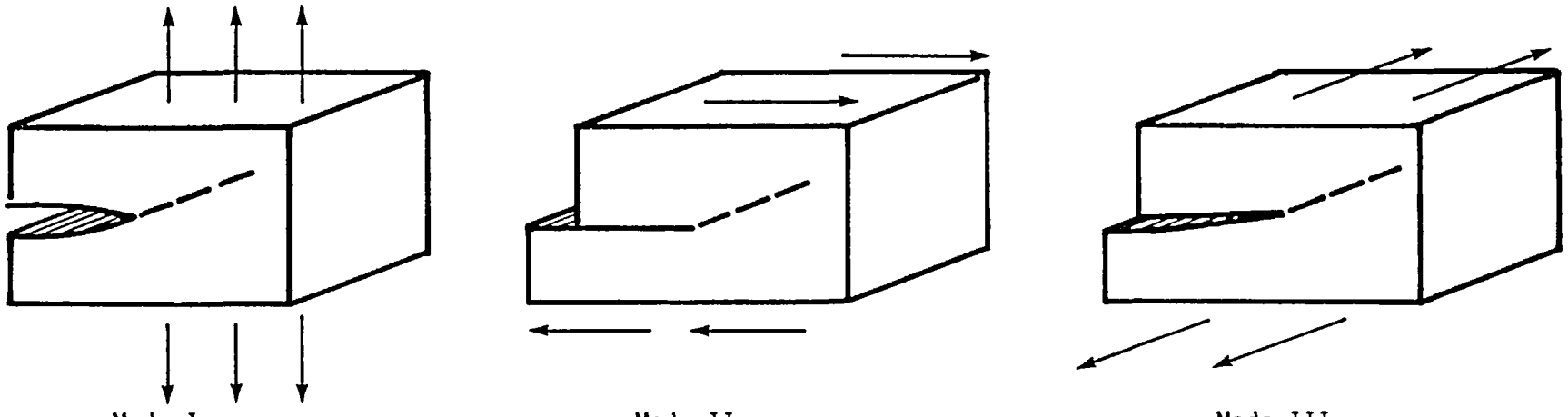

a) Crack Tip Loading Modes

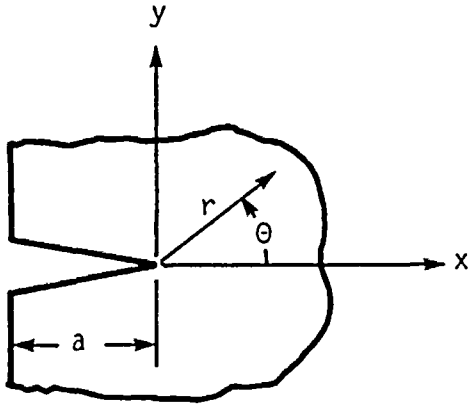

b) Near-Crack Tip Stress Component

All Stress Components Have the Form:

$$\sigma_{ij} = \frac{K_k}{\sqrt{2\pi r}} f_{ij}^{(k)}(\Theta)$$

Where i = x, y, z; j = x, y, z, and k=I,II,III.

No Summation is Implied and Stress Intensity Factor, K, is Proportional to

(Nominal Stress) $\sqrt{(\text{Crack Length})}$.

Figure 2.1 - Review of Linear Elastic Fracture Mechanics.

Crack growth rate-per-load-cycle (da/dN) is dependent on the stress intensity factor

$$da/dN = f(K). \tag{2.3}$$

Crack growth rate-per-time, t, can be similarly correlated

$$da/dt = g(K). \tag{2.4}$$

The subcritical crack growth life (N or t) can be determined by rearranging and integrating Eq. (2.3) or Eq. (2.4) over the appropriate domain of crack size so that

$$N = \int_{a_i}^{a_c} \frac{da}{f(K)} . \tag{2.5}$$

2.3 Calculation of K by the IF Method

With the exception of some special case solutions such as the center-cracked infinite plate problem mentioned earlier, the determination of K as a function of crack depth is a nontrivial problem when the body dimensions are finite and the stress distribution is varying in a nonlinear fashion. The influence function (IF) approach is used by BIGIF to compute K. The essential features in the formulation of IF method are described in (1-3), and the strengths of the method are that

(1) The application of elastic superposition allows the use of the "uncracked" stress distributions in the K analysis

(2) The influence function (h) itself is invariant with stress

and provides the vehicle to calculate the effect of the crack in redistributing any stress field.

The influence function (h) is a function of crack position (x), specified displacement boundary conditions (u) and geometry (k). The calculation of K for the general class of two-dimensional* problems in Mode I is

$$K = \int_L h(x,u,k)\ \sigma_{zz}(x)\ dx \qquad (2.6)$$

where L is the crack line and $\sigma_{zz}(x)$ is the "uncracked" stress distribution normal to the crack face. Once the influence function h has been obtained for a given crack configuration, the stress intensity factor for any uncracked stress distribution may be obtained accurately and rapidly from Eq. (2.6). For three-dimensional problems, K becomes a function of crack front position, s, so that Eq. (2.6) must be replaced with more complex formulas. The IF approach to this class of problems is to define one or more local averages $\bar{K}_i$ of K(s) over as many defined portions of the crack front. These local averages are also related to and may be calculated directly from the strain energy release rates resulting from defined crack growth and shape changes. Therefore, $\bar{K}$ has the same general properties as other elastic stress intensity factors including valid elastic superposition. Each dimension or parameter used to describe crack growth or shape change is called a degree-of-freedom (DOF) on K(s). Given sufficient discretization of the crack front into enough degrees-of-freedom, the $\bar{K}$ values will equal corresponding local values of K(s).

---

*The terms "two-dimensional" and "three-dimensional" refer to the level of elasticity theory required to solve the crack problem.

A general description of all IF solutions in the flaw model library of BIGIF is given in Section 4.0. All IF contained in the library were formulated for bodies with constant or infinitely thick (y direction) geometries. However, for each of the two-dimensional solutions in the library, an approximate procedure for computing K in a variable thickness part can be specified. In this case Eq. (2.6) is modified to yield

$$K = \frac{1}{t(a)} \int_0^a h(x,u,k) \quad t(x) \quad \sigma_{ij}(x) \quad dx \qquad (2.7)$$

where t(x) is the thickness variation. The influence function h(x,u,k) is not the correct one since it was formulated from the solution for a constant thickness plate. The errors associated with this approximation vary, and for certain linear thickness variations, Eq. (2.7) is exact. However, the most important effect of the distribution of load over the crack face area is accounted for in Eq. (2.7).

2.4 Crack Growth Rate Representation

A standard way to characterize the crack growth behavior of a material is to test a center-flawed specimen with a saw-cut slot in the center to act as a crack starter. The specimen is cyclically loaded at a low stress level until a fatigue crack grows far enough out of the slot to eliminate the effect of the slot-tip dimensions on crack growth. Crack length is periodically measured and recorded along with the number of load cycles. From this information, a curve for crack length versus cycles is determined as shown in Fig. 2.2a. The slope of this curve, da/dN, can then be computed at any crack length, "a". The stress intensity factor, K, can be calculated for the same

"a" and a plot made of da/dN versus K, as shown in Fig. 2.2b. In most cases, ΔK (see Fig. 2.3) which equals (1-R) K_{max} (or $K_{max} - K_{min}$), is used because it has the most pronounced effects on da/dN of all parameters. An R value (K_{min}/K_{max}) of 0.1 is commonly specified for the experiment (because testing with $K_{min} = 0$ is often difficult) although higher values such as R = 0.5, 0.9 are used for appropriate applications involving high steady stresses. A similar technique for determining crack growth under steady stress (da/dt versus K_{max}) can also be applied to quantify stress corrosion or creep cracking.

The da/dN versus ΔK curve thus produced is independent of loading and geometry and can be used for general life prediction. Empirical relations to express da/dN behavior have been proposed, the earliest and most well known is from Paris (2-1) which takes the form

$$da/dN = C\,\Delta K^n, \tag{2.8}$$

where C and n are constants determined from the relevant data. The advantages of the Paris rule is that it is simple in form (straight line on a log-log plot) and fits experimental data well in the middle range of ΔK away from threshold effects (low ΔK region) and K_{max} effects (high ΔK region). One major disadvantage of the Paris rule is that it does not account for mean stress effects (R variation) on fatigue crack propagation.

A popular expression which accounts for mean stress was developed by Forman (2-2):

$$da/dN = \frac{C\,\Delta K^n}{K_{IC}\,(1-R) - \Delta K} \tag{2.9}$$

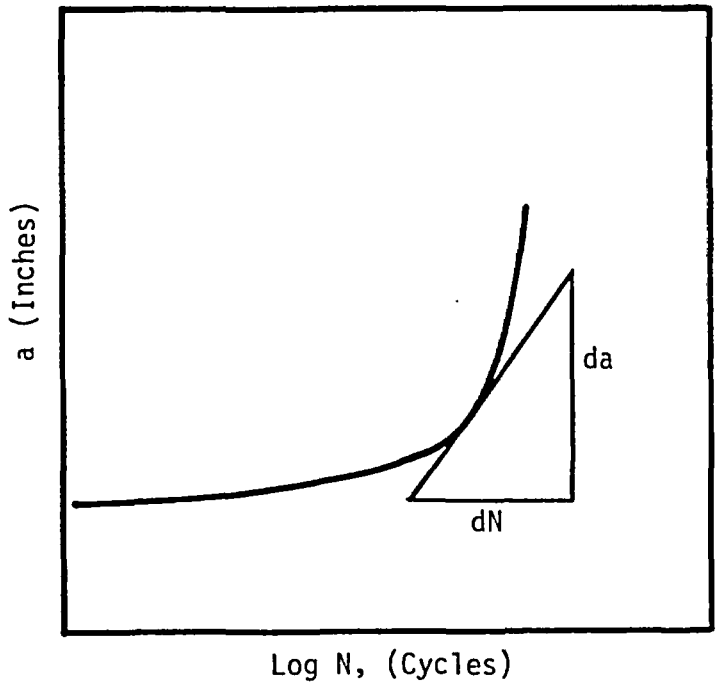

a) Crack length versus applied cycles.

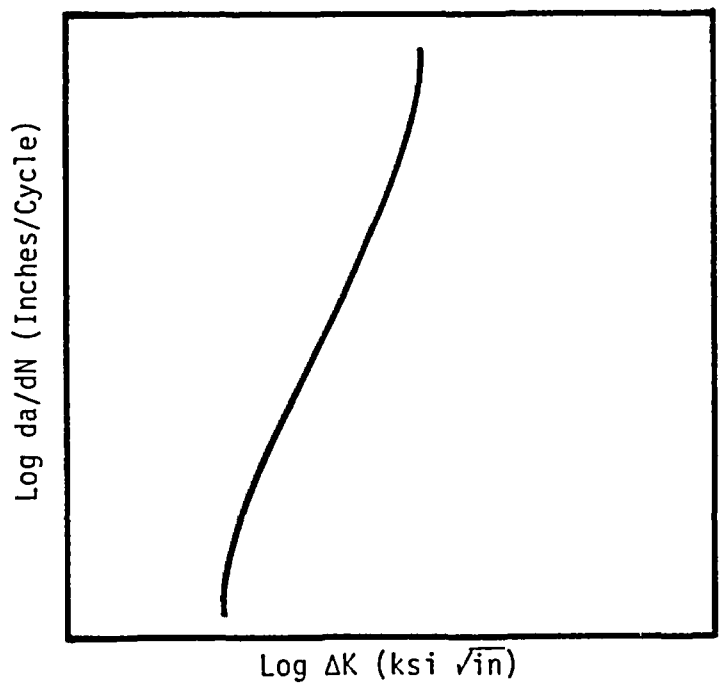

b) Crack growth rate representation

Figure 2.2 - Schematic of Fatigue Crack Growth Data Representation.

where C and n are material constants (not the same as those in Eq. (2.8)), and K_{IC} is the plane strain fracture toughness as originally proposed by Forman or can serve as an additional parameter for data fit. The added feature of Forman's relation is to correct for nonzero minimum stress and to increase the fatigue crack growth rate at the onset of failure.

Both the Paris and the Forman rules are available in BIGIF with additional options which allow the user to input tabular data. It is important to note that choice of the equational form and calculation of the constants need not follow a prescribed format as long as two conditions are met:

(1) The equation should agree with plotted median da/dN values to within say ±15% (this will contribute integrated life errors of (usually much) less than 15% if the second condition is also met).

(2) The equation must not be extrapolated outside the data range without extreme caution. It is surprisingly easy to inadvertantly violate this condition.

In general, the practice should be to "let the data draw the curve". For this purpose, the program also accepts the piecewise exponential data input for either a Paris-based relation or one based on Forman. When actual material data is not available, the analyst will have to rely on comparable literature data. A compilation of crack growth rate and toughness data for high strength alloys is provided in (2-3). Complete details of the options for da/dN specification are given in Section 3.0.

2.5 Fatigue Cycle Spectrum Description

There are two general classes of loading spectra which can occur in real loading histories; programmed loading and random loading. The BIGIF input is best suited for programmed loading; although there exist methods (2-4, 2-5) which can approximate random loading data with several cumulative programmed loads of fixed amplitudes and frequencies. A schematic showing the fatigue cycle definitions used in the BIGIF program is shown in Fig. 2.3. A group of constant amplitude cycles is defined as a transient. Currently, up to twenty transients can be grouped into a loading block (N). In a fatigue analysis, the loading block N is repeatedly applied to the structure and grows the crack from a_i to a_f, according to Eq. (2.5). The fatigue analysis will be terminated either when

$$K(a_f) \geq K_{IC} \tag{2.10}$$

or

$$a_f \geq w, \tag{2.11}$$

where w is the body width, whichever condition is satisfied first.

For a given stress intensity factor fatigue cycle, there exist five useful parameters as shown in Fig. 2.3. Once any two parameters are known, the remaining three are easily determined. These are K_{max}, K_{min}, $\Delta K = K_{max} - K_{min}$, $K_{mean} = (K_{max} + K_{min})/2$ and $R = K_{min}/K_{max}$. The most important for fatigue is ΔK, although all five quantities are printed as part of the solution output. Complete details of the input of the five parameters are given next in Section 3.0.

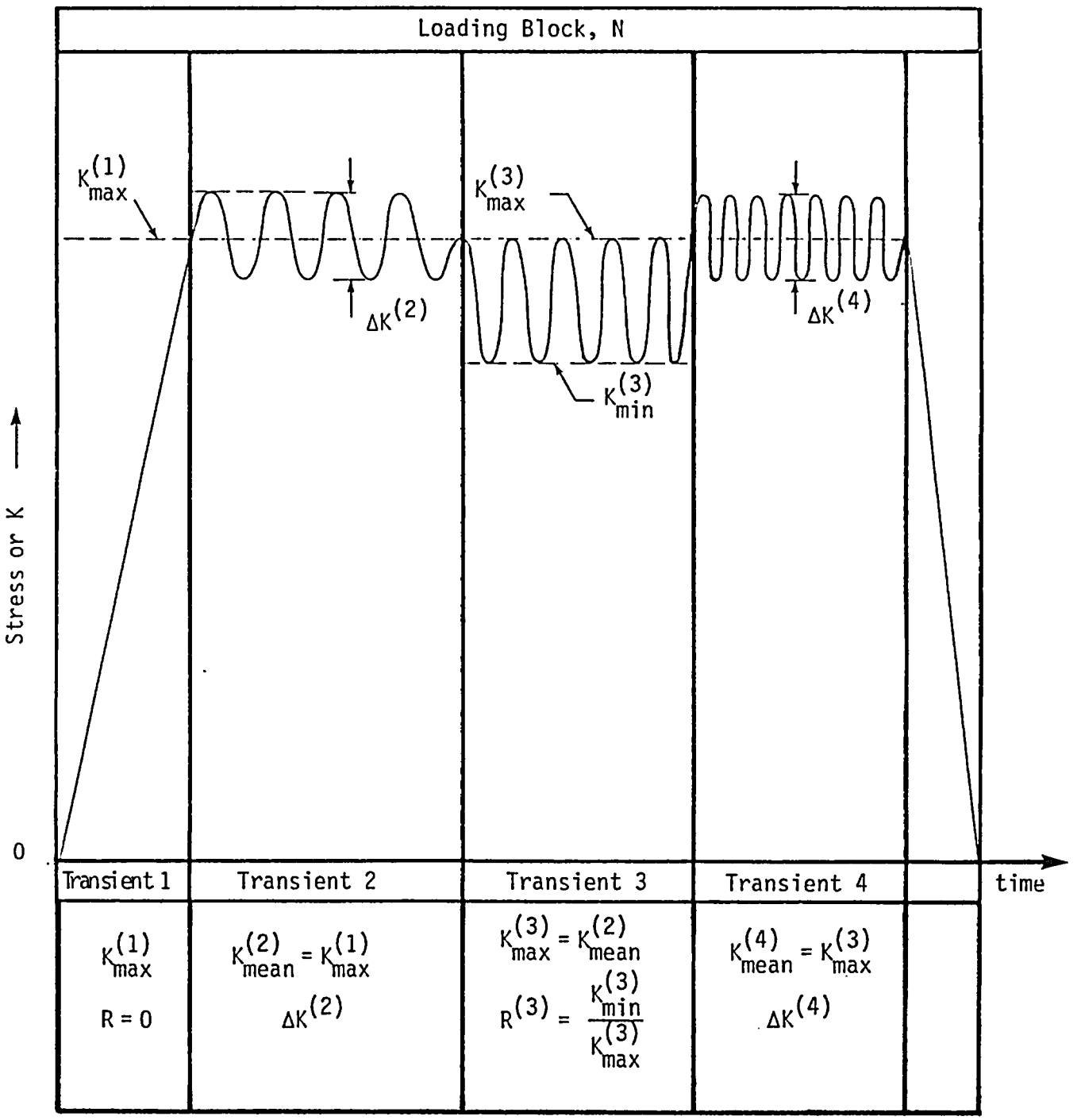

Figure 2.3 - Schematic Showing Five Cyclic Stress Intensity Factor Parameters.

REFERENCES

2-1 Paris, P. C., M. P. Gomez, W. E. Anderson. "A Rational Analytic Theory of Fatigue", The Trend in Engineering, Vol 13, No 1 (January 1961).

2-2 Forman, R. G., "Numerical Analysis of Crack Propagation in Cyclic Loaded Structures", Journal of Basic Engineering, pp. 459-464, (September 1967).

2-3 Damage Tolerant Design Handbook, "A Compilation of Fracture and Crack Growth Data for High Strength Alloys", Metals and Ceramics Information Center, Battelle Columbus NTIS HB-01 (September 1973).

2-4 Gurney, T. R., "The Rainflow Stress Counting Method", The Welding Institute Research Bulletin, pp. 205-206 (July 1975).

2-5 Fuchs, H. O., D. V. Nelson, M. A. Burke, T. L. Toomay, "Shortcuts in Cumulative Damage Analysis", Paper 730565 presented at SAE Automobile Engineering Meeting, Detroit (May 1973).

2-6 Miner, M. A. "Cumulative Damage in Fatigue," Trans. ASME, Vol. 67 pp. A159-A164 (September 1945).

3.0 DATA INPUT DESCRIPTION

3.1 General Coding Description

This section describes in detail, the data input required to run the BIGIF program. The data input stream is subdivided into six card series labeled A through F. A general overview and functional description of each card series is shown in Table 3.1. All input data is either of integer, real, or alphanumeric type and is read directly into core from fixed field card format. All variables which are labeled as integer are read under I5 format and must be right justified in the field. All decimal inputs (real) use F10.0 or F20.0 format and can appear anywhere within the field specification. Scientific notation may be substituted by specifying the input in E format in the usual way. Alphanumeric input uses any keyboard character and, like decimal input, can be specified anywhere in the field. Blank integer or real variable input will be interpreted as zero while blank alphanumeric input will be set equal to blank characters.

Complete but abbreviated card input instructions are provided in Appendix A. The Appendix is intended for use while completing input coding forms, punching cards, or working on a computer terminal, once the user has become familiar with the input variables and no longer needs to refer constantly to the full user's manual. Data coding forms structured for BIGIF input are provided in Appendix B. In the subsections which follow, each variable contained in the input stream will be described in detail. It is suggested that a copy of Appendix A be referred to while reading the remainder of this Section.

TABLE 3.1

CARD INPUT DESCRIPTION

Card Series	Sub-Series	Card Series Description
A		Job Title Card
B		Problem Control Card
C		Geometry Data
	C1	Initial Crack Dimensions
	C2	Body Dimensions and Crack Position
	C3A	Thickness Table Size
	C3B	Thickness Table Input
D		Material Properties Data
	D1	Material Toughness/Equational Input
	D2A	R Ratio and Table Size
	D2B	Crack Growth Rate Table Input
E		Transient Cyclic Spectrum
	E1	Transient Description
	E2A	Cycle Definition
	E2B	Stress Equational Constants
	E2C	Stress and K Table Input
F		Job Termination Card

3.2 Card A - Title Card

The first card beginning each problem is a single title card. This card contains an 80 character job title which will be echo printed at the top of each page which starts a new segment of the solution output. Any of the 64 ANSI characters can be used in the title.

3.3 Card B - Problem Control Card

The problem control card provides all the information to BIGIF necessary to specify type of analysis desired, the flaw model, the problem size, and other options. A listing of the current problem size limits is given in Table 3.2. The analysis selection parameter IFAT can either be zero for a single K calculation only or unity which specifies a complete fatigue analysis to be performed. NTRAN is the number of distinct constant amplitude transients to be used to define the loading block. The flaw model library index number, IFI, and the number of degrees-of-freedom, IDOF, define the flaw model to be used in the analysis. When IFAT = 0, K is calculated for each of NTRAN transients for IDOF initial crack dimensions specified in the geometry data (Card C1). A description of IFI and IDOF for the flaw models is presented in Section 4.0. A table summarizing the allowable combinations of IFI and IDOF for the models available is reproduced in this Section in Table 3.3.

A variable body thickness option, activated by setting the variable NTH = 1, is an approximate way to account for the variations in applied K due to changing body thickness. This feature is only available for two-dimensional flaw models (IFI ≡ 200's). When NTH is equal to zero, the

TABLE 3.2

FIRST PRODUCTION VERSION PROBLEM SIZE LIMITS

Input Variable Description	Limit
Number of Job Title Cards	1
Number of Transients	20
Number of da/dN vs. ΔK Points per R Curve Data Set	20
Number of R Curve Data Sets	5
Number of Stress Fields (Univariate Cubic Form)	40
Number of Stress Fields (Bivariate Cubic Form)	40
Number of Stress Fields (Linear Table, $\sigma(x)$)	40
Number of Stress Fields (Bilinear Table $\sigma(x,y)$)	40
Number of Stress Points, $\sigma(x)$	20
Number of Stress Points, $\sigma(x,y)$	225
Number of K(a) Distributions (Linear Table)	20
Number of K vs. a Data Points	20
Number of Thickness Points, t(x)	20

TABLE 3.3

FLAW MODEL LIBRARY IN BIGIF

Library Class	Model Index (IFI)	Crack Model Geometry Description	Degrees of Freedom (IDOF)	Finite Width Effects
Special Cases[1]	101	Center Cracked Infinite Plate in Tension	1	No
	102	Edge Crack Semi-Infinite Plate in Tension	1	No
Two-Dimensional	201	Center Cracked Plate, Mode I	1	Yes
	202	Center Cracked Plate, Mode II	1	Yes
	203	Center Cracked Plate, Mode III	1	Yes
	204	Edge Cracked Plate, Mode I	1	Yes[2]
	205	Edge Cracked Plate, Mode II (Inactive)	1	Yes
	206	Edge Cracked Plate, Mode III (Inactive)	1	Yes
Three-Dimensional	300	Nozzle Blend Radius Semi-Circular Corner Crack	1	No
	301	Buried Circular Crack	1	No
	302	Circular Surface Crack	1	No
	303	Circular Corner Crack	1	No
	304	Buried Elliptical Crack	4	No
	305	Elliptical Surface Crack	3	No
	306	Elliptical Corner Crack	2	No

[1]Special Cases does not involve influence function method nor numerical crack area integration to compute K.

[2]The influence function is accurate for $0 \leq a/w \leq 0.6$.

standard constant thickness is assumed. Refer to Section 2.3 for a technical discussion of the variable thickness option, and to Card C3 for the variable thickness input when NTH = 1.

The parameters IDADN and NR define the input format of material crack growth properties to be used in the analysis. IDADN specifies the fatigue crack growth relationship, and NR is the number of da/dN data sets corresponding to different R values. If IDADN = 1, a Paris rule, Eq. (2.8), is used to compute da/dN. For IDADN = 2, the user is to specify a table of points for da/dN vs. ΔK and the Paris relation is used to interpolate between data points and for extrapolation outside the tabular range. When IDADN = 3, 4, 5, or 6, a Forman's interpolation based on Eq. (2.9) will be used. Refer to the input description for Card Series D for description of each IDADN option. NR is not used and should be set to zero or left blank in the input field if IDADN = 1, 3, or 4.

Finally, the parameters INUM, INCL, and NDUB define the numerical integration scheme to be used in the analysis. INUM is an index defining the degree of refinement of the crack face discretization used for the integration of Eq. (2.6) or Eq. (2.7) for K. NDUB is the number of increments used to double the fastest growing crack dimension for the incremental crack growth used in the numerical integration of Eq. (2.5) for life N. There are three distinct integration breakups labeled as coarse, standard and refined corresponding to INUM = 1, 2, or 3. Table 3.4 summarizes the integration grid used for each scheme. If NDUB is input as zero, the crack growth increment will default to the values assigned for coarse, standard or refined analysis as shown in Table 3.4. The coarse breakup will suffice for simple problems involving more or less uniform stress behavior. A

TABLE 3.4

INTEGRATION POINT BREAKUP SCHEME

INUM	ANALYSIS TYPE	K ANALYSIS			LIFE ANALYSIS
		Two-Dimensional	Three-Dimensional[1]		(2-D or 3-D)
		INKX	INKX	INKY	NDUB[2]
1	Coarse (0-15%)[3]	5	3	9	2
2	Standard (0-6%)	15	6	18	4
3	Refined (0-3%)	30	12	36	8

[1] Grid breakup per quadrant. The parameters INKX and INKY are internal to the program described in the Programmer's Guide.

[2] NDUB may be input directly by the user; the default values listed are used when NDUB is input as blank or zero.

[3] Range of numerical integration errors for $\bar{K}$ computation from non-negative stress fields; the high end of the range occurs rarely. Grid breakup below is not drawn to scale, being denser than shown near the crack tip.

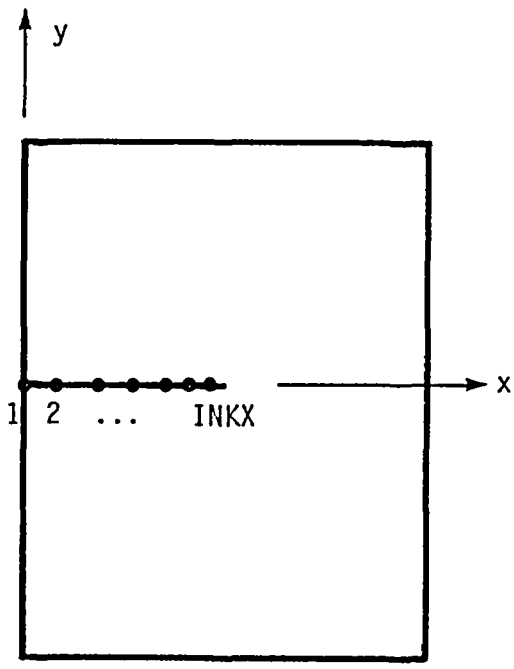

Two-Dimensional Model

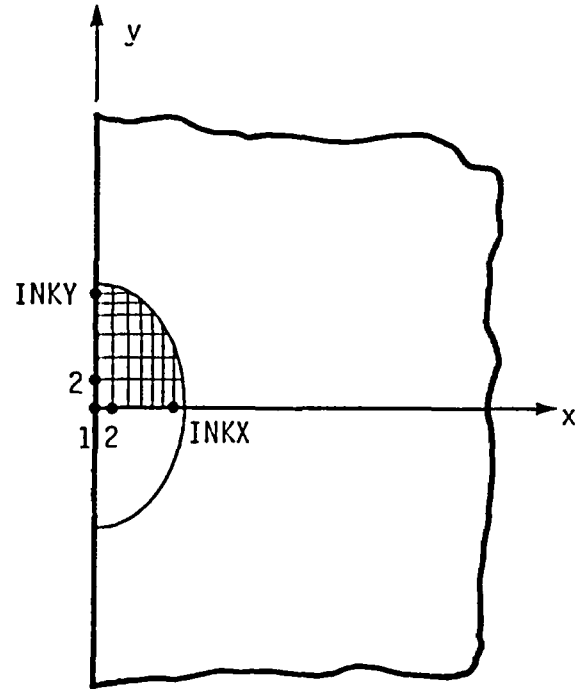

Three-Dimensional Model

standard scheme provides better accuracy than a coarse grid and will be sufficient for most problems encountered. The refined grid is for use when very high stress gradients are to be analyzed. INCL allows the user to specify either just the INUM analysis to be executed (INCL = 0), or 1 through INUM analyses to be executed (INCL = 1). This latter option will let the user compare the solutions for the different integration schemes in order to obtain a feel for the variation in accuracy and to make sure the numerical results are convergent.

3.4 Card Series C - Geometry Data

3.4.1 Card C1 - Initial Crack Dimensions

Card C1 defines the initial crack dimensions at the start of the analysis. The parameters AI(1) through AI(4) define the crack geometry for each IDOF. Refer to Section 4.0 for the definition of AI for each crack model in the library.

3.4.2 Card C2 - Body Dimensions and Crack Position

All pertinent body dimensions and crack position and orientation data is specified on the C2 card. This is accomplished using an array of eight parameters labeled G(1) through G(8). In this first production version, G(2) is not used and should be left blank. G(1) defines the body or model width, w. For crack models which are formulated for infinite bodies, G(1) will serve only to terminate the problem execution if the maximum crack depth exceeds w. G(3) through G(5) provide specific geometric input for the nozzle corner crack model (IFI = 300). G(3) is the nozzle blend radius

and G(4) and G(5) locates the crack plane in the model. Note: G(3) through G(5) are only used when IFI = 300 and should be left blank when other flaw models are selected. The remaining parameters G(6), G(7) and G(8) define the crack center position and the angular orientation in the two-dimensional crack plane. The user should refer to Section 4.0 for the required crack position data required for the flaw model selected.

3.4.3 Card Series C3 - Variable Thickness Data (NTH = 1)

Card Series C3 is a series of cards which defines the variable thickness of the body. These cards need only be used when NTH from Card B is unity. All thickness data is specified in tabular form. Card C3A is used to input the number of thickness points (NTPTS) in the table. NTPTS must be greater than unity. The next card (C3B) defines an x coordinate, XTH(N), and the corresponding body thickness, THK(N). Card C3B is repeated until the table is completed (N = 1 to NTPTS).

3.5 Card Series D - Material Properties Data

3.5.1 Card D1 - Material Toughness and Equational Parameter Card

Card D1 defines the material toughness (XKIC), and the da/dN parameters (C, XN, and RRATIO) when IDADN = 1, 3, or 4 from Card B. If IDADN = 1, a Paris' rule as discussed in Section 2.4 is used to compute the crack growth rate using parameter C and XN from

$$DADN = C\,(DK)^{XN}. \qquad (3.1)$$

Figure 3.1 illustrates the Paris rule relation for Eq. (3.1). When IDADN = 3 or 4, a Forman's rule is used to compute da/dN which is also discussed in Section 2.4. For IDADN = 3, the parameters C and XN are specified from R = 0 data and Forman's rule is used to predict da/dN for R ≠ 0 from

$$\text{DADN} = \frac{\text{C (DK)}^{\text{XN}}}{\text{XKIC (1-R) - DK}}, \tag{3.2}$$

as shown in Fig. 3.2. Another variation of Forman's rule (IDADN = 4) allows the user to input R ≠ 0 data. For this situation, the parameters C and XN are determined by the user from the data where R is specified as RRATIO(1). Forman's rule is used to ratio da/dN to other values of R from

$$\text{DADN} = \frac{\dfrac{\text{C (DK)}^{\text{XN}}}{\text{XKIC (1-R) - DK}}}{\dfrac{}{\text{XKIC (1-RRATIO(1)) - DK}}}, \tag{3.3}$$

as shown in Fig. 3.3.

3.5.2 Card D2 - Crack Growth Rate Data

Cards D2A and D2B are used only when IDADN = 2, 5, or 6 for inputting da/dN versus ΔK tabular points directly. For IDADN = 2, NR = 1 and the user is to specify a single table of da/dN points. Figure 3.4 illustrates the type of input required for this option. The Paris relation, Eq. (3.1) is used to interpolate between points and to extrapolate outside the tabular range. The local parameters C(I) and XN(I) are computed piecewise in BIGIF, for the linear line segments between the tabular entries. Extrapolation on the low or high end of the data is accomplished using the C(1) and XN(1) or C(NDK-1) and XN(NDK-1) values respectively, computed from the first two or last two DADN vs. DK points respectively.

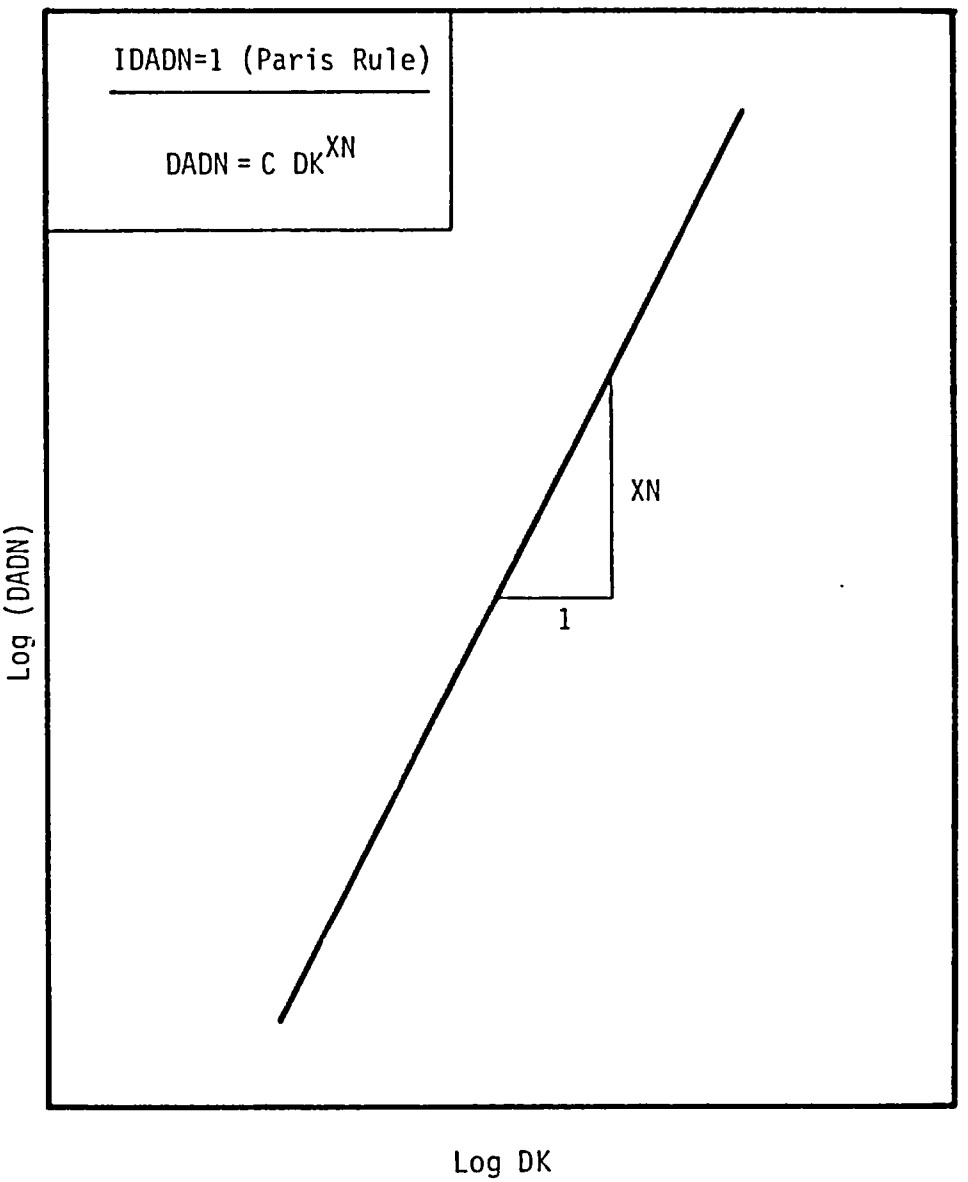

Figure 3.1 - Paris Rule Equational Form For IDADN=1.

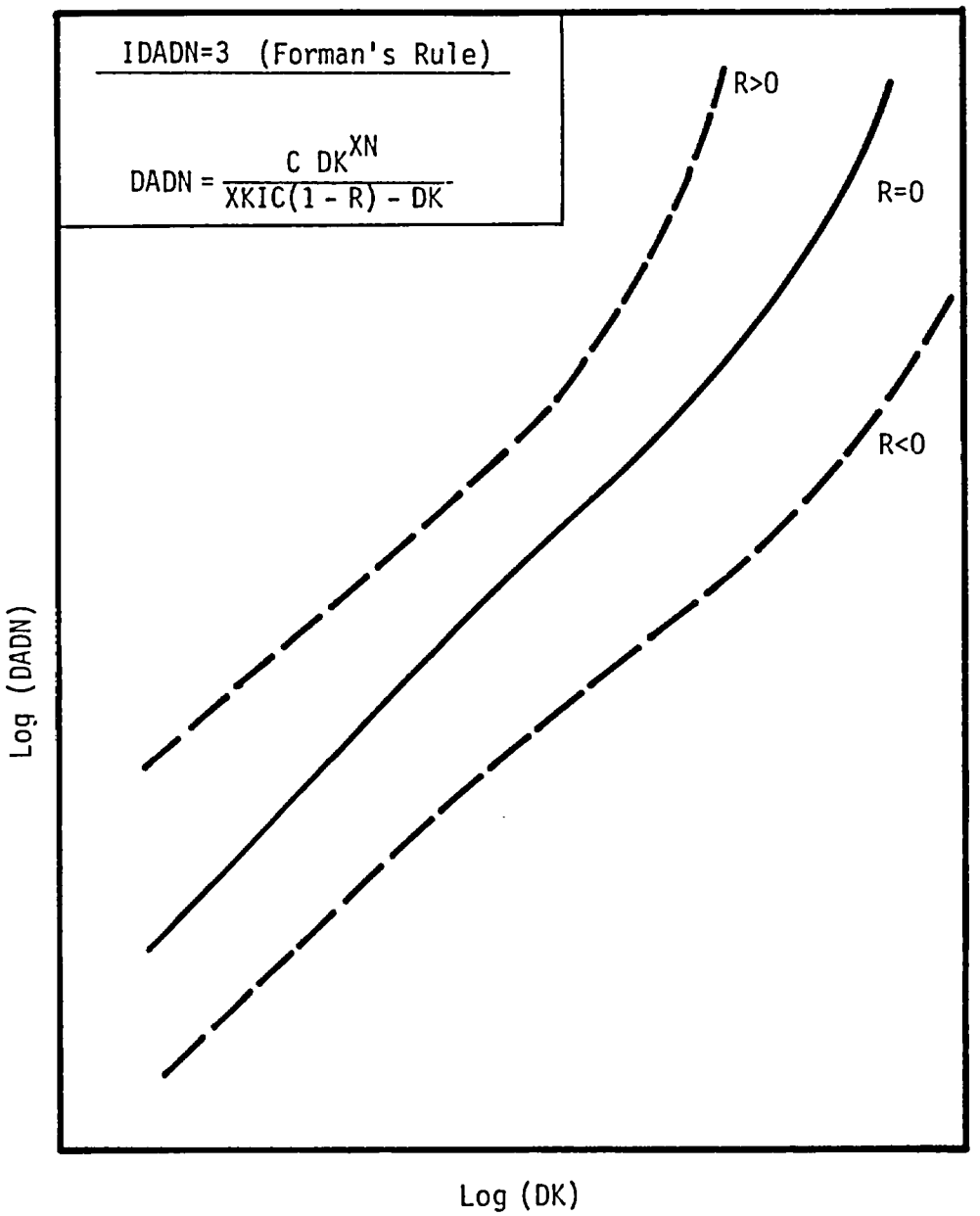

Figure 3.2 - Forman's Rule Equational Form at R=0 (IDADN=3)

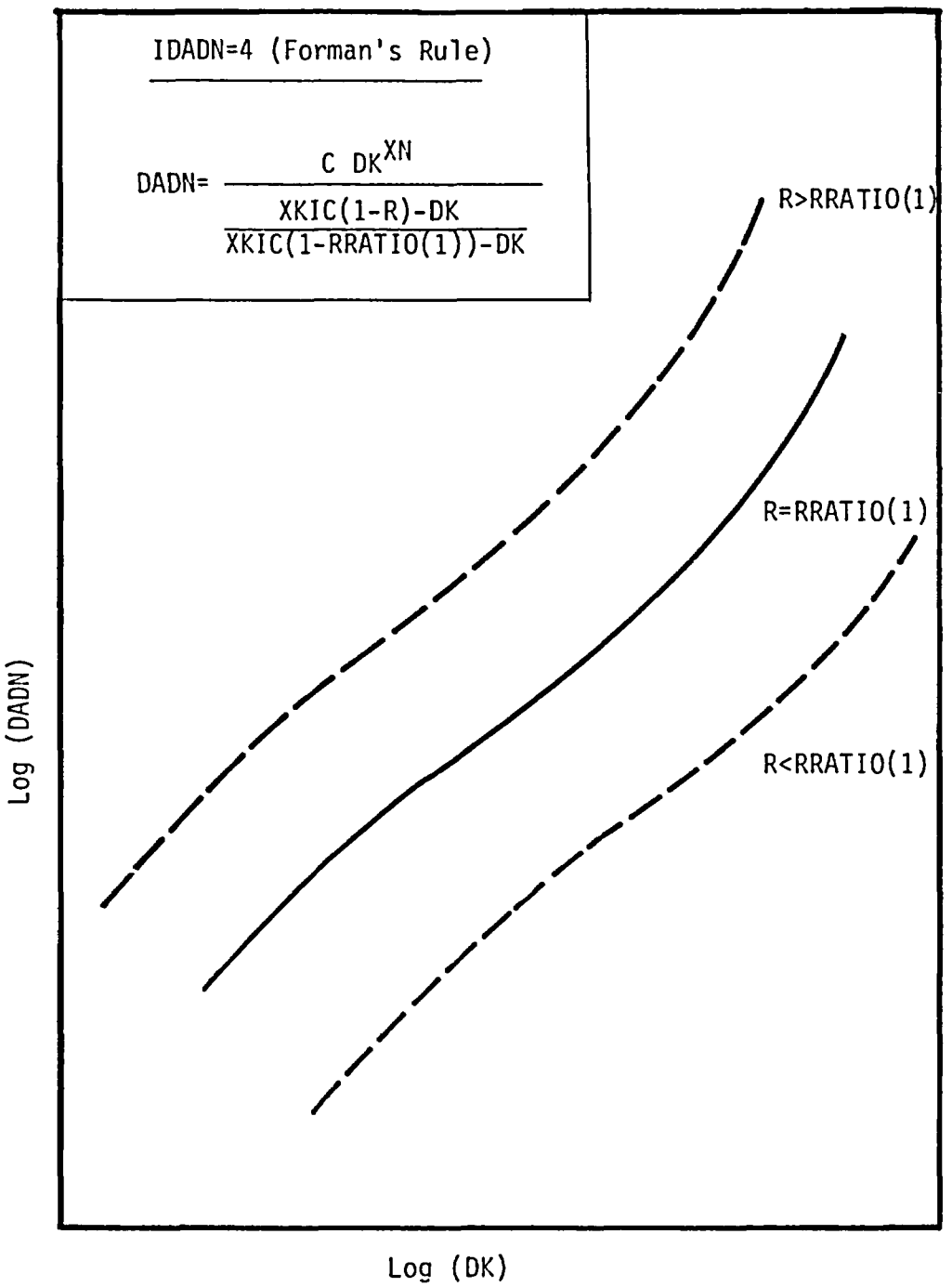

Figure 3.3 - Forman's Rule Equational Form, R=RRATIO(1) (IDADN=4)

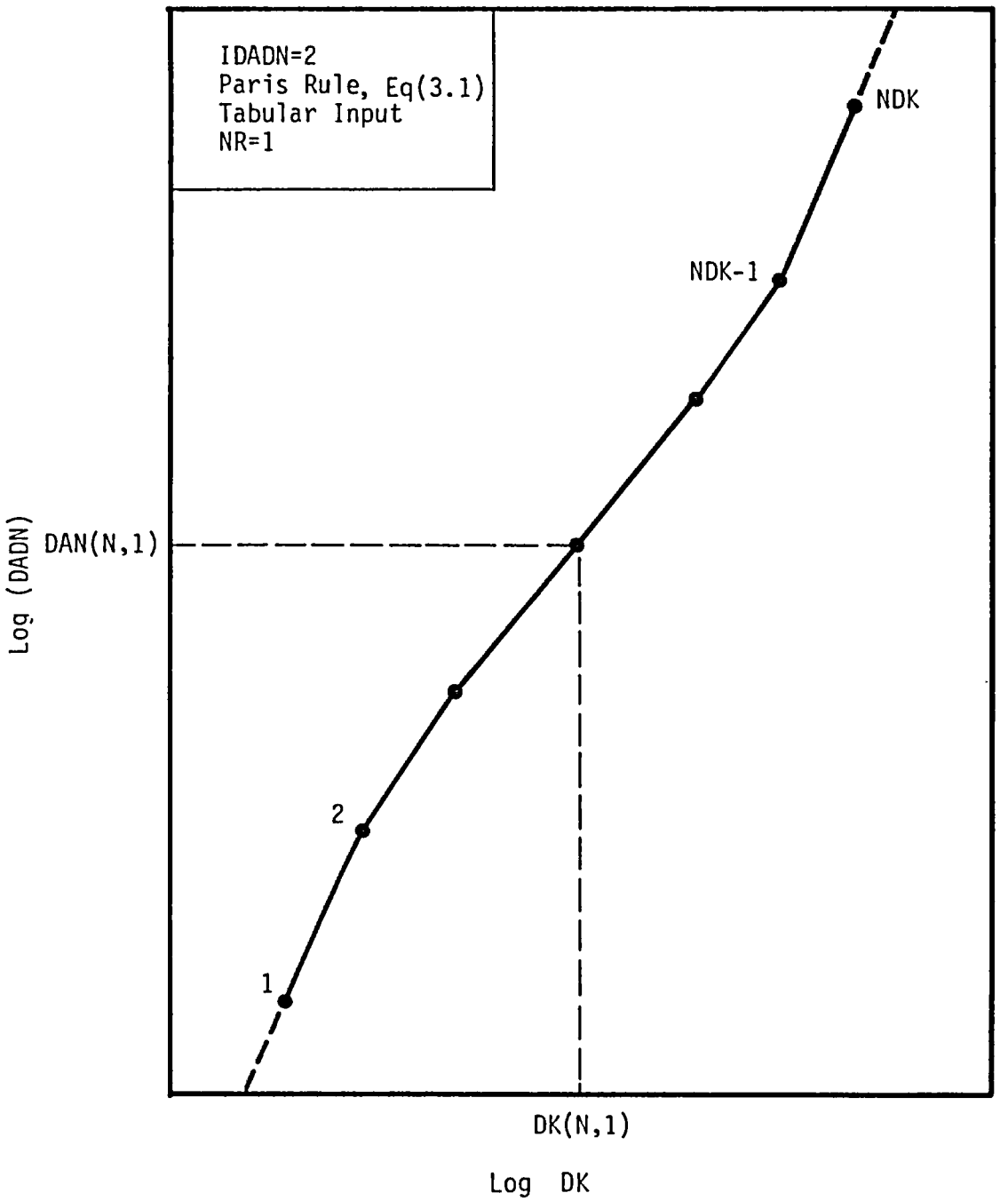

Figure 3.4 - Paris Rule Single Tabular Form (IDADN=2).

When IDADN = 5, or 6, the same general input scheme is followed where Figs. 3.5 and 3.6 illustrate the procedure. For the case of IDADN = 5, NR = 1 and a single table of DAN(NDK,1) versus DK(NDK,1) points is specified for a R = RRATIO(1) as shown in Fig. 3.5. Crack growth rate is computed by interpolation between DK values within the table, and extrapolation on DK and RRATIO using Forman's rule of Eq. (3.3). The parameters C(I) and XN(I) in Eq. (3.3) are computed piecewise in the program for the segments between the tabular entries. Similarly, extrapolation on the low or high end of the table is accomplished using the piecewise computed C and XN values determined from the first two or last two tabular entries respectively. When IDADN = 6, up to NR tabular sets, i.e., DAN(NDK,NR) versus DK(NDK,NR), can be specified with Forman's rule, Eq. (3.3), used internally in the program to interpolate between tabular points and for extrapolation outside the tabular range for DK and RRATIO. Figure 3.6 shows schematically the input for this da/dN option. Card D2B is repeated NDK-1 times to complete the data input for each NR table. Card Set D2 is repeated NR-1 times where the current limit is $1 \leq NR \leq 5$.

3.6 Card E - Transient Cycle Spectrum

3.6.1 Card E1 - Transient Description Card

For all NTRAN transients, an E1 card is required which allows the user to provide a 28 character alphanumeric title, TRANID(NT). A transient is defined as a group of constant amplitude cycles and the number of load cycles per transient is defined as DBK. A discussion of fatigue cycle definitions used in BIGIF is given in Section 2.5. A simple example of

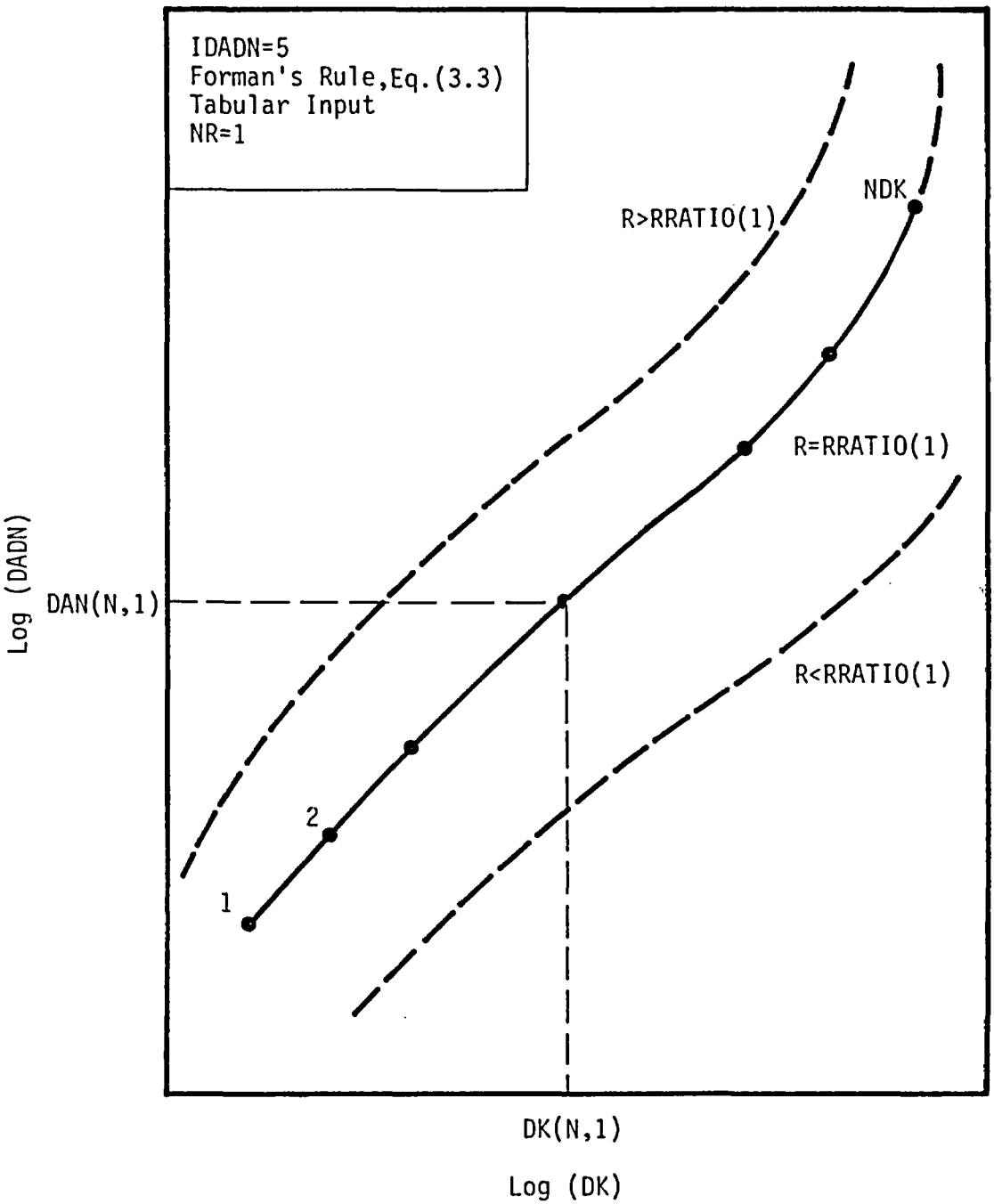

Figure 3.5 - Forman's Rule Single Tabular Input, (IDADN=5).

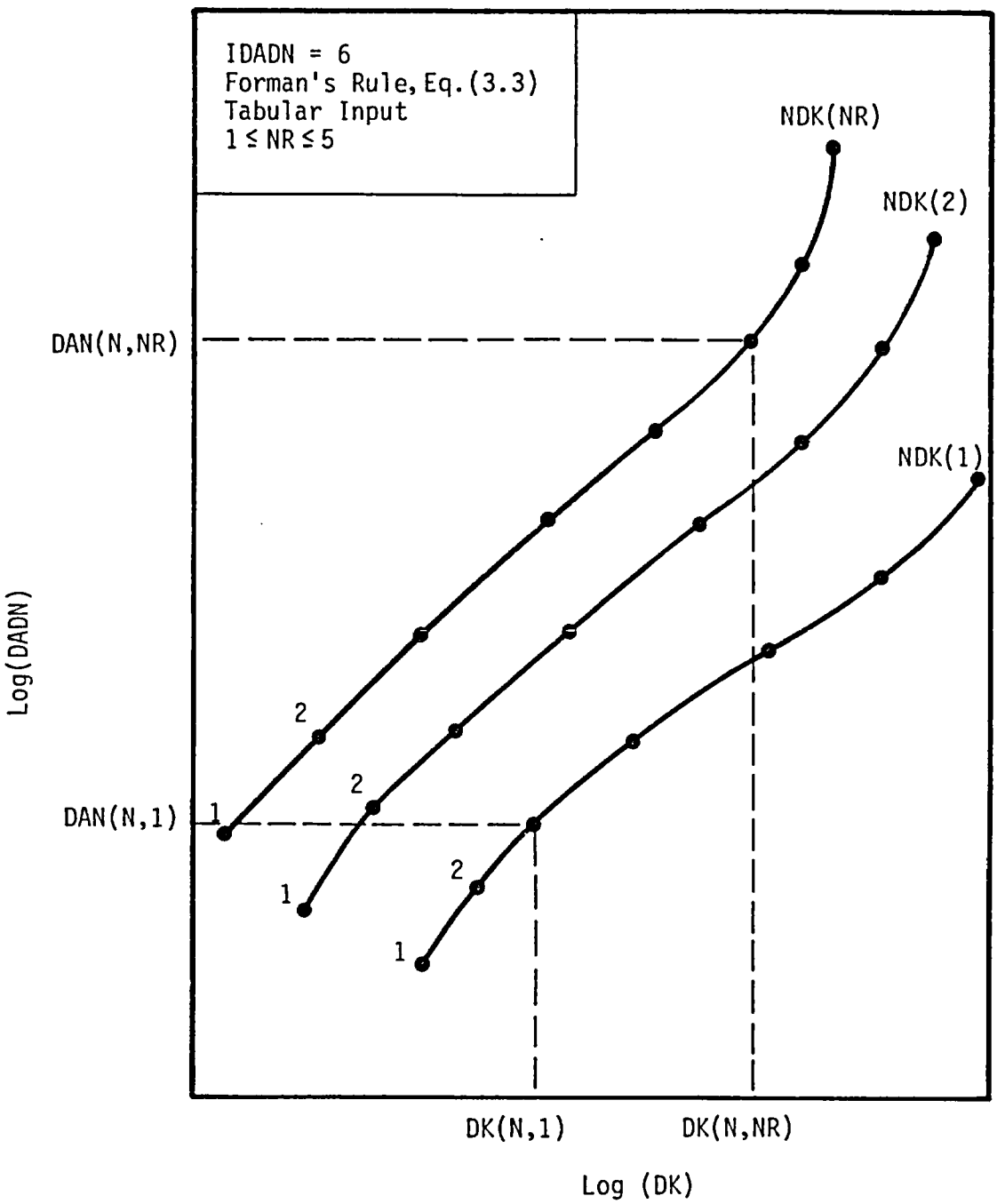

Figure 3.6 - Forman's Rule Multi-Tabular Input (IDADN=6).

a problem involving four transients which illustrates the physical meaning of DBK is shown in Fig. 3.7. A repeatable group of transients is defined as one block, N, and the number of blocks required to grow the flaw is computed from Eq. (2.5). The crack growth rate per block is computed by summing the crack growth rates in each cycle in the block, a form of linear cumulative damage law.

3.6.2 Cards E2A, E2B, and E2C - Cycle Definition Cards

For each transient, two sets of E2 cards are required to define the stress cycle. Card E2A is the fatigue cycle definition card. The meaning of the first parameter, AGLD, depends on the value of the next two parameters IPSRD and IPLD. The primary function of AGLD is to serve as a simple multiplying or scaling factor to ratio up or down the stress or K input. The parameter IPSRD defines which fatigue cycle component will be specified on this card. IPSRD can take on integer values from 0 to 4 corresponding to K_{max}, K_{min}, ΔK, R, or K_{mean} respectively. Except when IPSRD = 3, IPLD specifies the way either K_{max}, K_{min}, ΔK, or K_{mean} will be determined. When IPSRD = 3, then this E2A card will be used to specify a constant R ratio which will be set equal to AGLD.

The parameter IPLD is an index for specifying any one of eight possible stress field or K-input schemes. A summary of the IPLD options is given in Table 3.5. When IPLD = 1, 2, or 3, the K description defined by IPSRD will be computed using a stress field equation as listed in Table 3.5. The Q parameters in the equations are defined in Card E2B. For IPLD = 3, a special equation is used for $\sigma(x,y)$ based on the solution

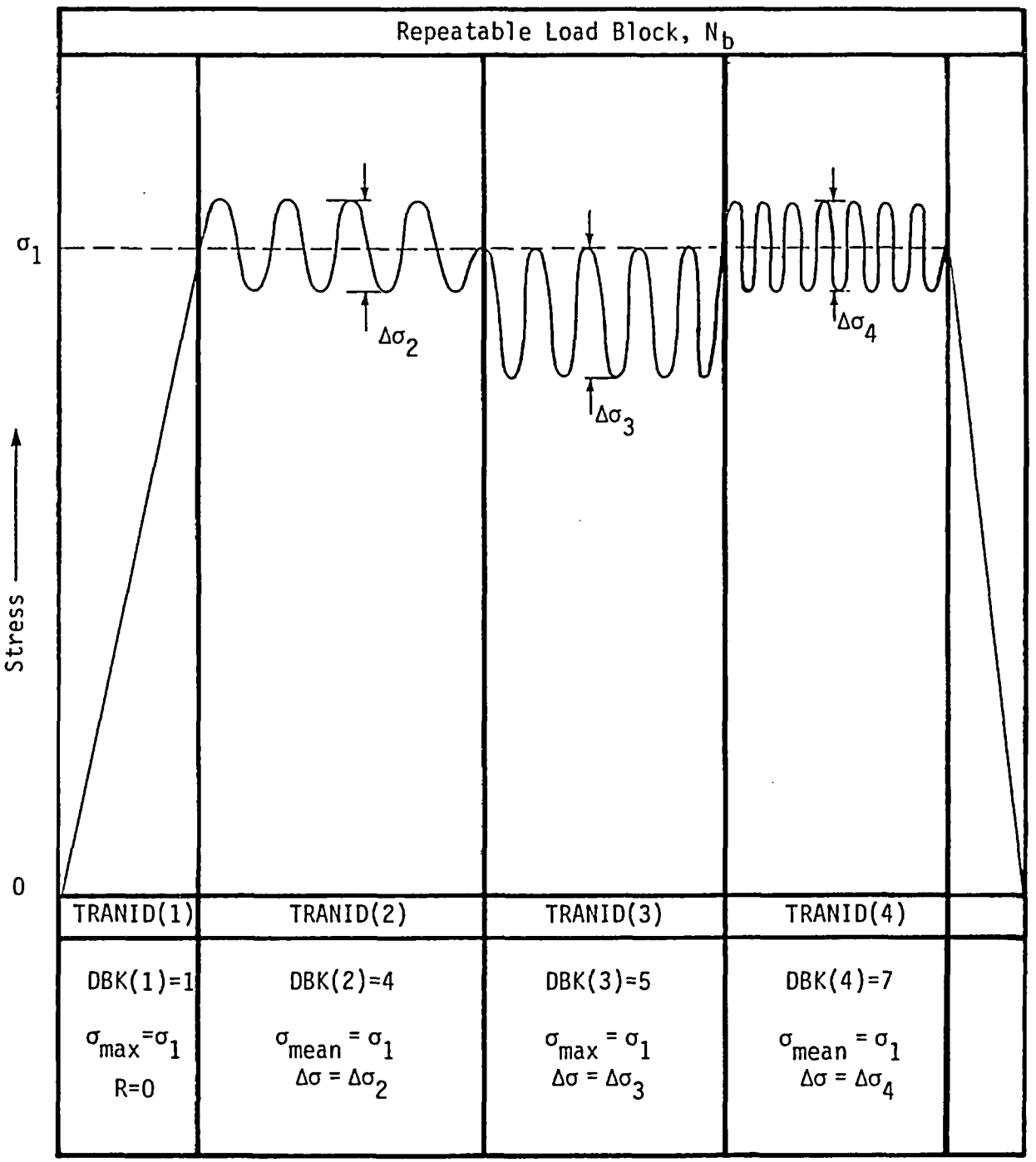

Figure 3.7 - Schematic Showing a Transient Cycle Spectrum Breakdown.

TABLE 3.5

SUMMARY OF IPLD PARAMETER OPTIONS FOR STRESS FIELD OR K INPUT IN CARD E2A

IPLD	DATA TYPE	FUNCTION	INPUT FORMAT	DESCRIPTION
0	Stress or K	See Below	None	K values to be copied from a previously specified transient.
1	Stress	$\sigma(x)$	Equational	Univariate cubic relation for $\sigma(x)$. $\sigma(x) = Q_1 + Q_2x + Q_3x^2 + Q_4x^3$.
2	Stress	$\sigma(x,y)$	Equational	Bivariate cubic relation for $\sigma(x,y)$. $\sigma(x,y) = Q_1 + Q_2x + Q_3x^2 + Q_4x^3 + Q_5y + Q_6xy + Q_7y^2 + Q_8x^2y + Q_9y^2x + Q_{10}y^3$.
3	Stress	$\sigma(x,y)$	Equational	Bivariate relation for $\sigma(x,y)$ with stress concentration option in two directions ($K_{tx} = Q_2$, $K_{ty} = Q_5$) which models the stress "die away" for a hole in a plate in tension of radius $r_x = Q_3$ and $r_y = Q_7$. $\sigma(x,y) = \left\{1 + (Q_2 - 1)\left[\frac{1}{4}\left(\frac{Q_3}{Q_3 + x}\right)^2 + \frac{3}{4}\left(\frac{Q_3}{Q_3 + x}\right)^4\right] + (Q_5 - 1)\left[\frac{1}{4}\left(\frac{Q_7}{Q_7 + y}\right)^2 + \frac{3}{4}\left(\frac{Q_7}{Q_7 + y}\right)^4\right]\right\} Q_1$ NOTE: Q_4 and Q_6 are not used.
4	Stress	$\sigma(x)$	Tabular	Linear interpolation stress table for $\sigma(x)$.
5	Stress	$\sigma(x,y)$	Tabular	Bilinear interpolation stress table for $\sigma(x,y)$.
6	K	K(a)	Tabular	Linear interpolational K versus a table. This option will overrule the K solution specified by IFI with IDOF = 1. This option should not be used if IDOF > 1.
7	K	K(a)	None	K calculated from a the special library of simple K formulas. (Use only if IFI ≡ 100 series flaw models.)

for the stress distribution, $\sigma(x)$, for a hole of radius Q_3 in a plate in tension. The equation for $\sigma(x,y)$ is constructed by using the $\sigma(x)$ solution for the hole problem in the two directions (x,y), and by allowing two different stress concentration effects, one in the x direction ($K_{tx} = Q_2$) and one for y ($K_{ty} = Q_5$). If the user leaves the Q_5 field blank, BIGIF assumes that no y-gradient exists and sets $Q_5 = 1$.

Two tabular stress inputs, one for a one-dimensional array $\sigma(x)$ (IPLD = 4), and another for a two-dimensional array $\sigma(x,y)$ (IPLD = 5) are provided for stress distributions which do not lend themselves to the equational format. For all tabular input, the table array size is specified by NPX and NPY. In addition to tabular stress, a tabular input for K(a) is also allowed (IPLD = 6). This feature will allow the user to input a K solution directly. This option will override the IFI flaw model K calculations for that transient for which IPLD = 6 was specified. The IPLD = 6 option, however, can only be used for IDOF = 1 crack models. Finally, IPLD = 7 is used only when IFI is defined for one of the 100 series flaw model. For this case, σ_{zz} in the flaw model is equal to AGLD.

A special input shortcut for the case when any particular transient K value appears more than once in the load block, can be used by specifying IPLD = 0. For this situation, the parameters KAME and IWO are used to locate the data of a previously specified transient for use in specifying the current E2 Card information. The previously defined transient number (KAME), and either the first (IWO = 1) or the second (IWO = 2) E2A Card from transient number KAME is all that is needed to locate the data. The items which will be used from the current E2A Card are AGLD, which will allow scaling

of the stress or K data from transient description (KAME, IWO), and IPSRD which will reassign this stress or K data for the computation of a different cyclic parameter. For example, as illustrated in Fig. 3.7, the transient description for K_{max} in the first transient (IPSRD = 0) could be copied for use in the next transient but redefined as K_{mean} (IPSRD = 4). As illustrated in Fig. 3.7, this feature allows the maximum K of one transient to serve as the mean K for another transient, and this option can be repeated as many times as necessary in specifying all the transient information in the loading block.

As mentioned earlier, all equational input for Q_i is accomplished with the E2B Card. Card E2B is not used if IPLD > 3. All tabular input for stress or K distribution data is done with Card E2C, and this card should only be used when IPLD = 4, 5, or 6. For one-dimensional tables (IPLD = 4, 6), a total of NPX cards are required. When a two-dimensional table is specified (IPLD = 5), a total of NPX times NPY cards are required to complete the table.

3.7 Card F - Job Termination Card

To ensure that all input for the problem is completed, the program will check the last card in the input stream for the word FINIS typed in the first five card columns. If this card is left out, the problem will not be run. Additional problems (Cards A through F) can be stacked for multiple job running.

APPENDIX A

BIGIF INPUT DESCRIPTION

This Appendix summarizes the detailed card input description of Section 3.0. It affords the user complete but abbreviated input instructions that can be utilized at a keypunch machine or computer terminal, without the need of the complete User's Manual.

CARD A - TITLE CARD

PARAMETER	TYPE	CARD COLUMNS	DESCRIPTION
TITLE (20)	ALPHANUMERIC	1-80	Job title card, 80 characters

CARD B - PROBLEM CONTROL CARD

PARAMETER	TYPE	CARD COLUMNS	DESCRIPTION
IFAT	INTEGER	5	Analysis selection 0 = Single K calculation 1 = Fatigue analysis
NTRAN	INTEGER	9-10	Number of distinct constant amplitude transients (20 maximum)
IFI	INTEGER	11-15	Crack model geometry index number
IDOF	INTEGER	16-20	Number of degrees of freedom (i.e., crack growth directions) for the crack model
NTH	INTEGER	25	Variable thickness specification 0 = Constant thickness 1 = Variable thickness
IDADN	INTEGER	30	Crack growth rate rule (Default = 1) 1 = Calculate da/dN using a Paris rule ($da/dN = C\Delta K^n$) 2 = Calculate da/dN from a table of data points (da/dN vs ΔK). Paris rule is used to interpolate between data points and for extrapolation outside the tabular range. 3 = Calculate da/dN using a Forman's Rule ($da/dN = C\Delta K^n / ((1-R) K_{IC} - \Delta K)$). 4 = Calculate da/dN using a Paris Rule given C, n for a specific value of R. Forman's Rule is used to ratio da/dN to other values of R. 5 = Calculate da/dN using Forman's Rule where a table of data points (da/dN vs. ΔK) for a single value of R is used to define C and n piecewise (between input points). Forman's Rule is used to ratio da/dN to other values of R. 6 = Calculate da/dN from a table of data points. Forman's Rule is used to interpolate between data points and for extrapolation outside the tabular range of R values.

PARAMETER	TYPE	CARD COLUMNS	DESCRIPTION
NR	INTEGER	34-35	Number of da/dN data sets to be specified on the D2 cards (set NR = 0 or leave blank if IDADN = 1, 3, or 4)
INUM	INTEGER	40	Integration increment scheme (Default = 1) 1 = Coarse integration scheme 2 = Standard 3 = Refined
INCL	INTEGER	45	Inclusive analysis option 0 = Perform only INUM analysis 1 = Perform 1 through INUM analysis, inclusively
NDUB	INTEGER	49-50	Number of crack growth increments to double the crack size. If NDUB = 0, the crack growth increment defaults to the following values depending on INUM: If INUM = 1 (Coarse), NDUB = 2 = 2 (Standard), NDUB = 4 = 3 (Refined), NDUB = 8 NDUB must be non-negative.

CARD SERIES C - GEOMETRY DATA

CARD C1 - Initial Crack Dimensions

PARAMETER	TYPE	CARD COLUMNS	DESCRIPTION
AI(1)	REAL	1-10	Initial crack size for the first degree of freedom (DOF) variable
AI(2)	REAL	11-20	Initial crack size for the second degree of freedom (DOF) variable
AI(3)	REAL	21-30	Initial crack size for the third degree of freedom (DOF) variable
AI(4)	REAL	31-40	Initial crack size for the fourth degree of freedom (DOF) variable

CARD C2 - Body Dimensions and Crack Position

PARAMETER	TYPE	CARD COLUMNS	
G(1)	REAL	1-10	Body width, w
G(2)	REAL	11-20	
G(3)	REAL	21-30	Nozzle blend radius, r_b (IFI = 300)
G(4)	REAL	31-40	Crack origin locator (IFI = 300)
G(5)	REAL	41-50	Crack origin position (IFI = 300)
G(6)	REAL	51-60	x Coordinate to crack center, x_c
G(7)	REAL	61-70	y Coordinate to crack center, y_c
G(8)	REAL	71-80	Crack orientation angle, ϕ (degrees)

CARDS C3A and C3B - Variable Thickness Data (USE ONLY IF NTH = 1)

CARD C3A - Selection of Thickness Data Input

PARAMETER	TYPE	CARD COLUMNS	DESCRIPTION
NTPTS	INTEGER	1-5	Number of tabular points defining thickness variation versus width (NTPTS > 1).

CARD C3B - Thickness Table Input

PARAMETER	TYPE	CARD COLUMNS	DESCRIPTION
XTH(N)	REAL	1-10	x Coordinate for specified thickness
THK(N)	REAL	11-20	Specified Thickness

(Repeat Cards C3B for N = 1 to NTPTS)

CARD SERIES D - MATERIAL PROPERTIES DATA

CARD D1 - Material Toughness and Equational Parameter Card

PARAMETER	TYPE	CARD COLUMNS	DESCRIPTION
XKIC	REAL	1-10	Static fracture toughness
C	REAL	11-20	Constant in da/dN rule (leave blank if IDADN = 2, 5, or 6)
XN	REAL	21-30	Exponent in da/dN rule (leave blank if IDADN = 2, 5, or 6)
RRATIO(1)	REAL	31-40	R ratio (leave blank if IDADN $\neq$ 4)

CARDS D2A and D2B - Crack Growth Rate Data (Use Only if IDADN = 2, 5, or 6)

CARD D2A - R-Ratio Specification and Table Size

PARAMETER	TYPE	CARD COLUMNS	DESCRIPTION
RRATIO(NR)	REAL	1-10	R ratio for the da/dN vs ΔK data to follow (not used when IDADN = 2)
NDK(NR)	INTEGER	11-15	Number of data points for the da/dN vs ΔK data table. $2 \leq$ NDK(NS) ≤ 20

CARD D2B - da/dN Table Input

PARAMETER	TYPE	CARD COLUMNS	DESCRIPTION
DK(1,NR)	REAL	1-10	The first value of ΔK in the da/dN vs ΔK table
DAN(1,NR)	REAL	11-20	The first value of da/dN in the da/dN vs ΔK table

Repeat Card D2B NDK(NR) - 1 times, i.e., total number of D2B cards is NDK(NR).

Repeat Card Set D2 (Card D2A and Card D2B) NR-1 times where $1 \leq$ NR ≤ 5.

CARD E - TRANSIENT CYCLE SPECTRUM

CARD E1 - Transient Description Card

PARAMETER	TYPE	CARD COLUMNS	DESCRIPTION
TRANID(NT)	ALPHANUMERIC	1-28	Title heading for the transient
DBK	REAL	31-50	Number of load cycles per block N

CARD E2 - Cycle Definition Cards (Two Sets of E2 Cards Per Transient)

CARD E2A - Fatigue Cycle Definition Card

PARAMETER	TYPE	CARD COLUMNS	DESCRIPTION
AGLD(1)	REAL	1-10	If IPSRD(1) $\neq$ 3 and/or IPLD(1) $\neq$ 7, the value of AGLD(1) is a directly multiplying factor or scaling factor to the stress equation or table, or K(a) table. If IPLD(1) = 7, AGLD(1) is used in the K equation as $K = AGLD(1)F\sqrt{\pi a}$. When IPSRD(1) = 3, then AGLD(1) specifies the value of R ratio, i.e., R = AGLD(1).
IPSRD(1)	INTEGER	15	Definition of first fatigue cycle parameter to be determined from user specified stress equations or tables, K vs a equations or tables, or from previously defined transient cycles. 0 = K_{max} to be determined from user-specified data 1 = K_{min} to be determined from user-specified data 2 = ΔK to be determined from user-specified data 3 = Constant R ratio to be specified by user. 4 = K_{mean} to be determined from user-specified data.

PARAMETER	TYPE	CARD COLUMNS	DESCRIPTION
IPLD(1)	INTEGER	20	Index defining the type of user data from which the above IPSRD(1) Quantity (K_{max}, K_{min}, etc.) to be determined from 0 = Data already specified in previous transient data; transient number is KAME(1) and cycle card IWO(1) 1 = Stress field $\sigma(x)$ which is a univariate cubic: $\sigma(x) = Q_1 + Q_2x + Q_3x^2 + Q_4x^3$ 2 = Stress field $\sigma(x,y)$ which is a bivariate cubic: $\sigma(x,y) = Q_1 + Q_2x + Q_3x^2 + Q_4x^3 + Q_5y + Q_6xy + Q_7y^2 + Q_8x^2y + Q_9y^2x + Q_{10}y^3$ 3 = $\sigma(x,y)$ which is bivariate relation based on a hole in a plate solution with a variable K_t option: $\sigma(x,y) = Q_1\left\{1+(Q_2 - 1)\left[\frac{1}{4}\left(\frac{Q_3}{Q_3 + x}\right)^2 + \frac{3}{4}\left(\frac{Q_3}{Q_3 + x}\right)^4\right] + (Q_5 - 1)\left[\frac{1}{4}\left(\frac{Q_7}{Q_7 + y}\right)^2 + \frac{3}{4}\left(\frac{Q_7}{Q_7 + y}\right)^4\right]\right\}$ 4 = Linear interpolation stress table for $\sigma(x)$ 5 = Bilinear interpolation stress table for $\sigma(x,y)$ 6 = Linear interpolation in a K(a) table 7 = K(a) calculated from a library of formulas ($K = \sigma F \sqrt{\pi a}$)
KAME(1)	INTEGER	25	If IPLD(1), = 0, KAME(1) specifies the transient number where the data is already specified (leave blank if IPLD(1) > 0)
IWO(1)	INTEGER	30	If IPLD(1) = 0, IWO(1) specifies which cycle definition card to use to specify data for this transient 1 = Use the first card from transient Number KAME(1) 2 = Use the second card from transient Number KAME(1) (Leave blank if IPLD(1) > 0)

PARAMETER	TYPE	CARD COLUMNS	DESCRIPTION
NPX	INTEGER	31-35	Number of table data points for σ or K in the x or a direction to be specified (use only if IPLD(1) = 4, 5, or 6, otherwise, leave blank)
NPY	INTEGER	36-40	Number of table data points for σ in the y direction to be specified (use only if IPLD(1) = 5, otherwise leave blank)

CARD E2B - Definition of Equational Constants for Stress, $\sigma(x)$ or $\sigma(x,y)$ (Do Not Use if IPLD(1) > 3)

PARAMETER	TYPE	CARD COLUMNS	DESCRIPTION
Q(1)	REAL	1-10	First constant in the stress equation
Q(2)	REAL	11-20	Second constant in the stress equation

Q(3), Q(4) up to Q(10) if needed to define all constants in stress equation. Two cards are required to define Q(1) through Q(10) if IPLD = 2 is used.

CARD E2C - Stress or Stress Intensity Factor Tabular Input (Necessary Only if IPLD(1) = 4, 5, or 6)

PARAMETER	TYPE	CARD COLUMNS	DESCRIPTION
CX(IX)	REAL	1-10	X or a distance in table for stress or K
CS(IX) or CY(IY)	REAL	11-20	Value of stress $\sigma(x)$, or K(a) if one dimensional table (IPLD(1) = 4,6). Value of y distance for stress if two dimensional table (IPLD(1) = 5).
CS(IX,IY)	REAL	21-30	Value of stress $\sigma(x,y)$ in bivariate table (only when IPLD(1) = 5)

Repeat Cards E2C NPX-1 times if one-dimensional table (IPLD(1) = 4,6) is specified.
Repeat Cards E2C (NPX)(NPY)-1 times if two-dimensional table (IPLD(1) = 5).

CARD F - JOB TERMINATION CARD

PARAMETER	TYPE	CARD COLUMNS	DESCRIPTION
FINIS	ALPHANUMERIC	1-5	Terminate job with the word FINIS

Card F must be the last card for the problem. Additional problems can be stacked one behind the other.

APPENDIX B

SAMPLE DATA INPUT CODING FORMS

BIGIF DATA CODING FORM 1	DATE	PAGE OF
NAME	JOB NO.	PRINT I for alpha 1 for numeric(not 1) PRINT Ø for alpha 0 for zero PRINT Z for letter Z
JOB DESCRIPTION		

A

1 10 20 30 40 50 60

TITLE(20)

B

1 5 10 15 20 25 30 35 40 45 50 61 70 80

IFAT	NTRAN	IFI	IDOF	NTH	IDADN	NR	INUM	INCL	NOUB

C1

1 11 21 31

AI(1)	AI(2)	AI(3)	AI(4)

C2

1 11 21 31 41 51

G(1)	G(2)	G(3)	G(4)	G(5)	G(6)

61 G(7) 71 G(8)

C3A

1 5

NTPTS

NOTE: USE C3A AND C3B ONLY IF NTH = 1 IN CARD B.

C3B

1 XTH(N)	11 THK(N)

NOTE: REPEAT CARD C3B NTPTS - 1 TIMES. CONTINUE ON FORM 5 IF TABLE INPUT EXCEEDS SPACE PROVIDED.

BIGIF DATA CODING FORM 2	DATE	PAGE OF
NAME	JOB NO.	PRINT I for alpha 1 for numeric (not l) PRINT Ø for alpha O for zero PRINT Z for letter Z
JOB DESCRIPTION		

D1

1 XKIC	11 C	21 XN	31 RRATIO(1)

D2A

1 RRATIO(NR)	15 NDK(NR)	NOTE: USE ONLY IF IDADN = 2, 5, or 6 IN CARD B. REPEAT CARDS D2A AND D2B NR-1 TIMES WHERE $1 \leq NR \leq 5$ CONTINUE ON FORM 5 IF NR > 1, OR IF TABLE INPUT EXCEEDS SPACE PROVIDED

D2B

1 DK(1,NR)	11 DAN(1,NR)	NOTE: REPEAT CARD D2B (NDK)(NR) - 1 TIMES. TOTAL NUMBER OF D2B CARDS IS (NDK)(NR).

BIGIF DATA CODING FORM 3A	DATE	PAGE OF
NAME	JOB NO.	PRINT I for alpha 1 for numeric(not 1) PRINT 8 for alpha 0 for zero PRINT Z for letter Z
JOB DESCRIPTION		

E1

1 TRANID(NT) 31	DBK(NT)

E2A

1 AGLD	15 IPSRD	20 IPLD	25 KAME	30 IWO	35 NPX	40 NPY	NOTE: FIRST OF TWO E2 CARD SERIES. USE FORM 3B FOR SECOND SERIES.

E2B

1 Q(1)	11 Q(2)	21 Q(3)	31 Q(4)	41 Q(5)	51 Q(6)
61 Q(7)	71 Q(8)	NEW E2B CARD →	1 Q(9)	11 Q(10)	NOTE: DO NOT USE ANY E2B CARDS IF IPLD > 3

E2C

1 CX(IX)	11 CS(IX) OR CY(IY)	21 CS(IX,IY)	NOTE: USE ONLY IF IPLD > 3. REPEAT CARD E2C NPX-1 TIMES IF ID TABLE IPLD = 4,6) OR (NPX) (NPY) - 1 TIMES IF 2D TABLE (IPLD = 5) CONTINUE ON FORM 5 IF TABLE INPUT EXCEEDS SPACE PROVIDED.

BIGIF CODING FORM 3B	DATE	PAGE OF
NAME	JOB NO.	PRINT I for alpha 1 for numeric(not 1) PRINT Ø for alpha 0 for zero PRINT Z for letter Z
JOB DESCRIPTION		

E2A

1	15	20	25	30	35	40	
AGLD	IPSRD	IPLD	KAME	IWO	NPX	NPY	NOTE: SECOND E2 CARD SERIES

E2B

1	11	21	31	41	51
Q(1)	Q(2)	Q(3)	Q(4)	Q(5)	Q(6)
61 Q(7)	71 Q(8)	NEW E2B CARD →	1 Q(9)	11 Q(10)	NOTE: DO NOT USE ANY E2B CARDS IF IPLD > 3

E2C

1 CX(IX)	11 CS(IX) or CY(IY)	21 CS(IX,IY)	NOTE: USE ONLY IF IPLD > 3. REPEAT CARD E2C NPX-1 TIMES IF 1D TABLE (IPLD = 4,6) OR (NPX) (NPY) - 1 TIMES IF 2D TABLE (IPLD = 5) CONTINUE ON FORM 5 IF TABLE INPUT EXCEEDS SPACE PROVIDED.

BIGIF DATA CODING FORM 4	DATE	PAGE OF
NAME	JOB NO.	PRINT I for alpha 1 for numeric(not 1) PRINT Ø for alpha 0 for zero PRINT Z for letter Z
JOB DESCRIPTION		

F

5

F	I	N	I	S
FINIS				

NOTE: MUST BE LAST CARD FOR THE PROBLEM IN THE INPUT DATA DECK.

MODEL NOTES:

BIGIF DATA CODING FORM 5	DATE	PAGE OF
NAME	JOB NO.	PRINT I for alpha 1 for numeric(not 1) PRINT O for alpha 0 for zero PRINT Z for letter Z
JOB DESCRIPTION		

C3B, D2B OR E2C

1	11	21

NOTE: FOR USE WHEN TABULAR INPUT FOR C3B, D2B, OR E2C EXCEEDS SPACE PROVIDED ON FORMS 1 THROUGH 4.

APPENDIX C

PROBLEM OUTPUT FOR EXAMPLE ANALYSES

C.1 Example 1 - Simple Edge Crack in an Unnotched Plate Under Tension

C.2 Example 2 - Through-Cracks in Notched Structures

C.3 Example 3 - Fatigue Analysis of a Weld Crack

C.4 Example 4 - Pressure Vessel Nozzle Corner Crack Under Two Loading Transients

APPENDIX C.1: Example 1 - Simple Edge Crack in an Unnotched Plate Under Tension

```
BIGIF:  BOUNDARY INTEGRAL EQUATION        EXAMPLE 1A - EDGE CRACK UNDER UNIFORM STRESS (NON-IF,IFI=102)        PMB10JAN78
        GENERATED INFLUENCE FUNCTIONS
        FOR USE IN FRACTURE MECHANICS
        PROBLEMS

A "->" MARKS THE OPTION SELECTED

        ANALYSIS SELECTION (IFAT)

              0 SINGLE K CALCULATION
          ->  1 FATIGUE ANALYSIS

        CRACK GEOMETRY MODEL INDEX NUMBER (IFI)

              0 K VALUES KNOWN, NO IF CALC.
            101 K = SIGMA*SQRT(PI*A)
          -> 102 K = 1.12* SIGMA* SQRT(PI*A)
            201 CENTER CRACKED PANEL, MODE I
            202 CENTER CRACKED PANEL, MODE II
            203 CENTER CRACKED PANEL, MODE III
            204 EDGE CRACK, MODE I
            205 EDGE CRACK, MODE II (INACTIVE)
            206 EDGE CRACK, MODE III (INACTIVE)
            207 SNOW PLAY (INACTIVE)
            300 NOZ BLEND RADIUS CORNERCRACK
            301 BURIED CIRCULAR CRACK
            302 SURFACE 1/2 CIRCULAR CRACK
            303 SURFACE 1/4 CIRCULAR CRACK
            304 4-DOF BURIED CRACK
            305 3-DOF SURFACE CRACK
            306 2-DOF CORNER CRACK


        VARIABLE THICKNESS SPECIFICATION (NTH)

          ->  0 CONSTANT BODY THICKNESS
              1 VARIABLE BODY THICKNESS


        CRACK GROWTH RATE RULE (IDADN)

          ->  1 PARIS RULE, INPUT C,XN (DEFAULT)
              2 INPUT TABULAR DA/DN, DELTA-K DATA
              3 FORMAN RULE, INPUT C,XN FOR EXPECTED R
              4 FORMAN RULE, INPUT C,XN AND R
              5 INPUT TABULAR DA/DN,DELTA-K DATA AND R
              6 SAME AS #5 BUT FOR UP TO FIVE R VALUES


        INTEGRATION INCREMENT SCHEME (INUM)

              1 COARSE INTEGRATION SCHEME (DEFAULT)
          ->  2 STANDARD
              3 REFINED


        SINGLE OR MULT INTEGRATION SCHEMES (INCL)

          ->  0 SINGLE
              1 MULTIPLE
```

INCREMENTS USED TO DOUBLE CRACK SIZE (NDUB)

COARSE = 2
-> STANDARD = 4
REFINED = 8

NUMBER OF DEGREES OF FREEDOM = 1

INITIAL A-VALUES FOR EACH DEGREE OF FREEDOM

CRACK LENGTH AI(1) = 0.50000E-02

GEOMETRY FACTORS

G(1)	0.10000E+04	BODY WIDTH
G(2)	0.0	
G(3)	0.0	
G(4)	0.0	
G(5)	0.0	
G(6)	0.0	X-COORD. TO CRACK CENTER (XC)
G(7)	0.0	Y-COORD. TO CRACK CENTER (YC)
G(8)	0.0	CRACK ORIENTATION ANGLE (PHI, DEGREES)

DA/DN OPTION SELECTED: 1

KIC =	0.65000E+02	FRACTURE TOUGHNESS
C =	0.45000E-09	COEFFICIENT
XN =	0.28000E+01	EXPONENT
AT R =	0.0	

LOAD TRANSIENTS: 1 TRANSIENT(S) IN PROBLEM EXAMPLE 1A - EDGE CRACK UNDER UNIFORM STRESS (NON-IF,IFI=102) PMB10JAN78

NUMBER	NAME	NUMBER OF CYCLES PER BLOCK	SPECIFIER	AGLD	IPSRD	IPLD	KAME	IWO	NPX	NPY
1	ONLY TRANSIENT	0.10000E+01	1	0.70000E+02	0	7	0	0	0	0
			2	0.0	1	7	0	0	0	0

DETAILED OUTPUT FOR ALL LOAD TRANSIENT(S) AND CRACK DEGREE(S) OF FREEDOM

INTEGRATION BREAKUP ********** * STANDARD * ********** EXAMPLE 1A - EDGE CRACK UNDER UNIFORM STRESS (NON-IF,IFI=102) PMB10JAN78

TRANSIENT NUMBER	DEGREE OF FREEDOM	CYCLES /BLOCK	KMAX	KMIN	KMEAN	DEL-K	R-RAT	TRANSIENT DA/DN (PER CYCLE)	DA/DN (PER BLOCK)	DOF CRACK SIZE	N
1	1	1.000	9.84	0.0	4.92	9.84	0.0	.2713E-06	.271E-06	.500E-02	.0
1	1	1.000	10.73	0.0	5.36	10.73	0.0	.3458E-06	.346E-06	.595E-02	3066.
1	1	1.000	11.70	0.0	5.85	11.70	0.0	.4408E-06	.441E-06	.707E-02	5926.
1	1	1.000	12.76	0.0	6.38	12.76	0.0	.5618E-06	.562E-06	.841E-02	8595.
1	1	1.000	13.91	0.0	6.96	13.91	0.0	.7160E-06	.716E-06	.100E-01	.1109E+05
1	1	1.000	15.17	0.0	7.59	15.17	0.0	.9126E-06	.913E-06	.119E-01	.1341E+05
1	1	1.000	16.55	0.0	8.27	16.55	0.0	.1163E-05	.116E-05	.141E-01	.1558E+05
1	1	1.000	18.05	0.0	9.02	18.05	0.0	.1483E-05	.148E-05	.168E-01	.1760E+05
1	1	1.000	19.68	0.0	9.84	19.68	0.0	.1890E-05	.189E-05	.200E-01	.1949E+05
1	1	1.000	21.46	0.0	10.73	21.46	0.0	.2408E-05	.241E-05	.238E-01	.2125E+05
1	1	1.000	23.40	0.0	11.70	23.40	0.0	.3070E-05	.307E-05	.283E-01	.2289E+05
1	1	1.000	25.52	0.0	12.76	25.52	0.0	.3913E-05	.391E-05	.336E-01	.2442E+05
1	1	1.000	27.83	0.0	13.91	27.83	0.0	.4987E-05	.499E-05	.400E-01	.2585E+05
1	1	1.000	30.35	0.0	15.17	30.35	0.0	.6356E-05	.636E-05	.476E-01	.2719E+05
1	1	1.000	33.09	0.0	16.55	33.09	0.0	.8101E-05	.810E-05	.566E-01	.2843E+05
1	1	1.000	36.09	0.0	18.05	36.09	0.0	.1033E-04	.103E-04	.673E-01	.2959E+05
1	1	1.000	39.36	0.0	19.68	39.36	0.0	.1316E-04	.132E-04	.800E-01	.3068E+05
1	1	1.000	42.92	0.0	21.46	42.92	0.0	.1677E-04	.168E-04	.951E-01	.3169E+05
1	1	1.000	46.80	0.0	23.40	46.80	0.0	.2138E-04	.214E-04	.113	.3263E+05
1	1	1.000	51.04	0.0	25.52	51.04	0.0	.2725E-04	.272E-04	.135	.3351E+05
1	1	1.000	55.66	0.0	27.83	55.66	0.0	.3473E-04	.347E-04	.160	.3434E+05
1	1	1.000	60.70	0.0	30.35	60.70	0.0	.4427E-04	.443E-04	.190	.3510E+05
1	1	1.000	66.19	0.0	33.09	66.19	0.0	.5642E-04	.564E-04	.226	.3582E+05
1	1	1.000	72.18	0.0	36.09	72.18	0.0	.7191E-04	.719E-04	.269	.3648E+05

1	1	1.000	78.71	0.0	39.36	78.71	0.0	.9165E-04	.917E-04	.320	.3711E+05

STRUCTURE HAS FAILED--KMAX.GT.KIC IN DADN SUBROUTINE. NEXT CRACK SIZE EXCEEDS CRITICAL CRACK SIZE.

1	1	1.000	85.84	0.0	42.92	85.84	0.0	.9165E-04	.917E-03	.381	.3723E+05

FATIGUE CRACK GROWTH ANALYSIS SUMMARY

CRACK DIMENSION(S) A(I)	ALTERNATING STRESS INTENSITY FACTOR(S) FOR FIRST INPUT LOAD TRANSIENT DELTA K(I)	TOTAL CRACK GROWTH RATE(S) DADN(I)	NUMBER OF CYCLES OR BLOCKS TO GROW CRACK FROM INITIAL SIZE N
A1	DK1	DADN1	N
0.005	9.839	0.2713E-06	.0
0.006	10.730	0.3458E-06	3066.
0.007	11.701	0.4408E-06	5926.
0.008	12.760	0.5618E-06	8595.
0.010	13.915	0.7160E-06	.1109E+05
0.012	15.174	0.9126E-06	.1341E+05
0.014	16.547	0.1163E-05	.1558E+05
0.017	18.045	0.1483E-05	.1760E+05
0.020	19.678	0.1890E-05	.1949E+05
0.024	21.459	0.2408E-05	.2125E+05
0.028	23.402	0.3070E-05	.2289E+05
0.034	25.520	0.3913E-05	.2442E+05
0.040	27.829	0.4987E-05	.2585E+05
0.048	30.348	0.6356E-05	.2719E+05
0.057	33.095	0.8101E-05	.2843E+05
0.067	36.090	0.1033E-04	.2959E+05
0.080	39.357	0.1316E-04	.3068E+05
0.095	42.919	0.1677E-04	.3169E+05
0.113	46.803	0.2138E-04	.3263E+05
0.135	51.039	0.2725E-04	.3351E+05
0.160	55.659	0.3473E-04	.3434E+05
0.190	60.696	0.4427E-04	.3510E+05
0.226	66.190	0.5642E-04	.3582E+05
0.269	72.180	0.7191E-04	.3648E+05
0.320	78.713	0.9165E-04	.3711E+05
0.381	85.837	0.9165E-03	.3723E+05

STRUCTURE FAILED, KMAX .GT. KIC

```
BIGIF:  BOUNDARY INTEGRAL EQUATION        EXAMPLE 1B - EDGE CRACK UNDER UNIFORM STRESS (IF SOLUTION,IFI=204)    PMB10JAN78
        GENERATED INFLUENCE FUNCTIONS
        FOR USE IN FRACTURE MECHANICS
        PROBLEMS

A "->" MARKS THE OPTION SELECTED

        ANALYSIS SELECTION (IFAT)

              0 SINGLE K CALCULATION
          ->  1 FATIGUE ANALYSIS

        CRACK GEOMETRY MODEL INDEX NUMBER (IFI)

              0 K VALUES KNOWN, NO IF CALC.
            101 K = SIGMA*SQRT(PI*A)
            102 K = 1.12* SIGMA* SQRT(PI*A)
            201 CENTER CRACKED PANEL, MODE I
            202 CENTER CRACKED PANEL, MODE II
            203 CENTER CRACKED PANEL, MODE III
          -> 204 EDGE CRACK, MODE I
            205 EDGE CRACK, MODE II (INACTIVE)
            206 EDGE CRACK, MODE III (INACTIVE)
            207 SNOW PLAY (INACTIVE)
            300 NOZ BLEND RADIUS CORNERCRACK
            301 BURIED CIRCULAR CRACK
            302 SURFACE 1/2 CIRCULAR CRACK
            303 SURFACE 1/4 CIRCULAR CRACK
            304 4-DOF BURIED CRACK
            305 3-DOF SURFACE CRACK
            306 2-DOF CORNER CRACK


        VARIABLE THICKNESS SPECIFICATION (NTH)

          ->  0 CONSTANT BODY THICKNESS
              1 VARIABLE BODY THICKNESS


        CRACK GROWTH RATE RULE (IDADN)

          ->  1 PARIS RULE, INPUT C,XN (DEFAULT)
              2 INPUT TABULAR DA/DN, DELTA-K DATA
              3 FORMAN RULE, INPUT C,XN FOR EXPECTED R
              4 FORMAN RULE, INPUT C,XN AND R
              5 INPUT TABULAR DA/DN,DELTA-K DATA AND R
              6 SAME AS #5 BUT FOR UP TO FIVE R VALUES


        INTEGRATION INCREMENT SCHEME (INUM)

              1 COARSE INTEGRATION SCHEME (DEFAULT)
          ->  2 STANDARD
              3 REFINED


        SINGLE OR MULT INTEGRATION SCHEMES (INCL)

          ->  0 SINGLE
              1 MULTIPLE
```

INCREMENTS USED TO DOUBLE CRACK SIZE (NDUB)

COARSE = 2
-> STANDARD = 4
REFINED = 8

GEOMETRY AND MATERIAL CRACK GROWTH INPUT

EXAMPLE 1B - EDGE CRACK UNDER UNIFORM STRESS (IF SOLUTION,IFI=204) PMB10JAN78

NUMBER OF DEGREES OF FREEDOM = 1

INITIAL A-VALUES FOR EACH DEGREE OF FREEDOM

CRACK LENGTH AI(1) = 0.50000E-02

GEOMETRY FACTORS

G(1)	0.10000E+04	BODY WIDTH
G(2)	0.0	
G(3)	0.0	
G(4)	0.0	
G(5)	0.0	
G(6)	0.0	X-COORD. TO CRACK CENTER (XC)
G(7)	0.0	Y-COORD. TO CRACK CENTER (YC)
G(8)	0.0	CRACK ORIENTATION ANGLE (PHI, DEGREES)

DA/DN OPTION SELECTED: 1

KIC =	0.85000E+02	FRACTURE TOUGHNESS
C =	0.45000E-09	COEFFICIENT
XN =	0.28000E+01	EXPONENT
AT R =	0.0	

LOAD TRANSIENTS: 1 TRANSIENT(S) IN PROBLEM EXAMPLE 1B - EDGE CRACK UNDER UNIFORM STRESS (IF SOLUTION,IFI=204) PMB10JAN78

NUMBER	NAME	NUMBER OF CYCLES PER BLOCK	SPECIFIER	AGLD	IPSRD	IPLD	KAME	IWO	NPX	NPY
1	ONLY TRANSIENT	0.10000E+01	1	0.70000E+02	0	1	0	0	0	0

NEEDED ADDITIONAL INFORMATION
(DEPENDS ON VALUE OF IPLD)

COEFFICIENTS OF EQUATION FOR UNCRACKED STRESS FIELD

Q(1) = 0.10000E+01
Q(2) = 0.0
Q(3) = 0.0
Q(4) = 0.0

			2	0.0	3	0	0	0	0	0

DETAILED OUTPUT FOR ALL LOAD TRANSIENT(S) AND CRACK DEGREE(S) OF FREEDOM

INTEGRATION BREAKUP ********** * STANDARD * ********** EXAMPLE 1B - EDGE CRACK UNDER UNIFORM STRESS (IF SOLUTION,IFI=204) PMB10JAN78

TRANSIENT NUMBER	DEGREE OF FREEDOM	CYCLES /BLOCK	KMAX	KMIN	KMEAN	DEL-K	R-RAT	TRANSIENT DA/DN (PER CYCLE)	DA/DN (PER BLOCK)	DOF CRACK SIZE	N
1	1	1.000	9.97	0.0	4.99	9.97	0.0	.2819E-06	.282E-06	.500E-02	.0
1	1	1.000	10.88	0.0	5.44	10.88	0.0	.3594E-06	.359E-06	.595E-02	2950.
1	1	1.000	11.86	0.0	5.93	11.86	0.0	.4580E-06	.458E-06	.707E-02	5703.
1	1	1.000	12.94	0.0	6.47	12.94	0.0	.5838E-06	.584E-06	.841E-02	8271.
1	1	1.000	14.11	0.0	7.05	14.11	0.0	.7441E-06	.744E-06	.100E-01	.1067E+05
1	1	1.000	15.38	0.0	7.69	15.38	0.0	.9484E-06	.948E-06	.119E-01	.1290E+05
1	1	1.000	16.78	0.0	8.39	16.78	0.0	.1209E-05	.121E-05	.141E-01	.1499E+05
1	1	1.000	18.29	0.0	9.15	18.29	0.0	.1541E-05	.154E-05	.168E-01	.1694E+05
1	1	1.000	19.95	0.0	9.98	19.95	0.0	.1964E-05	.196E-05	.200E-01	.1875E+05
1	1	1.000	21.76	0.0	10.88	21.76	0.0	.2503E-05	.250E-05	.238E-01	.2045E+05
1	1	1.000	23.72	0.0	11.86	23.72	0.0	.3190E-05	.319E-05	.283E-01	.2203E+05
1	1	1.000	25.87	0.0	12.94	25.87	0.0	.4066E-05	.407E-05	.336E-01	.2350E+05
1	1	1.000	28.21	0.0	14.11	28.21	0.0	.5182E-05	.518E-05	.400E-01	.2488E+05
1	1	1.000	30.77	0.0	15.38	30.77	0.0	.6605E-05	.660E-05	.476E-01	.2616E+05
1	1	1.000	33.55	0.0	16.78	33.55	0.0	.8418E-05	.842E-05	.566E-01	.2736E+05
1	1	1.000	36.59	0.0	18.29	36.59	0.0	.1073E-04	.107E-04	.673E-01	.2848E+05
1	1	1.000	39.90	0.0	19.95	39.90	0.0	.1367E-04	.137E-04	.800E-01	.2952E+05
1	1	1.000	43.51	0.0	21.76	43.51	0.0	.1743E-04	.174E-04	.951E-01	.3050E+05
1	1	1.000	47.45	0.0	23.72	47.45	0.0	.2222E-04	.222E-04	.113	.3140E+05
1	1	1.000	51.74	0.0	25.87	51.74	0.0	.2832E-04	.283E-04	.135	.3225E+05
1	1	1.000	56.43	0.0	28.21	56.43	0.0	.3609E-04	.361E-04	.160	.3304E+05
1	1	1.000	61.53	0.0	30.77	61.53	0.0	.4600E-04	.460E-04	.190	.3378E+05
1	1	1.000	67.10	0.0	33.55	67.10	0.0	.5863E-04	.586E-04	.226	.3447E+05
1	1	1.000	73.18	0.0	36.59	73.18	0.0	.7473E-04	.747E-04	.269	.3511E+05

1	1	1.000	79.80	0.0	39.90	79.80	0.0	.9524E-04	.952E-04	.320	.3571E+05

STRUCTURE HAS FAILED--KMAX.GT.KIC IN DADN SUBROUTINE. NEXT CRACK SIZE EXCEEDS CRITICAL CRACK SIZE.

1	1	1.000	87.02	0.0	43.51	87.02	0.0	.9524E-04	.952E-03	.381	.3582E+05

FATIGUE CRACK GROWTH ANALYSIS SUMMARY

CRACK DIMENSION(S) A(I)	ALTERNATING STRESS INTENSITY FACTOR(S) FOR FIRST INPUT LOAD TRANSIENT DELTA K(I)	TOTAL CRACK GROWTH RATE(S) DADN(I)	NUMBER OF CYCLES OR BLOCKS TO GROW CRACK FROM INITIAL SIZE N
A1	DK1	DADN1	N
0.005	9.975	0.2819E-06	.0
0.006	10.878	0.3594E-06	2950.
0.007	11.862	0.4580E-06	5703.
0.008	12.936	0.5838E-06	8271.
0.010	14.107	0.7441E-06	.1067E+05
0.012	15.384	0.9484E-06	.1290E+05
0.014	16.776	0.1209E-05	.1499E+05
0.017	18.294	0.1541E-05	.1694E+05
0.020	19.950	0.1964E-05	.1875E+05
0.024	21.756	0.2503E-05	.2045E+05
0.028	23.725	0.3190E-05	.2203E+05
0.034	25.872	0.4066E-05	.2350E+05
0.040	28.214	0.5182E-05	.2488E+05
0.048	30.767	0.6605E-05	.2616E+05
0.057	33.552	0.8418E-05	.2736E+05
0.067	36.589	0.1073E-04	.2848E+05
0.080	39.899	0.1367E-04	.2952E+05
0.095	43.512	0.1743E-04	.3050E+05
0.113	47.450	0.2222E-04	.3140E+05
0.135	51.744	0.2832E-04	.3225E+05
0.160	56.427	0.3609E-04	.3304E+05
0.190	61.535	0.4600E-04	.3378E+05
0.226	67.104	0.5863E-04	.3447E+05
0.269	73.177	0.7473E-04	.3511E+05
0.320	79.800	0.9524E-04	.3571E+05
0.381	87.023	0.9524E-03	.3582E+05

STRUCTURE FAILED, KMAX .GT. KIC

APPENDIX C.2: Example 2 - Through-Cracks in Notched Structures

```
BIGIF:  BOUNDARY INTEGRAL EQUATION        EXAMPLE 2A - CRACK IN SMALL RADIUS NOTCH WITH HIGH KT (KT=5)          PMB10JAN78
        GENERATED INFLUENCE FUNCTIONS
        FOR USE IN FRACTURE MECHANICS
        PROBLEMS

A "->" MARKS THE OPTION SELECTED

        ANALYSIS SELECTION (IFAT)

              0 SINGLE K CALCULATION
          ->  1 FATIGUE ANALYSIS

        CRACK GEOMETRY MODEL INDEX NUMBER (IFI)

              0 K VALUES KNOWN, NO IF CALC.
            101 K = SIGMA*SQRT(PI*A)
            102 K = 1.12* SIGMA* SQRT(PI*A)
            201 CENTER CRACKED PANEL, MODE I
            202 CENTER CRACKED PANEL, MODE II
            203 CENTER CRACKED PANEL, MODE III
          -> 204 EDGE CRACK, MODE I
            205 EDGE CRACK, MODE II (INACTIVE)
            206 EDGE CRACK, MODE III (INACTIVE)
            207 SNOW PLAY (INACTIVE)
            300 NOZ BLEND RADIUS CORNERCRACK
            301 BURIED CIRCULAR CRACK
            302 SURFACE 1/2 CIRCULAR CRACK
            303 SURFACE 1/4 CIRCULAR CRACK
            304 4-DOF BURIED CRACK
            305 3-DOF SURFACE CRACK
            306 2-DOF CORNER CRACK


        VARIABLE THICKNESS SPECIFICATION (NTH)

          ->  0 CONSTANT BODY THICKNESS
              1 VARIABLE BODY THICKNESS


        CRACK GROWTH RATE RULE (IDADN)

          ->  1 PARIS RULE, INPUT C,XN (DEFAULT)
              2 INPUT TABULAR DA/DN, DELTA-K DATA
              3 FORMAN RULE, INPUT C,XN FOR EXPECTED R
              4 FORMAN RULE, INPUT C,XN AND R
              5 INPUT TABULAR DA/DN,DELTA-K DATA AND R
              6 SAME AS #5 BUT FOR UP TO FIVE R VALUES


        INTEGRATION INCREMENT SCHEME (INUM)

              1 COARSE INTEGRATION SCHEME (DEFAULT)
          ->  2 STANDARD
              3 REFINED


        SINGLE OR MULT INTEGRATION SCHEMES (INCL)

          ->  0 SINGLE
              1 MULTIPLE
```

INCREMENTS USED TO DOUBLE CRACK SIZE (NDUB)

COARSE = 2
-> STANDARD = 4
REFINED = 8

NUMBER OF DEGREES OF FREEDOM = 1

INITIAL A-VALUES FOR EACH DEGREE OF FREEDOM

CRACK LENGTH AI(1) = 0.10000E-01

GEOMETRY FACTORS

G(1)	0.10000E+04	BODY WIDTH
G(2)	0.0	
G(3)	0.0	
G(4)	0.0	
G(5)	0.0	
G(6)	0.0	X-COORD. TO CRACK CENTER (XC)
G(7)	0.0	Y-COORD. TO CRACK CENTER (YC)
G(8)	0.0	CRACK ORIENTATION ANGLE (PHI, DEGREES)

DA/DN OPTION SELECTED: 1

KIC =	0.85000E+02	FRACTURE TOUGHNESS
C =	0.15000E-08	COEFFICIENT
XN =	0.28000E+01	EXPONENT
AT R =	0.0	

LOAD TRANSIENTS: 1 TRANSIENT(S) IN PROBLEM EXAMPLE 2A - CRACK IN SMALL RADIUS NOTCH WITH HIGH KT (KT=5) PMB10JAN78

NUMBER	NAME	NUMBER OF CYCLES PER BLOCK	SPECIFIER	AGLD	IPSRD	IPLD	KAME	IWO	NPX	NPY
1	ONE TRANSIENT	0.10000E+01	1	0.10000E+01	0	3	0	0	0	0

NEEDED ADDITIONAL INFORMATION
(DEPENDS ON VALUE OF IPLD)

COEFFICIENTS OF EQUATION FOR UNCRACKED STRESS FIELD

Q(1) = 0.50000E+02
Q(2) = 0.50000E+01
Q(3) = 0.50000E-02
Q(5) = 0.0
Q(7) = 0.0

			2	0.0	3	0	0	0	0	0

DETAILED OUTPUT FOR ALL LOAD TRANSIENT(S) AND CRACK DEGREE(S) OF FREEDOM

INTEGRATION BREAKUP ********** * STANDARD * ********** EXAMPLE 2A - CRACK IN SMALL RADIUS NOTCH WITH HIGH KT (KT=5) PMB10JAN78

TRANSIENT NUMBER	DEGREE OF FREEDOM	CYCLES /BLOCK	KMAX	KMIN	KMEAN	DEL-K	R-RAT	TRANSIENT DA/DN (PER CYCLE)	DA/DN (PER BLOCK)	DOF CRACK SIZE	N
1	1	1.000	16.54	0.0	8.27	16.54	0.0	.3870E-05	.387E-05	.100E-01	.0
1	1	1.000	17.02	0.0	8.51	17.02	0.0	.4192E-05	.419E-05	.119E-01	469.4
1	1	1.000	17.58	0.0	8.79	17.58	0.0	.4596E-05	.460E-05	.141E-01	981.4
1	1	1.000	18.25	0.0	9.13	18.25	0.0	.5103E-05	.510E-05	.168E-01	1533.
1	1	1.000	19.03	0.0	9.52	19.03	0.0	.5738E-05	.574E-05	.200E-01	2120.
1	1	1.000	19.94	0.0	9.97	19.94	0.0	.6532E-05	.653E-05	.238E-01	2737.
1	1	1.000	20.97	0.0	10.48	20.97	0.0	.7524E-05	.752E-05	.283E-01	3377.
1	1	1.000	22.14	0.0	11.07	22.14	0.0	.8763E-05	.876E-05	.336E-01	4034.
1	1	1.000	23.47	0.0	11.73	23.47	0.0	.1031E-04	.103E-04	.400E-01	4702.
1	1	1.000	24.95	0.0	12.48	24.95	0.0	.1225E-04	.122E-04	.476E-01	5373.
1	1	1.000	26.62	0.0	13.31	26.62	0.0	.1468E-04	.147E-04	.566E-01	6041.
1	1	1.000	28.48	0.0	14.24	28.48	0.0	.1774E-04	.177E-04	.673E-01	6701.
1	1	1.000	30.55	0.0	15.28	30.55	0.0	.2159E-04	.216E-04	.800E-01	7349.
1	1	1.000	32.86	0.0	16.43	32.86	0.0	.2647E-04	.265E-04	.951E-01	7979.
1	1	1.000	35.42	0.0	17.71	35.42	0.0	.3265E-04	.326E-04	.113	8588.
1	1	1.000	38.25	0.0	19.12	38.25	0.0	.4050E-04	.405E-04	.135	9173.
1	1	1.000	41.39	0.0	20.69	41.39	0.0	.5050E-04	.505E-04	.160	9733.
1	1	1.000	44.85	0.0	22.42	44.85	0.0	.6324E-04	.632E-04	.190	.1026E+05
1	1	1.000	48.67	0.0	24.33	48.67	0.0	.7950E-04	.795E-04	.226	.1077E+05
1	1	1.000	52.87	0.0	26.44	52.87	0.0	.1003E-03	.100E-03	.269	.1125E+05
1	1	1.000	57.49	0.0	28.74	57.49	0.0	.1267E-03	.127E-03	.320	.1169E+05
1	1	1.000	62.55	0.0	31.28	62.55	0.0	.1605E-03	.161E-03	.381	.1212E+05
1	1	1.000	68.10	0.0	34.05	68.10	0.0	.2037E-03	.204E-03	.453	.1251E+05
1	1	1.000	74.17	0.0	37.09	74.17	0.0	.2587E-03	.259E-03	.538	.1288E+05

1	1	1.000	80.81	0.0	40.41	80.81	0.0	.3289E-03	.329E-03	.640	.1323E+05

STRUCTURE HAS FAILED--KMAX.GT.KIC IN DADN SUBROUTINE. NEXT CRACK SIZE EXCEEDS CRITICAL CRACK SIZE.

1	1	1.000	88.07	0.0	44.03	88.07	0.0	.3289E-03	.329E-02	.761	.1330E+05

FATIGUE CRACK GROWTH ANALYSIS SUMMARY

CRACK DIMENSION(S) A(I)	ALTERNATING STRESS INTENSITY FACTOR(S) FOR FIRST INPUT LOAD TRANSIENT DELTA K(I)	TOTAL CRACK GROWTH RATE(S) DADN(I)	NUMBER OF CYCLES OR BLOCKS TO GROW CRACK FROM INITIAL SIZE N
A1	DK1	DADN1	N
0.010	16.537	0.3870E-05	.0
0.012	17.015	0.4192E-05	469.4
0.014	17.584	0.4596E-05	981.4
0.017	18.253	0.5103E-05	1533.
0.020	19.034	0.5738E-05	2120.
0.024	19.936	0.6532E-05	2737.
0.028	20.968	0.7524E-05	3377.
0.034	22.141	0.8763E-05	4034.
0.040	23.466	0.1031E-04	4702.
0.048	24.955	0.1225E-04	5373.
0.057	26.622	0.1468E-04	6041.
0.067	28.482	0.1774E-04	6701.
0.080	30.553	0.2159E-04	7349.
0.095	32.858	0.2647E-04	7979.
0.113	35.415	0.3265E-04	8588.
0.135	38.249	0.4050E-04	9173.
0.160	41.385	0.5050E-04	9733.
0.190	44.849	0.6324E-04	.1026E+05
0.226	48.668	0.7950E-04	.1077E+05
0.269	52.871	0.1003E-03	.1125E+05
0.320	57.488	0.1267E-03	.1169E+05
0.381	62.553	0.1605E-03	.1212E+05
0.453	68.102	0.2037E-03	.1251E+05
0.538	74.173	0.2587E-03	.1288E+05
0.640	80.813	0.3289E-03	.1323E+05
0.761	88.068	0.3289E-02	.1330E+05

STRUCTURE FAILED, KMAX .GT. KIC

```
BIGIF:  BOUNDARY INTEGRAL EQUATION        EXAMPLE 2B - CRACK IN LARGE RADIUS NOTCH WITH LOW KT (KT=2.45)        PMB10JAN78
        GENERATED INFLUENCE FUNCTIONS
        FOR USE IN FRACTURE MECHANICS
        PROBLEMS

A "->" MARKS THE OPTION SELECTED

        ANALYSIS SELECTION (IFAT)

              0 SINGLE K CALCULATION
          ->  1 FATIGUE ANALYSIS

        CRACK GEOMETRY MODEL INDEX NUMBER (IFI)

              0 K VALUES KNOWN, NO IF CALC.
            101 K = SIGMA*SQRT(PI*A)
            102 K = 1.12* SIGMA* SQRT(PI*A)
            201 CENTER CRACKED PANEL, MODE I
            202 CENTER CRACKED PANEL, MODE II
            203 CENTER CRACKED PANEL, MODE III
          -> 204 EDGE CRACK, MODE I
            205 EDGE CRACK, MODE II (INACTIVE)
            206 EDGE CRACK, MODE III (INACTIVE)
            207 SNOW PLAY (INACTIVE)
            300 NOZ BLEND RADIUS CORNERCRACK
            301 BURIED CIRCULAR CRACK
            302 SURFACE 1/2 CIRCULAR CRACK
            303 SURFACE 1/4 CIRCULAR CRACK
            304 4-DOF BURIED CRACK
            305 3-DOF SURFACE CRACK
            306 2-DOF CORNER CRACK


        VARIABLE THICKNESS SPECIFICATION (NTH)

          ->  0 CONSTANT BODY THICKNESS
              1 VARIABLE BODY THICKNESS


        CRACK GROWTH RATE RULE (IDADN)

          ->  1 PARIS RULE, INPUT C,XN (DEFAULT)
              2 INPUT TABULAR DA/DN, DELTA-K DATA
              3 FORMAN RULE, INPUT C,XN FOR EXPECTED R
              4 FORMAN RULE, INPUT C,XN AND R
              5 INPUT TABULAR DA/DN,DELTA-K DATA AND R
              6 SAME AS #5 BUT FOR UP TO FIVE R VALUES


        INTEGRATION INCREMENT SCHEME (INUM)

              1 COARSE INTEGRATION SCHEME (DEFAULT)
          ->  2 STANDARD
              3 REFINED


        SINGLE OR MULT INTEGRATION SCHEMES (INCL)

          ->  0 SINGLE
              1 MULTIPLE
```

INCREMENTS USED TO DOUBLE CRACK SIZE (NDUB)

COARSE = 2
-> STANDARD = 4
REFINED = 8

GEOMETRY AND MATERIAL CRACK GROWTH INPUT — EXAMPLE 2B - CRACK IN LARGE RADIUS NOTCH WITH LOW KT (KT=2.45) — PMB10JAN78

NUMBER OF DEGREES OF FREEDOM = 1

INITIAL A-VALUES FOR EACH DEGREE OF FREEDOM

CRACK LENGTH AI(1) = 0.10000E-01

GEOMETRY FACTORS

G(1)	0.10000E+04	BODY WIDTH
G(2)	0.0	
G(3)	0.0	
G(4)	0.0	
G(5)	0.0	
G(6)	0.0	X-COORD. TO CRACK CENTER (XC)
G(7)	0.0	Y-COORD. TO CRACK CENTER (YC)
G(8)	0.0	CRACK ORIENTATION ANGLE (PHI, DEGREES)

DA/DN OPTION SELECTED: 1

KIC =	0.85000E+02	FRACTURE TOUGHNESS
C =	0.15000E-08	COEFFICIENT
XN =	0.28000E+01	EXPONENT
AT R =	0.0	

LOAD TRANSIENTS: 1 TRANSIENT(S) IN PROBLEM EXAMPLE 2B - CRACK IN LARGE RADIUS NOTCH WITH LOW KT (KT=2.45) PMB10JAN78

NUMBER	NAME	NUMBER OF CYCLES PER BLOCK	SPECIFIER	AGLD	IPSRD	IPLD	KAME	IWO	NPX	NPY
1	ONE TRANSIENT	0.10000E+01	1	0.73500E+00	0	3	0	0	0	0

NEEDED ADDITIONAL INFORMATION
(DEPENDS ON VALUE OF IPLD)

COEFFICIENTS OF EQUATION FOR UNCRACKED STRESS FIELD

Q(1) = 0.50000E+02
Q(2) = 0.24500E+01
Q(3) = 0.37500E+00
Q(5) = 0.0
Q(7) = 0.0

			2	0.0	3	0	0	0	0	0

DETAILED OUTPUT FOR ALL LOAD TRANSIENT(S) AND CRACK DEGREE(S) OF FREEDOM

INTEGRATION BREAKUP ********** * STANDARD * **********

EXAMPLE 2B - CRACK IN LARGE RADIUS NOTCH WITH LOW KT (KT=2.45) PMB10JAN78

TRANSIENT NUMBER	DEGREE OF FREEDOM	CYCLES /BLOCK	KMAX	KMIN	KMEAN	DEL-K	R-RAT	TRANSIENT DA/DN (PER CYCLE)	DA/DN (PER BLOCK)	DOF CRACK SIZE	N
1	1	1.000	17.56	0.0	8.78	17.56	0.0	.4580E-05	.458E-05	.100E-01	.0
1	1	1.000	19.04	0.0	9.52	19.04	0.0	.5741E-05	.574E-05	.119E-01	366.7
1	1	1.000	20.61	0.0	10.31	20.61	0.0	.7175E-05	.717E-05	.141E-01	715.1
1	1	1.000	22.30	0.0	11.15	22.30	0.0	.8937E-05	.894E-05	.168E-01	1047.
1	1	1.000	24.08	0.0	12.04	24.08	0.0	.1109E-04	.111E-04	.200E-01	1365.
1	1	1.000	25.97	0.0	12.99	25.97	0.0	.1370E-04	.137E-04	.238E-01	1670.
1	1	1.000	27.96	0.0	13.98	27.96	0.0	.1684E-04	.168E-04	.283E-01	1965.
1	1	1.000	30.04	0.0	15.02	30.04	0.0	.2059E-04	.206E-04	.336E-01	2251.
1	1	1.000	32.20	0.0	16.10	32.20	0.0	.2501E-04	.250E-04	.400E-01	2530.
1	1	1.000	34.43	0.0	17.22	34.43	0.0	.3017E-04	.302E-04	.476E-01	2805.
1	1	1.000	36.73	0.0	18.36	36.73	0.0	.3614E-04	.361E-04	.566E-01	3076.
1	1	1.000	39.06	0.0	19.53	39.06	0.0	.4296E-04	.430E-04	.673E-01	3347.
1	1	1.000	41.43	0.0	20.72	41.43	0.0	.5065E-04	.507E-04	.800E-01	3618.
1	1	1.000	43.82	0.0	21.91	43.82	0.0	.5926E-04	.593E-04	.951E-01	3894.
1	1	1.000	46.22	0.0	23.11	46.22	0.0	.6880E-04	.688E-04	.113	4175.
1	1	1.000	48.63	0.0	24.31	48.63	0.0	.7931E-04	.793E-04	.135	4464.
1	1	1.000	51.05	0.0	25.53	51.05	0.0	.9089E-04	.909E-04	.160	4763.
1	1	1.000	53.51	0.0	26.76	53.51	0.0	.1037E-03	.104E-03	.190	5074.
1	1	1.000	56.03	0.0	28.02	56.03	0.0	.1180E-03	.118E-03	.226	5399.
1	1	1.000	58.65	0.0	29.33	58.65	0.0	.1341E-03	.134E-03	.269	5739.
1	1	1.000	61.42	0.0	30.71	61.42	0.0	.1525E-03	.153E-03	.320	6094.
1	1	1.000	64.39	0.0	32.19	64.39	0.0	.1741E-03	.174E-03	.381	6465.
1	1	1.000	67.61	0.0	33.81	67.61	0.0	.1996E-03	.200E-03	.453	6850.
1	1	1.000	71.16	0.0	35.58	71.16	0.0	.2303E-03	.230E-03	.538	7249.

1	1	1.000	75.08	0.0	37.54	75.08	0.0	.2676E-03	.268E-03	.640	7658.
1	1	1.000	79.43	0.0	39.72	79.43	0.0	.3134E-03	.313E-03	.761	8075.
1	1	1.000	84.28	0.0	42.14	84.28	0.0	.3700E-03	.370E-03	.905	8496.

STRUCTURE HAS FAILED--KMAX.GT.KIC IN DADN SUBROUTINE. NEXT CRACK SIZE EXCEEDS CRITICAL CRACK SIZE.

1	1	1.000	89.68	0.0	44.84	89.68	0.0	.3700E-03	.370E-02	1.08	8580.

STANDARD BREAKUP EXAMPLE 2B - CRACK IN LARGE RADIUS NOTCH WITH LOW KT (KT=2.45) PMB10JAN78

FATIGUE CRACK GROWTH ANALYSIS SUMMARY

CRACK DIMENSION(S) A(I)	ALTERNATING STRESS INTENSITY FACTOR(S) FOR FIRST INPUT LOAD TRANSIENT DELTA K(I)	TOTAL CRACK GROWTH RATE(S) DADN(I)	NUMBER OF CYCLES OR BLOCKS TO GROW CRACK FROM INITIAL SIZE N
A1	DK1	DADN1	N
0.010	17.561	0.4580E-05	.0
0.012	19.037	0.5741E-05	366.7
0.014	20.615	0.7175E-05	715.1
0.017	22.297	0.8937E-05	1047.
0.020	24.083	0.1109E-04	1365.
0.024	25.972	0.1370E-04	1670.
0.028	27.959	0.1684E-04	1965.
0.034	30.038	0.2059E-04	2251.
0.040	32.200	0.2501E-04	2530.
0.048	34.434	0.3017E-04	2805.
0.057	36.726	0.3614E-04	3076.
0.067	39.063	0.4296E-04	3347.
0.080	41.431	0.5065E-04	3618.
0.095	43.820	0.5926E-04	3894.
0.113	46.218	0.6880E-04	4175.
0.135	48.627	0.7931E-04	4464.
0.160	51.052	0.9089E-04	4763.
0.190	53.511	0.1037E-03	5074.
0.226	56.032	0.1180E-03	5399.
0.269	58.652	0.1341E-03	5739.
0.320	61.419	0.1525E-03	6094.
0.381	64.387	0.1741E-03	6465.
0.453	67.613	0.1996E-03	6850.
0.538	71.156	0.2303E-03	7249.
0.640	75.077	0.2676E-03	7658.
0.761	79.434	0.3134E-03	8075.
0.905	84.282	0.3700E-03	8496.
1.076	89.677	0.3700E-02	8580.

STRUCTURE FAILED, KMAX .GT. KIC

APPENDIX C.3: Example 3 - Fatigue Analysis of a Weld Crack

```
BIGIF:  BOUNDARY INTEGRAL EQUATION        EXAMPLE 3A - CENTER-CRACKED FINITE WIDTH PLATE (CYCLIC + RESIDUALS)   PMB01DEC76
        GENERATED INFLUENCE FUNCTIONS
        FOR USE IN FRACTURE MECHANICS
        PROBLEMS

A "->" MARKS THE OPTION SELECTED

        ANALYSIS SELECTION (IFAT)

                0 SINGLE K CALCULATION
            ->  1 FATIGUE ANALYSIS

        CRACK GEOMETRY MODEL INDEX NUMBER (IFI)

                0 K VALUES KNOWN, NO IF CALC.
              101 K = SIGMA*SQRT(PI*A)
              102 K = 1.12* SIGMA* SQRT(PI*A)
            -> 201 CENTER CRACKED PANEL, MODE I
              202 CENTER CRACKED PANEL, MODE II
              203 CENTER CRACKED PANEL, MODE III
              204 EDGE CRACK, MODE I
              205 EDGE CRACK, MODE II (INACTIVE)
              206 EDGE CRACK, MODE III (INACTIVE)
              207 SNOW PLAY (INACTIVE)
              300 NOZ BLEND RADIUS CORNERCRACK
              301 BURIED CIRCULAR CRACK
              302 SURFACE 1/2 CIRCULAR CRACK
              303 SURFACE 1/4 CIRCULAR CRACK
              304 4-DOF BURIED CRACK
              305 3-DOF SURFACE CRACK
              306 2-DOF CORNER CRACK


        VARIABLE THICKNESS SPECIFICATION (NTH)

            ->  0 CONSTANT BODY THICKNESS
                1 VARIABLE BODY THICKNESS


        CRACK GROWTH RATE RULE (IDADN)

                1 PARIS RULE, INPUT C,XN (DEFAULT)
                2 INPUT TABULAR DA/DN, DELTA-K DATA
            ->  3 FORMAN RULE, INPUT C,XN FOR EXPECTED R
                4 FORMAN RULE, INPUT C,XN AND R
                5 INPUT TABULAR DA/DN,DELTA-K DATA AND R
                6 SAME AS #5 BUT FOR UP TO FIVE R VALUES


        INTEGRATION INCREMENT SCHEME (INUM)

                1 COARSE INTEGRATION SCHEME (DEFAULT)
                2 STANDARD
            ->  3 REFINED


        SINGLE OR MULT INTEGRATION SCHEMES (INCL)

            ->  0 SINGLE
                1 MULTIPLE
```

INCREMENTS USED TO DOUBLE CRACK SIZE (NDUB)

COARSE = 2
STANDARD = 4
-> REFINED = 8

CRACK GROWTH INPUT

NUMBER OF DEGREES OF FREEDOM = 1

INITIAL A-VALUES FOR EACH DEGREE OF FREEDOM

CRACK LENGTH AI(1) = 0.12500E+00

GEOMETRY FACTORS

G(1)	0.50000E+01	BODY WIDTH
G(2)	0.0	
G(3)	0.0	
G(4)	0.0	
G(5)	0.0	
G(6)	0.0	X-COORD. TO CRACK CENTER (XC)
G(7)	0.0	Y-COORD. TO CRACK CENTER (YC)
G(8)	0.0	CRACK ORIENTATION ANGLE (PHI, DEGREES)

DA/DN OPTION SELECTED: 3

KIC =	0.15000E+03	FRACTURE TOUGHNESS
C =	0.14000E-06	COEFFICIENT
XN =	0.27400E+01	EXPONENT
AT R =	0.0	

LOAD TRANSIENTS: 1 TRANSIENT(S) IN PROBLEM EXAMPLE 3A - CENTER-CRACKED FINITE WIDTH PLATE (CYCLIC + RESIDUALS) PMB01DEC76

NUMBER	NAME	NUMBER OF CYCLES PER BLOCK	SPECIFIER	AGLD	IPSRD	IPLD	KAME	IWO	NPX	NPY
1	CYCLIC STRESS + RESIDUALS	0.10000E+01	1	0.10000E+01	1	4	0	0	11	0

NEEDED ADDITIONAL INFORMATION
(DEPENDS ON VALUE OF IPLD)

STRESS FUNCTION SIGMA(X)

X	SIGMA(X)
0.0	0.52500E+02
0.40000E+00	0.48500E+02
0.80000E+00	0.38000E+02
0.12000E+01	0.20000E+02
0.16000E+01	0.75000E+01
0.18000E+01	0.37000E+01
0.24000E+01	-0.90000E+01
0.30000E+01	-0.17000E+02
0.36000E+01	-0.22000E+02
0.45000E+01	-0.35500E+02
0.50000E+01	-0.37500E+02

			2	0.25000E+02	2	4	0	0	2	0

NEEDED ADDITIONAL INFORMATION
(DEPENDS ON VALUE OF IPLD)

STRESS FUNCTION SIGMA(X)

X	SIGMA(X)
0.0	0.10000E+01
0.50000E+01	0.10000E+01

DETAILED OUTPUT FOR ALL LOAD TRANSIENT(S) AND CRACK DEGREE(S) OF FREEDOM

INTEGRATION BREAKUP ********** * REFINED * **********

EXAMPLE 3A - CENTER-CRACKED FINITE WIDTH PLATE (CYCLIC + RESIDUALS) PMB01DEC76

TRANSIENT NUMBER	DEGREE OF FREEDOM	CYCLES /BLOCK	KMAX	KMIN	KMEAN	DEL-K	R-RAT	TRANSIENT DA/DN (PER CYCLE)	DA/DN (PER BLOCK)	DOF CRACK SIZE	N
1	1	1.000	48.20	32.49	40.34	15.71	0.674	.7994E-05	.799E-05	.125	.0
1	1	1.000	50.29	33.88	42.09	16.41	0.674	.9184E-05	.918E-05	.136	1317.
1	1	1.000	52.47	35.33	43.90	17.13	0.673	.1056E-04	.106E-04	.149	2567.
1	1	1.000	54.73	36.84	45.79	17.89	0.673	.1217E-04	.122E-04	.162	3751.
1	1	1.000	57.10	38.41	47.75	18.69	0.673	.1404E-04	.140E-04	.177	4870.
1	1	1.000	59.55	40.03	49.79	19.52	0.672	.1622E-04	.162E-04	.193	5928.
1	1	1.000	62.11	41.72	51.92	20.39	0.672	.1878E-04	.188E-04	.210	6925.
1	1	1.000	64.77	43.48	54.12	21.30	0.671	.2178E-04	.218E-04	.229	7863.
1	1	1.000	67.54	45.29	56.42	22.24	0.671	.2533E-04	.253E-04	.250	8744.
1	1	1.000	70.42	47.18	58.80	23.24	0.670	.2952E-04	.295E-04	.273	9569.
1	1	1.000	73.41	49.14	61.27	24.27	0.669	.3450E-04	.345E-04	.297	.1034E+05
1	1	1.000	76.52	51.16	63.84	25.36	0.669	.4045E-04	.405E-04	.324	.1106E+05
1	1	1.000	79.75	53.25	66.50	26.50	0.668	.4760E-04	.476E-04	.354	.1172E+05
1	1	1.000	83.11	55.42	69.26	27.69	0.667	.5622E-04	.562E-04	.386	.1234E+05
1	1	1.000	86.54	57.61	72.08	28.93	0.666	.6663E-04	.666E-04	.420	.1291E+05
1	1	1.000	89.96	59.72	74.84	30.24	0.664	.7907E-04	.791E-04	.458	.1343E+05
1	1	1.000	93.41	61.80	77.61	31.61	0.662	.9409E-04	.941E-04	.500	.1391E+05
1	1	1.000	96.89	63.84	80.37	33.05	0.659	.1124E-03	.112E-03	.545	.1435E+05
1	1	1.000	100.40	65.83	83.12	34.56	0.656	.1348E-03	.135E-03	.595	.1475E+05
1	1	1.000	103.92	67.76	85.84	36.16	0.652	.1624E-03	.162E-03	.648	.1511E+05
1	1	1.000	107.45	69.62	88.53	37.84	0.648	.1968E-03	.197E-03	.707	.1544E+05
1	1	1.000	110.98	71.37	91.17	39.61	0.643	.2400E-03	.240E-03	.771	.1573E+05
1	1	1.000	114.31	72.82	93.57	41.48	0.637	.2929E-03	.293E-03	.841	.1599E+05
1	1	1.000	117.12	73.65	95.38	43.47	0.629	.3535E-03	.353E-03	.917	.1623E+05

1	1	1.000	119.50	73.92	96.71	45.59	0.619	.4224E-03	.422E-03	1.00	.1644E+05
1	1	1.000	121.42	73.58	97.50	47.84	0.606	.4981E-03	.498E-03	1.09	.1664E+05
1	1	1.000	122.82	72.56	97.69	50.26	0.591	.5769E-03	.577E-03	1.19	.1682E+05
1	1	1.000	124.07	71.21	97.64	52.86	0.574	.6672E-03	.667E-03	1.30	.1699E+05
1	1	1.000	125.20	69.52	97.36	55.68	0.555	.7706E-03	.771E-03	1.41	.1716E+05
1	1	1.000	126.02	67.27	96.65	58.75	0.534	.8807E-03	.881E-03	1.54	.1731E+05
1	1	1.000	126.73	64.61	95.67	62.11	0.510	.1005E-02	.101E-02	1.68	.1746E+05
1	1	1.000	127.81	61.96	94.89	65.84	0.485	.1177E-02	.118E-02	1.83	.1760E+05
1	1	1.000	128.81	58.79	93.80	70.02	0.456	.1383E-02	.138E-02	2.00	.1773E+05
1	1	1.000	129.70	54.95	92.33	74.76	0.424	.1629E-02	.163E-02	2.18	.1785E+05
1	1	1.000	130.50	50.29	90.39	80.21	0.385	.1927E-02	.193E-02	2.38	.1796E+05
1	1	1.000	131.99	45.38	88.68	86.61	0.344	.2412E-02	.241E-02	2.59	.1806E+05
1	1	1.000	134.56	40.25	87.41	94.32	0.299	.3329E-02	.333E-02	2.83	.1814E+05
1	1	1.000	138.55	34.68	86.61	103.87	0.250	.5464E-02	.546E-02	3.08	.1820E+05
1	1	1.000	145.55	29.32	87.43	116.23	0.201	.1797E-01	.180E-01	3.36	.1822E+05

STRUCTURE HAS FAILED--KMAX.GT.KIC IN DADN SUBROUTINE. NEXT CRACK SIZE EXCEEDS CRITICAL CRACK SIZE.

1	1	1.000	156.92	23.67	90.30	133.25	0.151	.1797E-01	.180	3.67	.1823E+05

REFINED BREAKUP EXAMPLE 3A - CENTER-CRACKED FINITE WIDTH PLATE (CYCLIC + RESIDUALS) PMB01DEC76

FATIGUE CRACK GROWTH ANALYSIS SUMMARY

CRACK DIMENSION(S) A(I)	ALTERNATING STRESS INTENSITY FACTOR(S) FOR FIRST INPUT LOAD TRANSIENT DELTA K(I)	TOTAL CRACK GROWTH RATE(S) DADN(I)	NUMBER OF CYCLES OR BLOCKS TO GROW CRACK FROM INITIAL SIZE N
A1	DK1	DADN1	N
0.125	15.710	0.7994E-05	.0
0.136	16.407	0.9184E-05	1317.
0.149	17.134	0.1056E-04	2567.
0.162	17.895	0.1217E-04	3751.
0.177	18.690	0.1404E-04	4870.
0.193	19.520	0.1622E-04	5928.
0.210	20.388	0.1878E-04	6925.
0.229	21.296	0.2178E-04	7863.
0.250	22.244	0.2533E-04	8744.
0.273	23.236	0.2952E-04	9569.
0.297	24.274	0.3450E-04	.1034E+05
0.324	25.359	0.4045E-04	.1106E+05
0.354	26.496	0.4760E-04	.1172E+05
0.386	27.686	0.5622E-04	.1234E+05
0.420	28.933	0.6663E-04	.1291E+05
0.458	30.240	0.7907E-04	.1343E+05
0.500	31.611	0.9409E-04	.1391E+05
0.545	33.051	0.1124E-03	.1435E+05
0.595	34.565	0.1348E-03	.1475E+05
0.648	36.158	0.1624E-03	.1511E+05
0.707	37.837	0.1968E-03	.1544E+05
0.771	39.610	0.2400E-03	.1573E+05
0.841	41.485	0.2929E-03	.1599E+05
0.917	43.474	0.3535E-03	.1623E+05
1.000	45.589	0.4224E-03	.1644E+05
1.090	47.844	0.4981E-03	.1664E+05
1.189	50.257	0.5769E-03	.1682E+05
1.297	52.863	0.6672E-03	.1699E+05
1.414	55.679	0.7706E-03	.1716E+05
1.542	58.748	0.8807E-03	.1731E+05
1.682	62.113	0.1005E-02	.1746E+05
1.834	65.843	0.1177E-02	.1760E+05
2.000	70.021	0.1383E-02	.1773E+05
2.181	74.756	0.1629E-02	.1785E+05
2.378	80.207	0.1927E-02	.1796E+05
2.594	86.611	0.2412E-02	.1806E+05
2.828	94.315	0.3329E-02	.1814E+05
3.084	103.866	0.5464E-02	.1820E+05
3.364	116.235	0.1797E-01	.1822E+05
3.668	133.254	0.1797E+00	.1823E+05

STRUCTURE FAILED, KMAX .GT. KIC

```
BIGIF:  BOUNDARY INTEGRAL EQUATION        EXAMPLE 3B - CENTER-CRACKED FINITE WIDTH PLATE (CYCLIC STRESS ONLY)   PMB01DEC76
        GENERATED INFLUENCE FUNCTIONS
        FOR USE IN FRACTURE MECHANICS
        PROBLEMS

A "->" MARKS THE OPTION SELECTED

        ANALYSIS SELECTION (IFAT)

                0 SINGLE K CALCULATION
             -> 1 FATIGUE ANALYSIS

        CRACK GEOMETRY MODEL INDEX NUMBER (IFI)

                0 K VALUES KNOWN, NO IF CALC.
              101 K = SIGMA*SQRT(PI*A)
              102 K = 1.12* SIGMA* SQRT(PI*A)
             -> 201 CENTER CRACKED PANEL, MODE I
              202 CENTER CRACKED PANEL, MODE II
              203 CENTER CRACKED PANEL, MODE III
              204 EDGE CRACK, MODE I
              205 EDGE CRACK, MODE II (INACTIVE)
              206 EDGE CRACK, MODE III (INACTIVE)
              207 SNOW PLAY (INACTIVE)
              300 NOZ BLEND RADIUS CORNERCRACK
              301 BURIED CIRCULAR CRACK
              302 SURFACE 1/2 CIRCULAR CRACK
              303 SURFACE 1/4 CIRCULAR CRACK
              304 4-DOF BURIED CRACK
              305 3-DOF SURFACE CRACK
              306 2-DOF CORNER CRACK


        VARIABLE THICKNESS SPECIFICATION (NTH)

             -> 0 CONSTANT BODY THICKNESS
                1 VARIABLE BODY THICKNESS


        CRACK GROWTH RATE RULE (IDADN)

                1 PARIS RULE, INPUT C,XN (DEFAULT)
                2 INPUT TABULAR DA/DN, DELTA-K DATA
             -> 3 FORMAN RULE, INPUT C,XN FOR EXPECTED R
                4 FORMAN RULE, INPUT C,XN AND R
                5 INPUT TABULAR DA/DN,DELTA-K DATA AND R
                6 SAME AS #5 BUT FOR UP TO FIVE R VALUES


        INTEGRATION INCREMENT SCHEME (INUM)

                1 COARSE INTEGRATION SCHEME (DEFAULT)
                2 STANDARD
             -> 3 REFINED


        SINGLE OR MULT INTEGRATION SCHEMES (INCL)

             -> 0 SINGLE
                1 MULTIPLE
```

INCREMENTS USED TO DOUBLE CRACK SIZE (NDUB)

COARSE = 2
STANDARD = 4
-> REFINED = 8

NUMBER OF DEGREES OF FREEDOM = 1

INITIAL A-VALUES FOR EACH DEGREE OF FREEDOM

CRACK LENGTH AI(1) = 0.12500E+00

GEOMETRY FACTORS

G(1)	0.50000E+01	BODY WIDTH
G(2)	0.0	
G(3)	0.0	
G(4)	0.0	
G(5)	0.0	
G(6)	0.0	X-COORD. TO CRACK CENTER (XC)
G(7)	0.0	Y-COORD. TO CRACK CENTER (YC)
G(8)	0.0	CRACK ORIENTATION ANGLE (PHI, DEGREES)

DA/DN OPTION SELECTED: 3

KIC =	0.15000E+03	FRACTURE TOUGHNESS
C =	0.14000E-06	COEFFICIENT
XN =	0.27400E+01	EXPONENT
AT R =	0.0	

LOAD TRANSIENTS: 1 TRANSIENT(S) IN PROBLEM EXAMPLE 3B - CENTER-CRACKED FINITE WIDTH PLATE (CYCLIC STRESS ONLY) PMB01DEC76

NUMBER	NAME	NUMBER OF CYCLES PER BLOCK	SPECIFIER	AGLD	IPSRD	IPLD	KAME	IWO	NPX	NPY
1	CYCLIC STRESS ONLY	0.10000E+01	1	0.0	3	0	0	0	0	0
			2	0.25000E+02	2	4	0	0	2	0

NEEDED ADDITIONAL INFORMATION
(DEPENDS ON VALUE OF IPLD)

STRESS FUNCTION SIGMA(X)

X	SIGMA(X)
0.0	0.10000E+01
0.50000E+01	0.10000E+01

DETAILED OUTPUT FOR ALL LOAD TRANSIENT(S) AND CRACK DEGREE(S) OF FREEDOM

INTEGRATION BREAKUP ********** * REFINED * **********

EXAMPLE 3B - CENTER-CRACKED FINITE WIDTH PLATE (CYCLIC STRESS ONLY) PMB01DEC76

TRANSIENT NUMBER	DEGREE OF FREEDOM	CYCLES /BLOCK	KMAX	KMIN	KMEAN	DEL-K	R-RAT	TRANSIENT DA/DN (PER CYCLE)	DA/DN (PER BLOCK)	DOF CRACK SIZE	N
1	1	1.000	15.71	0.0	7.85	15.71	0.0	.1975E-05	.198E-05	.125	.0
1	1	1.000	16.41	0.0	8.20	16.41	0.0	.2236E-05	.224E-05	.136	5373.
1	1	1.000	17.13	0.0	8.57	17.13	0.0	.2532E-05	.253E-05	.149	.1055E+05
1	1	1.000	17.89	0.0	8.95	17.89	0.0	.2869E-05	.287E-05	.162	.1553E+05
1	1	1.000	18.69	0.0	9.35	18.69	0.0	.3251E-05	.325E-05	.177	.2032E+05
1	1	1.000	19.52	0.0	9.76	19.52	0.0	.3686E-05	.369E-05	.193	.2494E+05
1	1	1.000	20.39	0.0	10.19	20.39	0.0	.4180E-05	.418E-05	.210	.2937E+05
1	1	1.000	21.30	0.0	10.65	21.30	0.0	.4743E-05	.474E-05	.229	.3364E+05
1	1	1.000	22.24	0.0	11.12	22.24	0.0	.5384E-05	.538E-05	.250	.3774E+05
1	1	1.000	23.24	0.0	11.62	23.24	0.0	.6115E-05	.612E-05	.273	.4167E+05
1	1	1.000	24.27	0.0	12.14	24.27	0.0	.6950E-05	.695E-05	.297	.4545E+05
1	1	1.000	25.36	0.0	12.68	25.36	0.0	.7903E-05	.790E-05	.324	.4907E+05
1	1	1.000	26.50	0.0	13.25	26.50	0.0	.8994E-05	.899E-05	.354	.5254E+05
1	1	1.000	27.69	0.0	13.84	27.69	0.0	.1024E-04	.102E-04	.386	.5587E+05
1	1	1.000	28.93	0.0	14.47	28.93	0.0	.1168E-04	.117E-04	.420	.5906E+05
1	1	1.000	30.24	0.0	15.12	30.24	0.0	.1332E-04	.133E-04	.458	.6210E+05
1	1	1.000	31.61	0.0	15.81	31.61	0.0	.1522E-04	.152E-04	.500	.6501E+05
1	1	1.000	33.05	0.0	16.53	33.05	0.0	.1741E-04	.174E-04	.545	.6778E+05
1	1	1.000	34.56	0.0	17.28	34.56	0.0	.1994E-04	.199E-04	.595	.7042E+05
1	1	1.000	36.16	0.0	18.08	36.16	0.0	.2287E-04	.229E-04	.648	.7294E+05
1	1	1.000	37.84	0.0	18.92	37.84	0.0	.2629E-04	.263E-04	.707	.7533E+05
1	1	1.000	39.61	0.0	19.80	39.61	0.0	.3028E-04	.303E-04	.771	.7759E+05
1	1	1.000	41.48	0.0	20.74	41.48	0.0	.3497E-04	.350E-04	.841	.7973E+05
1	1	1.000	43.47	0.0	21.74	43.47	0.0	.4050E-04	.405E-04	.917	.8175E+05

1	1	1.000	45.59	0.0	22.79	45.59	0.0	.4706E-04	.471E-04	1.00	.8364E+05
1	1	1.000	47.84	0.0	23.92	47.84	0.0	.5490E-04	.549E-04	1.09	.8542E+05
1	1	1.000	50.26	0.0	25.13	50.26	0.0	.6434E-04	.643E-04	1.19	.8707E+05
1	1	1.000	52.86	0.0	26.43	52.86	0.0	.7589E-04	.759E-04	1.30	.8861E+05
1	1	1.000	55.68	0.0	27.84	55.68	0.0	.9010E-04	.901E-04	1.41	.9002E+05
1	1	1.000	58.75	0.0	29.37	58.75	0.0	.1079E-03	.108E-03	1.54	.9131E+05
1	1	1.000	62.11	0.0	31.06	62.11	0.0	.1305E-03	.130E-03	1.68	.9249E+05
1	1	1.000	65.84	0.0	32.92	65.84	0.0	.1599E-03	.160E-03	1.83	.9353E+05
1	1	1.000	70.02	0.0	35.01	70.02	0.0	.1991E-03	.199E-03	2.00	.9446E+05
1	1	1.000	74.76	0.0	37.38	74.76	0.0	.2532E-03	.253E-03	2.18	.9526E+05
1	1	1.000	80.21	0.0	40.10	80.21	0.0	.3310E-03	.331E-03	2.38	.9593E+05
1	1	1.000	86.61	0.0	43.31	86.61	0.0	.4498E-03	.450E-03	2.59	.9649E+05
1	1	1.000	94.32	0.0	47.16	94.32	0.0	.6468E-03	.647E-03	2.83	.9691E+05
1	1	1.000	103.87	0.0	51.93	103.87	0.0	.1017E-02	.102E-02	3.08	.9722E+05
1	1	1.000	116.23	0.0	58.12	116.23	0.0	.1891E-02	.189E-02	3.36	.9741E+05
1	1	1.000	133.25	0.0	66.63	133.25	0.0	.5544E-02	.554E-02	3.67	.9750E+05

STRUCTURE HAS FAILED--KMAX.GT.KIC IN DADN SUBROUTINE. NEXT CRACK SIZE EXCEEDS CRITICAL CRACK SIZE.

1	1	1.000	159.07	0.0	79.53	159.07	0.0	.5544E-02	.554E-01	4.00	.9751E+05

FATIGUE CRACK GROWTH ANALYSIS SUMMARY

CRACK DIMENSION(S) A(I)	ALTERNATING STRESS INTENSITY FACTOR(S) FOR FIRST INPUT LOAD TRANSIENT DELTA K(I)	TOTAL CRACK GROWTH RATE(S) DADN(I)	NUMBER OF CYCLES OR BLOCKS TO GROW CRACK FROM INITIAL SIZE N
A1	DK1	DADN1	N
0.125	15.710	0.1975E-05	.0
0.136	16.407	0.2236E-05	5373.
0.149	17.134	0.2532E-05	.1055E+05
0.162	17.895	0.2869E-05	.1553E+05
0.177	18.690	0.3251E-05	.2032E+05
0.193	19.520	0.3686E-05	.2494E+05
0.210	20.388	0.4180E-05	.2937E+05
0.229	21.296	0.4743E-05	.3364E+05
0.250	22.244	0.5384E-05	.3774E+05
0.273	23.236	0.6115E-05	.4167E+05
0.297	24.274	0.6950E-05	.4545E+05
0.324	25.359	0.7903E-05	.4907E+05
0.354	26.496	0.8994E-05	.5254E+05
0.386	27.686	0.1024E-04	.5587E+05
0.420	28.933	0.1168E-04	.5906E+05
0.458	30.240	0.1332E-04	.6210E+05
0.500	31.611	0.1522E-04	.6501E+05
0.545	33.051	0.1741E-04	.6778E+05
0.595	34.565	0.1994E-04	.7042E+05
0.648	36.158	0.2287E-04	.7294E+05
0.707	37.837	0.2629E-04	.7533E+05
0.771	39.610	0.3028E-04	.7759E+05
0.841	41.485	0.3497E-04	.7973E+05
0.917	43.474	0.4050E-04	.8175E+05
1.000	45.589	0.4706E-04	.8364E+05
1.090	47.844	0.5490E-04	.8542E+05
1.189	50.257	0.6434E-04	.8707E+05
1.297	52.863	0.7589E-04	.8861E+05
1.414	55.679	0.9010E-04	.9002E+05
1.542	58.748	0.1079E-03	.9131E+05
1.682	62.113	0.1305E-03	.9249E+05
1.834	65.843	0.1599E-03	.9353E+05
2.000	70.021	0.1991E-03	.9446E+05
2.181	74.756	0.2532E-03	.9526E+05
2.378	80.207	0.3310E-03	.9593E+05
2.594	86.611	0.4498E-03	.9649E+05
2.828	94.315	0.6468E-03	.9691E+05
3.084	103.866	0.1017E-02	.9722E+05
3.364	116.235	0.1891E-02	.9741E+05
3.668	133.254	0.5544E-02	.9750E+05
4.000	159.068	0.5544E-01	.9751E+05

STRUCTURE FAILED, KMAX .GT. KIC

APPENDIX C.4: Example 4 - Pressure Vessel Nozzle Corner Crack Under Two Loading Transients

BIGIF: BOUNDARY INTEGRAL EQUATION GENERATED INFLUENCE FUNCTIONS FOR USE IN FRACTURE MECHANICS PROBLEMS

EXAMPLE 4 - NOZZLE CORNER CRACK UNDER PRESSURE + THERMAL STRESS

PMB01DEC76

A "->" MARKS THE OPTION SELECTED

ANALYSIS SELECTION (IFAT)

```
      0 SINGLE K CALCULATION
->    1 FATIGUE ANALYSIS
```

CRACK GEOMETRY MODEL INDEX NUMBER (IFI)

```
      0 K VALUES KNOWN, NO IF CALC.
    101 K = SIGMA*SQRT(PI*A)
    102 K = 1.12* SIGMA* SQRT(PI*A)
    201 CENTER CRACKED PANEL, MODE I
    202 CENTER CRACKED PANEL, MODE II
    203 CENTER CRACKED PANEL, MODE III
    204 EDGE CRACK, MODE I
    205 EDGE CRACK, MODE II (INACTIVE)
    206 EDGE CRACK, MODE III (INACTIVE)
    207 SNOW PLAY (INACTIVE)
-> 300 NOZ BLEND RADIUS CORNERCRACK
    301 BURIED CIRCULAR CRACK
    302 SURFACE 1/2 CIRCULAR CRACK
    303 SURFACE 1/4 CIRCULAR CRACK
    304 4-DOF BURIED CRACK
    305 3-DOF SURFACE CRACK
    306 2-DOF CORNER CRACK
```

VARIABLE THICKNESS SPECIFICATION (NTH)

```
->    0 CONSTANT BODY THICKNESS
      1 VARIABLE BODY THICKNESS
```

CRACK GROWTH RATE RULE (IDADN)

```
      1 PARIS RULE, INPUT C,XN (DEFAULT)
      2 INPUT TABULAR DA/DN, DELTA-K DATA
      3 FORMAN RULE, INPUT C,XN FOR EXPECTED R
      4 FORMAN RULE, INPUT C,XN AND R
      5 INPUT TABULAR DA/DN,DELTA-K DATA AND R
->    6 SAME AS #5 BUT FOR UP TO FIVE R VALUES
```

INTEGRATION INCREMENT SCHEME (INUM)

```
      1 COARSE INTEGRATION SCHEME (DEFAULT)
->    2 STANDARD
      3 REFINED
```

SINGLE OR MULT INTEGRATION SCHEMES (INCL)

```
      0 SINGLE
->    1 MULTIPLE
```

INCREMENTS USED TO DOUBLE CRACK SIZE (NDUB)

-> COARSE = 2
-> STANDARD = 4
REFINED = 8

NUMBER OF DEGREES OF FREEDOM = 1

INITIAL A-VALUES FOR EACH DEGREE OF FREEDOM

CRACK LENGTH AI(1) = 0.40000E-02

GEOMETRY FACTORS

G(1)	0.10000E+04	BODY WIDTH
G(2)	0.0	
*G(3)	0.24400E+01	NOZZLE BLEND RADIUS (RB)
*G(4)	0.30000E+01	CRACK ORIGIN LOCATOR (NOZZLE SIDE = 1, BLEND RADIUS ARC = 2, VESSEL SIDE = 3)
*G(5)	0.15000E+02	CRACK ORIGIN POSITION
G(6)	0.0	
G(7)	0.0	
G(8)	0.0	

DA/DN OPTION SELECTED: 6

KIC = 0.30000E+03 FRACTURE TOUGHNESS

THERE ARE SETS OF INPUT DATA FOR 4 R-RATIOS

R-RATIO = 0.0 6 POINTS INPUT

DELTA-K	DA/DN
0.50000E+00	0.10000E-27
0.52000E+01	0.10000E-07
0.55000E+01	0.20000E-07
0.65000E+01	0.70000E-07
0.75000E+01	0.13000E-06
0.83000E+02	0.10000E-02

R-RATIO = 0.50000E+00 6 POINTS INPUT

DELTA-K	DA/DN
0.35300E+00	0.10000E-27
0.36800E+01	0.10000E-07
0.38900E+01	0.20000E-07
0.46000E+01	0.70000E-07
0.53000E+01	0.13000E-06
0.58700E+02	0.10000E-02

R-RATIO = 0.90000E+00 6 POINTS INPUT

DELTA-K	DA/DN
0.15810E+00	0.10000E-27
0.16440E+01	0.10000E-07
0.17390E+01	0.20000E-07

*NOTE: In this example, these dimensions do not affect results since K(a) is specified rather than calculated.

```
0.20600E+01 0.70000E-07
0.23700E+01 0.13000E-06
0.26200E+02 0.10000E-02

R-RATIO =  0.99000E+00      6 POINTS INPUT
    DELTA-K      DA/DN
0.50000E-01 0.10000E-27
0.52000E+00 0.10000E-07
0.55000E+00 0.20000E-07
0.65000E+00 0.70000E-07
0.75000E+00 0.13000E-06
0.83000E+01 0.10000E-02
```

LOAD TRANSIENTS: 2 TRANSIENT(S) IN PROBLEM EXAMPLE 4 - NOZZLE CORNER CRACK UNDER PRESSURE + THERMAL STRESS PMB01DEC76

NUMBER	NAME	NUMBER OF CYCLES PER BLOCK	SPECIFIER	AGLD	IPSRD	IPLD	KAME	IWO	NPX	NPY
1	PRES + THERM WITH R=0	0.15000E+02	1	0.0	3	0	0	0	0	0
			2	0.10000E+01	2	6	0	0	9	0

NEEDED ADDITIONAL INFORMATION
(DEPENDS ON VALUE OF IPLD)

K VERSUS A TABLE

X	K(A)
0.0	0.0
0.12500E+00	0.59200E+02
0.25000E+00	0.81400E+02
0.50000E+00	0.10830E+03
0.10000E+01	0.13580E+03
0.20000E+01	0.14950E+03
0.40000E+01	0.13880E+03
0.60000E+01	0.20000E+03
0.90000E+01	0.10000E+04

2	THERMALS ONLY	0.60000E+02	1	0.10000E+01	1	6	0	0	9	0

NEEDED ADDITIONAL INFORMATION
(DEPENDS ON VALUE OF IPLD)

K VERSUS A TABLE

X	K(A)
0.0	0.0
0.12500E+00	0.16000E+02
0.25000E+00	0.22600E+02
0.50000E+00	0.31600E+02
0.10000E+01	0.43600E+02
0.20000E+01	0.57700E+02
0.40000E+01	0.69800E+02
0.60000E+01	0.10000E+03
0.90000E+01	0.50000E+03

			2	0.10000E+01	0	6	1	2	0	0

DETAILED OUTPUT FOR ALL LOAD TRANSIENT(S) AND CRACK DEGREE(S) OF FREEDOM

INTEGRATION BREAKUP ********** * COARSE * **********

EXAMPLE 4 - NOZZLE CORNER CRACK UNDER PRESSURE + THERMAL STRESS PMB01DEC76

TRANSIENT NUMBER	DEGREE OF FREEDOM	CYCLES /BLOCK	KMAX	KMIN	KMEAN	DEL-K	R-RAT	TRANSIENT DA/DN (PER CYCLE)	DA/DN (PER BLOCK)	DOF CRACK SIZE	N
1	1	15.00	10.59	0.0	5.30	10.59	0.0	.4695E-06	.241E-04	.400E-02	.0
2	1	60.00	10.59	2.86	6.73	7.73	0.270	.2850E-06			
1	1	15.00	12.59	0.0	6.30	12.59	0.0	.8949E-06	.460E-04	.566E-02	47.27
2	1	60.00	12.59	3.40	8.00	9.19	0.270	.5422E-06			
1	1	15.00	14.98	0.0	7.49	14.98	0.0	.1706E-05	.875E-04	.800E-02	82.39
2	1	60.00	14.98	4.05	9.51	10.93	0.270	.1031E-05			
1	1	15.00	17.81	0.0	8.91	17.81	0.0	.3251E-05	.166E-03	.113E-01	108.5
2	1	60.00	17.81	4.81	11.31	13.00	0.270	.1961E-05			
1	1	15.00	21.18	0.0	10.59	21.18	0.0	.6197E-05	.316E-03	.160E-01	127.9
2	1	60.00	21.18	5.72	13.45	15.46	0.270	.3725E-05			
1	1	15.00	25.19	0.0	12.59	25.19	0.0	.1181E-04	.602E-03	.226E-01	142.3
2	1	60.00	25.19	6.81	16.00	18.38	0.270	.7074E-05			
1	1	15.00	29.95	0.0	14.98	29.95	0.0	.2251E-04	.114E-02	.320E-01	153.1
2	1	60.00	29.95	8.10	19.02	21.86	0.270	.1342E-04			
1	1	15.00	35.62	0.0	17.81	35.62	0.0	.4291E-04	.217E-02	.453E-01	161.1
2	1	60.00	35.62	9.63	22.62	25.99	0.270	.2543E-04			
1	1	15.00	42.36	0.0	21.18	42.36	0.0	.8178E-04	.411E-02	.640E-01	167.1
2	1	60.00	42.36	11.45	26.90	30.91	0.270	.4813E-04			
1	1	15.00	50.37	0.0	25.19	50.37	0.0	.1559E-03	.779E-02	.905E-01	171.5
2	1	60.00	50.37	13.61	31.99	36.76	0.270	.9092E-04			
1	1	15.00	59.84	0.0	29.92	59.84	0.0	.2959E-03	.147E-01	.128	174.9
2	1	60.00	59.84	16.19	38.01	43.65	0.271	.1705E-03			
1	1	15.00	70.10	0.0	35.05	70.10	0.0	.5333E-03	.260E-01	.181	177.5
2	1	60.00	70.10	19.24	44.67	50.86	0.274	.3002E-03			
1	1	15.00	82.17	0.0	41.09	82.17	0.0	.9635E-03	.461E-01	.256	179.5
2	1	60.00	82.17	22.86	52.52	59.32	0.278	.5280E-03			
1	1	15.00	94.61	0.0	47.30	94.61	0.0	.1628E-02	.759E-01	.362	181.3
2	1	60.00	94.61	27.02	60.81	67.59	0.286	.8583E-03			
1	1	15.00	109.09	0.0	54.55	109.09	0.0	.2766E-02	.125	.512	182.8
2	1	60.00	109.09	31.95	70.52	77.15	0.293	.1395E-02			
1	1	15.00	121.80	0.0	60.90	121.80	0.0	.4169E-02	.181	.724	184.2
2	1	60.00	121.80	37.49	79.65	84.31	0.308	.1974E-02			

1	1	15.00	136.19	0.0	68.10	136.19	0.0	.6318E-02	.262	1.02	185.5
2	1	60.00	136.19	44.01	90.10	92.19	0.323	.2787E-02			
1	1	15.00	142.53	0.0	71.26	142.53	0.0	.7483E-02	.294	1.45	187.0
2	1	60.00	142.53	50.52	96.53	92.00	0.354	.3027E-02			
1	1	15.00	149.19	0.0	74.60	149.19	0.0	.8870E-02	.329	2.05	189.0
2	1	60.00	149.19	58.05	103.62	91.14	0.389	.3268E-02			
1	1	15.00	144.25	0.0	72.12	144.25	0.0	.7824E-02	.271	2.90	191.8
2	1	60.00	144.25	63.64	103.94	80.60	0.441	.2555E-02			
1	1	15.00	142.05	0.0	71.02	142.05	0.0	.7389E-02	.232	4.10	196.6
2	1	60.00	142.05	71.40	106.72	70.64	0.503	.2012E-02			
1	1	15.00	194.18	0.0	97.09	194.18	0.0	.2366E-01	.745	5.79	200.0
2	1	60.00	194.18	97.13	145.66	97.05	0.500	.6502E-02			

STRUCTURE HAS FAILED--KMAX.GT.KIC IN DADN SUBROUTINE. NEXT CRACK SIZE EXCEEDS CRITICAL CRACK SIZE.

1	1	15.00	799.68	0.0	399.84	799.68	0.0	.2366E-01	7.45	8.19	200.6
2	1	60.00	799.68	399.84	599.76	399.84	0.500	.6502E-02			

FATIGUE CRACK GROWTH ANALYSIS SUMMARY

CRACK DIMENSION(S) A(I)	ALTERNATING STRESS INTENSITY FACTOR(S) FOR FIRST INPUT LOAD TRANSIENT DELTA K(I)	TOTAL CRACK GROWTH RATE(S) DADN(I)	NUMBER OF CYCLES OR BLOCKS TO GROW CRACK FROM INITIAL SIZE N
A1	DK1	DADN1	N
0.004	10.590	0.2414E-04	.0
0.006	12.594	0.4596E-04	47.27
0.008	14.977	0.8746E-04	82.39
0.011	17.810	0.1664E-03	108.5
0.016	21.180	0.3165E-03	127.9
0.023	25.187	0.6016E-03	142.3
0.032	29.953	0.1143E-02	153.1
0.045	35.620	0.2170E-02	161.1
0.064	42.360	0.4115E-02	167.1
0.091	50.375	0.7793E-02	171.5
0.128	59.839	0.1467E-01	174.9
0.181	70.101	0.2601E-01	177.5
0.256	82.174	0.4613E-01	179.5
0.362	94.609	0.7592E-01	181.3
0.512	109.092	0.1252E+00	182.8
0.724	121.803	0.1810E+00	184.2
1.024	136.194	0.2620E+00	185.5
1.448	142.527	0.2939E+00	187.0
2.048	149.192	0.3291E+00	189.0
2.896	144.246	0.2707E+00	191.8
4.096	142.047	0.2316E+00	196.6
5.793	194.184	0.7450E+00	200.0
8.192	799.681	0.7450E+01	200.6

STRUCTURE FAILED, KMAX .GT. KIC

DETAILED OUTPUT FOR ALL LOAD TRANSIENT(S) AND CRACK DEGREE(S) OF FREEDOM

INTEGRATION BREAKUP ********** * STANDARD * ********** EXAMPLE 4 - NOZZLE CORNER CRACK UNDER PRESSURE + THERMAL STRESS PMB01DEC76

TRANSIENT NUMBER	DEGREE OF FREEDOM	CYCLES /BLOCK	KMAX	KMIN	KMEAN	DEL-K	R-RAT	TRANSIENT DA/DN (PER CYCLE)	DA/DN (PER BLOCK)	DOF CRACK SIZE	N
1	1	15.00	10.59	0.0	5.30	10.59	0.0	.4695E-06	.241E-04	.400E-02	.0
2	1	60.00	10.59	2.86	6.73	7.73	0.270	.2850E-06			
1	1	15.00	11.55	0.0	5.77	11.55	0.0	.6482E-06	.333E-04	.476E-02	26.35
2	1	60.00	11.55	3.12	7.33	8.43	0.270	.3931E-06			
1	1	15.00	12.59	0.0	6.30	12.59	0.0	.8949E-06	.460E-04	.566E-02	49.05
2	1	60.00	12.59	3.40	8.00	9.19	0.270	.5422E-06			
1	1	15.00	13.73	0.0	6.87	13.73	0.0	.1236E-05	.634E-04	.673E-02	68.63
2	1	60.00	13.73	3.71	8.72	10.02	0.270	.7478E-06			
1	1	15.00	14.98	0.0	7.49	14.98	0.0	.1706E-05	.875E-04	.800E-02	85.50
2	1	60.00	14.98	4.05	9.51	10.93	0.270	.1031E-05			
1	1	15.00	16.33	0.0	8.17	16.33	0.0	.2355E-05	.121E-03	.951E-02	100.0
2	1	60.00	16.33	4.41	10.37	11.92	0.270	.1422E-05			
1	1	15.00	17.81	0.0	8.91	17.81	0.0	.3251E-05	.166E-03	.113E-01	112.6
2	1	60.00	17.81	4.81	11.31	13.00	0.270	.1961E-05			
1	1	15.00	19.42	0.0	9.71	19.42	0.0	.4488E-05	.229E-03	.135E-01	123.4
2	1	60.00	19.42	5.25	12.34	14.17	0.270	.2703E-05			
1	1	15.00	21.18	0.0	10.59	21.18	0.0	.6197E-05	.316E-03	.160E-01	132.7
2	1	60.00	21.18	5.72	13.45	15.46	0.270	.3725E-05			
1	1	15.00	23.10	0.0	11.55	23.10	0.0	.8555E-05	.436E-03	.190E-01	140.8
2	1	60.00	23.10	6.24	14.67	16.85	0.270	.5134E-05			
1	1	15.00	25.19	0.0	12.59	25.19	0.0	.1181E-04	.602E-03	.226E-01	147.7
2	1	60.00	25.19	6.81	16.00	18.38	0.270	.7074E-05			
1	1	15.00	27.47	0.0	13.73	27.47	0.0	.1631E-04	.829E-03	.269E-01	153.7
2	1	60.00	27.47	7.42	17.45	20.04	0.270	.9744E-05			
1	1	15.00	29.95	0.0	14.98	29.95	0.0	.2251E-04	.114E-02	.320E-01	158.9
2	1	60.00	29.95	8.10	19.02	21.86	0.270	.1342E-04			
1	1	15.00	32.66	0.0	16.33	32.66	0.0	.3108E-04	.157E-02	.381E-01	163.3
2	1	60.00	32.66	8.83	20.75	23.84	0.270	.1848E-04			
1	1	15.00	35.62	0.0	17.81	35.62	0.0	.4291E-04	.217E-02	.453E-01	167.2
2	1	60.00	35.62	9.63	22.62	25.99	0.270	.2543E-04			
1	1	15.00	38.84	0.0	19.42	38.84	0.0	.5924E-04	.299E-02	.538E-01	170.5
2	1	60.00	38.84	10.50	24.67	28.35	0.270	.3500E-04			

1	1	15.00	42.36	0.0	21.18	42.36	0.0	.8178E-04	.411E-02	.640E-01	173.3
2	1	60.00	42.36	11.45	26.90	30.91	0.270	.4813E-04			
1	1	15.00	46.19	0.0	23.10	46.19	0.0	.1129E-03	.566E-02	.761E-01	175.8
2	1	60.00	46.19	12.48	29.34	33.71	0.270	.6617E-04			
1	1	15.00	50.37	0.0	25.19	50.37	0.0	.1559E-03	.779E-02	.905E-01	178.0
2	1	60.00	50.37	13.61	31.99	36.76	0.270	.9092E-04			
1	1	15.00	54.93	0.0	27.47	54.93	0.0	.2152E-03	.107E-01	.108	179.8
2	1	60.00	54.93	14.85	34.89	40.09	0.270	.1248E-03			
1	1	15.00	59.84	0.0	29.92	59.84	0.0	.2959E-03	.147E-01	.128	181.4
2	1	60.00	59.84	16.19	38.01	43.65	0.271	.1705E-03			
1	1	15.00	64.75	0.0	32.37	64.75	0.0	.3968E-03	.195E-01	.152	182.8
2	1	60.00	64.75	17.65	41.20	47.10	0.273	.2261E-03			
1	1	15.00	70.10	0.0	35.05	70.10	0.0	.5333E-03	.260E-01	.181	184.1
2	1	60.00	70.10	19.24	44.67	50.86	0.274	.3002E-03			
1	1	15.00	75.94	0.0	37.97	75.94	0.0	.7182E-03	.347E-01	.215	185.2
2	1	60.00	75.94	20.98	48.46	54.96	0.276	.3993E-03			
1	1	15.00	82.17	0.0	41.09	82.17	0.0	.9635E-03	.461E-01	.256	186.2
2	1	60.00	82.17	22.86	52.52	59.32	0.278	.5280E-03			
1	1	15.00	88.12	0.0	44.06	88.12	0.0	.1250E-02	.591E-01	.304	187.2
2	1	60.00	88.12	24.85	56.49	63.27	0.282	.6721E-03			
1	1	15.00	94.61	0.0	47.30	94.61	0.0	.1628E-02	.759E-01	.362	188.0
2	1	60.00	94.61	27.02	60.81	67.59	0.286	.8583E-03			
1	1	15.00	101.68	0.0	50.84	101.68	0.0	.2129E-02	.979E-01	.431	188.8
2	1	60.00	101.68	29.39	65.53	72.30	0.289	.1099E-02			
1	1	15.00	109.09	0.0	54.55	109.09	0.0	.2766E-02	.125	.512	189.5
2	1	60.00	109.09	31.95	70.52	77.15	0.293	.1395E-02			
1	1	15.00	115.17	0.0	57.59	115.17	0.0	.3385E-02	.150	.609	190.2
2	1	60.00	115.17	34.60	74.89	80.57	0.300	.1655E-02			
1	1	15.00	121.80	0.0	60.90	121.80	0.0	.4169E-02	.181	.724	190.9
2	1	60.00	121.80	37.49	79.65	84.31	0.308	.1974E-02			
1	1	15.00	129.03	0.0	64.52	129.03	0.0	.5167E-02	.219	.861	191.6
2	1	60.00	129.03	40.65	84.84	88.39	0.315	.2365E-02			
1	1	15.00	136.19	0.0	68.10	136.19	0.0	.6318E-02	.262	1.02	192.3
2	1	60.00	136.19	44.01	90.10	92.19	0.323	.2787E-02			
1	1	15.00	139.22	0.0	69.61	139.22	0.0	.6857E-02	.277	1.22	193.0
2	1	60.00	139.22	47.12	93.17	92.10	0.338	.2900E-02			
1	1	15.00	142.53	0.0	71.26	142.53	0.0	.7483E-02	.294	1.45	193.8
2	1	60.00	142.53	50.52	96.53	92.00	0.354	.3027E-02			
1	1	15.00	146.13	0.0	73.06	146.13	0.0	.8211E-02	.314	1.72	194.7
2	1	60.00	146.13	54.23	100.18	91.90	0.371	.3172E-02			

1	1	15.00	149.19	0.0	74.60	149.19	0.0	.8870E-02	.329	2.05	195.7
2	1	60.00	149.19	58.05	103.62	91.14	0.389	.3268E-02			
1	1	15.00	146.83	0.0	73.41	146.83	0.0	.8358E-02	.301	2.44	197.0
2	1	60.00	146.83	60.72	103.77	86.10	0.414	.2920E-02			
1	1	15.00	144.25	0.0	72.12	144.25	0.0	.7824E-02	.271	2.90	198.6
2	1	60.00	144.25	63.64	103.94	80.60	0.441	.2555E-02			
1	1	15.00	141.43	0.0	70.72	141.43	0.0	.7271E-02	.240	3.44	200.7
2	1	60.00	141.43	66.82	104.13	74.61	0.472	.2179E-02			
1	1	15.00	142.05	0.0	71.02	142.05	0.0	.7389E-02	.232	4.10	203.5
2	1	60.00	142.05	71.40	106.72	70.64	0.503	.2012E-02			
1	1	15.00	166.99	0.0	83.49	166.99	0.0	.1349E-01	.424	4.87	205.9
2	1	60.00	166.99	83.71	125.35	83.28	0.501	.3696E-02			
1	1	15.00	194.18	0.0	97.09	194.18	0.0	.2366E-01	.745	5.79	207.4
2	1	60.00	194.18	97.13	145.66	97.05	0.500	.6502E-02			

STRUCTURE HAS FAILED--KMAX.GT.KIC IN DADN SUBROUTINE. NEXT CRACK SIZE EXCEEDS CRITICAL CRACK SIZE.

1	1	15.00	454.48	0.0	227.24	454.48	0.0	.2366E-01	7.45	6.89	207.7
2	1	60.00	454.48	227.24	340.86	227.24	0.500	.6502E-02			

FATIGUE CRACK GROWTH ANALYSIS SUMMARY

CRACK DIMENSION(S) A(I)	ALTERNATING STRESS INTENSITY FACTOR(S) FOR FIRST INPUT LOAD TRANSIENT DELTA K(I)	TOTAL CRACK GROWTH RATE(S) DADN(I)	NUMBER OF CYCLES OR BLOCKS TO GROW CRACK FROM INITIAL SIZE N
A1	DK1	DADN1	N
0.004	10.590	0.2414E-04	.0
0.005	11.548	0.3331E-04	26.35
0.006	12.594	0.4596E-04	49.05
0.007	13.734	0.6340E-04	68.63
0.008	14.977	0.8746E-04	85.50
0.010	16.332	0.1206E-03	100.0
0.011	17.810	0.1664E-03	112.6
0.013	19.422	0.2295E-03	123.4
0.016	21.180	0.3165E-03	132.7
0.019	23.097	0.4364E-03	140.8
0.023	25.187	0.6016E-03	147.7
0.027	27.467	0.8293E-03	153.7
0.032	29.953	0.1143E-02	158.9
0.038	32.664	0.1575E-02	163.3
0.045	35.620	0.2170E-02	167.2
0.054	38.844	0.2988E-02	170.5
0.064	42.360	0.4115E-02	173.3
0.076	46.194	0.5664E-02	175.8
0.091	50.375	0.7793E-02	178.0
0.108	54.934	0.1072E-01	179.8
0.128	59.839	0.1467E-01	181.4
0.152	64.748	0.1951E-01	182.8
0.181	70.101	0.2601E-01	184.1
0.215	75.938	0.3473E-01	185.2
0.256	82.174	0.4613E-01	186.2
0.304	88.122	0.5907E-01	187.2
0.362	94.609	0.7592E-01	188.0
0.431	101.682	0.9788E-01	188.8
0.512	109.092	0.1252E+00	189.5
0.609	115.172	0.1501E+00	190.2
0.724	121.803	0.1810E+00	190.9
0.861	129.034	0.2194E+00	191.6
1.024	136.194	0.2620E+00	192.3
1.218	139.224	0.2768E+00	193.0
1.448	142.527	0.2939E+00	193.8
1.722	146.129	0.3135E+00	194.7
2.048	149.192	0.3291E+00	195.7
2.435	146.826	0.3005E+00	197.0
2.896	144.246	0.2707E+00	198.6
3.444	141.433	0.2398E+00	200.7
4.096	142.047	0.2316E+00	203.5
4.871	166.987	0.4241E+00	205.9
5.793	194.184	0.7450E+00	207.4
6.889	454.479	0.7450E+01	207.7

STRUCTURE FAILED, KMAX .GT. KIC

APPENDIX D

CONVERSION FACTORS FOR LEFM UNITS

Quantity	To Convert From	To	Multiply by
Length	in	m	2.54×10^{-2}
	in	cm	2.54
Area	in^2	m^2	6.4516×10^{-4}
	in^2	cm^2	6.4516
Force	lbf	N	4.448222
Stress	psi	Pa	6.894757×10^{3}
	ksi	MN/m^2	6.894757
Energy	Ft-lbf	J	1.355818
	in-lbf	Nm	1.129848×10^{-1}
Fracture Toughness	$ksi\sqrt{in}$	$Pa\sqrt{m}$	1.0988×10^{-6}
	$ksi\sqrt{in}$	$MN/m^{3/2}$	1.0988
	$ksi\sqrt{in}$	$MN/cm^{3/2}$	1.0988×10^{-3}

List of Symbols:

in = inches	N = Newton	Pa = Pascal (N/m^2)
m = meters	MN = Mega-Newton	psi = $pounds/in^2$
cm = centimeters	Nm = Newton meter	ksi = $kilopounds/in^2$
lbf = pounds force	J = Joule	

4.0 FLAW MODEL LIBRARY

4.1 Library Description

The flaw model library in the BIGIF program is divided into three classes: a special case (non-IF) class, a two-dimensional IF model class, and a three-dimensional IF model class. In the first production version of BIGIF, there are thirteen flaw models, two in the special library class, four general two-dimensional models, and seven general three-dimensional models. A summary of these three model classes showing the capabilities and options is given in Table 4.1. The model degrees-of-freedom (IDOF), crack shape, and crack mode describe the general behavior of the model. IDOF refers to the number of degress-of-freedom where each degree of freedom is a distinct independent crack front coordinate which is allowed to change during the analysis. If IDOF = 1 and the crack shape is circular, the radius is the only degree of freedom and the crack front will grow in fatigue as a series of concentric circular arcs of ever-increasing radii. The crack mode refers to the crack face opening direction; I is normal or perpendicular opening mode, II is in-plane shearing mode and III is out-of-plane shearing mode. Finite body width effects, if included, account for the proximity of the surface(s). A variable body thickness specification is allowed for the two-dimensional models where the effect of a non-uniform thickness is approximately accounted for in the model discussed in Section 2.5. All flaw models in BIGIF were formulated from plane or solid rectangular bodies ($r = \infty$); therefore, none of the models can handle curved geometries. In most applications, however, the situation of large r/w and/or small a/r makes any curvature

TABLE 4.1

FLAW MODEL LIBRARY IN BIGIF

Library Class	Class Index (IFI)	Crack Geometry Description	Degrees-of-Freedom (IDOF)	Crack Shape	Crack Mode	Finite Width Effects	Variable Thickness (NTH)	Curvature	Stress Input[1]
Special Cases	101	Center Cracked Infinite Plate in Tension	1	Straight	I	No	No	No	Uniform
	102	Edge Crack Semi-Infinite Plate in Tension	1	Straight	I	No	No	No	Uniform
Two-Dimensional	201	Center Cracked Plate, Mode I	1	Straight	I	Yes	Yes	No	General[2]
	202	Center Cracked Plate, Mode II	1	Straight	II	Yes	Yes	No	General[2]
	203	Center Cracked Plate, Mode III	1	Straight	III	Yes	Yes	No	General[2]
	204	Edge Cracked Plate, Mode I	1	Straight	I	Yes[3]	Yes	No	General
	205	Edge Cracked Plate, Mode II (Inactive)	1	Straight	II	Yes	Yes	No	General
	206	Edge Cracked Plate, Mode III (Inactive)	1	Straight	III	Yes	Yes	No	General
Three-Dimensional	300	Nozzle Blend Radius Circular Corner Crack	1	1/2 Circular	I	No	No	No	General
	301	Buried Circular Crack	1	Circular	I	No	No	No	General
	302	Circular Surface Crack	1	1/2 Circular	I	No	No	No	General
	303	Circular Corner Crack	1	1/4 Circular	I	No	No	No	General
	304	Buried Elliptical Crack	4	Elliptical	I	No	No	No	General
	305	Elliptical Surface Crack	3	1/2 Elliptical	I	No	No	No	General
	306	Elliptical Corner Crack	2	1/4 Elliptical	I	No	No	No	General

Notes:

1) General stress input for two-dimensional crack model implies any $\sigma(x)$ variation; for three-dimensional models, the general stress variation is $\sigma(x,y)$.

2) $\sigma(x)$ must be symmetric about the z axis.

3) The influence function is accurate for $0 \leq a/w \leq 0.6$

effects* on influence functions small enough to be neglected.

The special case non-IF category, designated by the 100-series class index (IFI), involves stress intensity factor (K) solutions in the literature for uniform or other simple stress fields. It is the intent of the special case series to allow the user to select these simple solutions when it is known that the stress variation is not important. This will result in computer cost savings over inputting uniform stress states into the "general stress" two- or three-dimensional models.

The "general stress" two-dimensional (200 series) and three-dimensional (300 series) IF model libraries contain powerful crack solutions for K under any general varying applied stress distribution. For two-dimensional geometries the general stress input is a univariate stress field, $\sigma(x)$, and for the three-dimensional case, either $\sigma(x)$ or a bivariate distribution $\sigma(x,y)$ is assumed. In some cases, $\bar{K}$ computational errors are estimated from known errors for numerical influence functions. The errors quoted below do not include the numerical integration errors of Table 3.4

Sections 4.2 through 4.4 give full details for all flaw models within BIGIF. Two Cartesian coordinate systems are used in specifying flaw model input. The global coordinate system (x,y) is used to specify the stress functions $\sigma(x)$ and/or $\sigma(x,y)$ and a local coordinate system (x',y') for the crack defines the crack origin and orientation relative to the global system.

---

*The effects of curvature and finite width on the uncracked stress field $\sigma(x,y)$ are almost always non-negligible and must be accounted for in the stress analysis. However, the IF, which represent the influence of a unit crack face load on K, are often much weaker functions of physical dimensions not involving the crack.

The crack origin coordinates (x_c, y_c) and angular position (ϕ) expressed in degrees are shown in Fig. 4.1.

4.2 Special Cases ($100 \leq IFI \leq 199$)

4.2.1 Center Cracked Infinite Plate in Tension (IFI = 101)

The problem of the center through-crack or "tunnel crack" in an infinitely wide plate under uniform tension was originally solved by Irwin (4-1, 4-2) for the general case of the buried ellipse in the limit as the major axis approaches infinity. These results are also reported by Paris and Sih (4-3). For this problem, the Mode I stress intensity factor in terms of half-crack length, a, and applied stress, σ_{zz}, is

$$K_I = \sigma_{zz}\sqrt{\pi a} \ . \qquad (4.1)$$

Table 4.2 shows the crack geometry and summarizes the model capabilities and data input. The applied stress, σ_{zz} is constant and is defined as AGLD from Card E2A.

This simple model has no capability for modeling finite width or variable thickness effects; to obtain those features, even for uniform stress problems, the analyst must use the general center cracked plate model (IFI = 201). The model has only one DOF in that the crack tips ($x = \pm a$) can only propagate in equal increments. Although finite width effects are neglected, the body width, w, is still required as input if the user desires

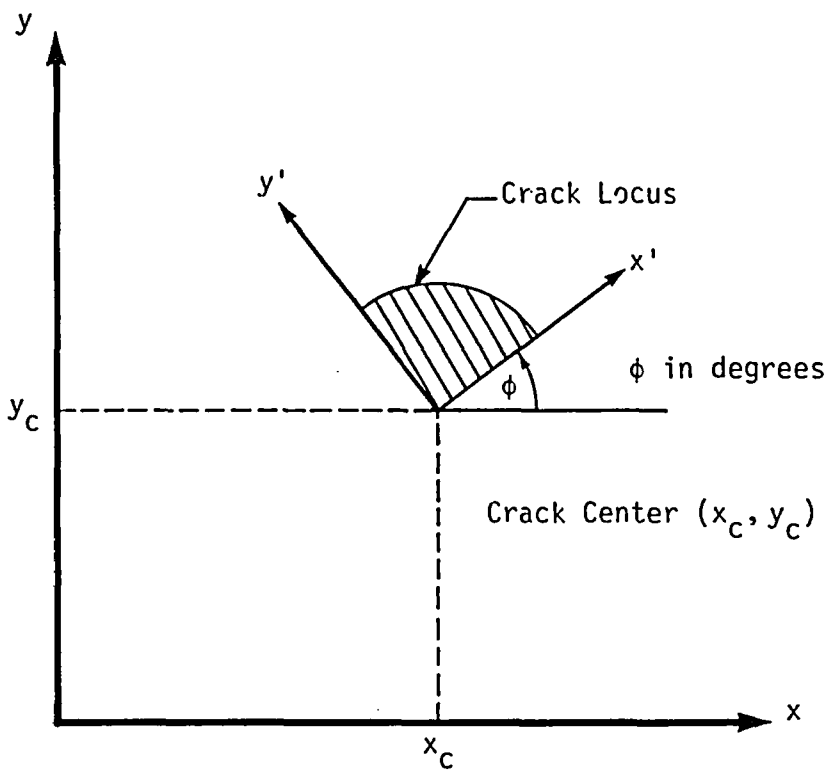

Figure 4.1 - Definition of Global and Local Coordinate Systems.

Table 4.2
IFI = 101 - CENTER-CRACKED INFINITE PLATE IN TENSION

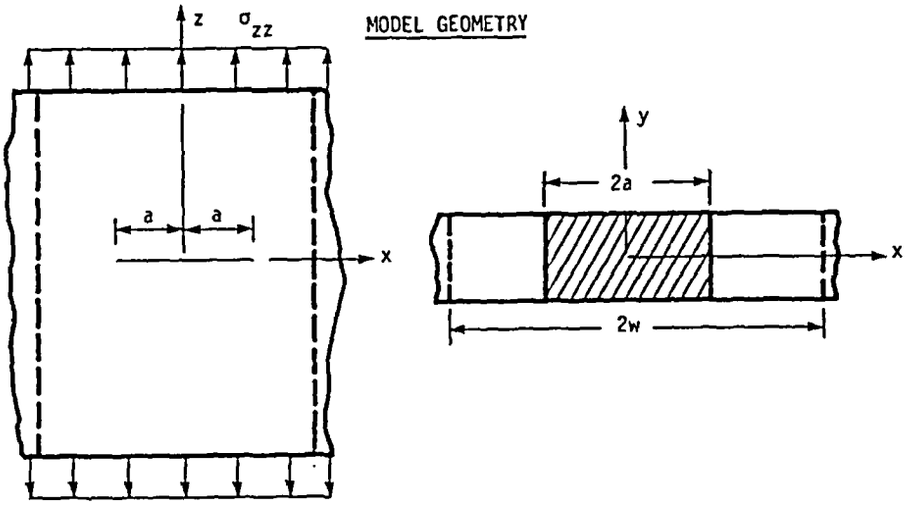

MODEL DESCRIPTION

MODEL FEATURES	PARAMETER	OPTION FEATURED
Model Index Number	IFI	101
Number of Degrees of Freedom	IDOF	1
Crack Front Shape	--	Straight
Crack Opening Mode	--	Mode I
Finite Width Effects	w	No
Variable Thickness Effects	NTH	No

DATA INPUT DESCRIPTION

INPUT DESCRIPTION	PARAMETER	INPUT FORMAT	CARD SERIES	REMARKS
Variable Thickness	NTH	Constant	B	Set NTH = 0 or leave blank
Initial Crack Size, a_i	AI(1)	Constant	C1	
Body Width, w	G(1)	Constant	C2	Only used to terminate analysis when ($a \geq w$)
Crack Coordinates, x_c	G(6)	Constant	C2	Leave blank ($x_c = 0$)
y_c	G(7)	Constant	C2	Leave blank ($y_c = 0$)
Crack Orientation, ϕ	G(8)	Constant	C2	Leave Blank ($\phi = 0$)
Stress Input Option	IPLD	Constant	E2A	Set IPLD = 7
Stress, σ_{zz}	AGLD	Constant	E2A	σ_{zz} = AGLD

to terminate the fatigue analysis (IFAT = 1) when $a \geq w$; otherwise, the problem will stop only when K_I = XKIC.

4.2.2 Edge Cracked Infinite Plate in Tension (IFI = 102)

The problem of the edge cracked plate in tension is similar to the center-cracked plate except a surface correction factor is used to account for the free surface effects of the front surface. The overall effect of the front surface gives rise to approximately a 12% increase in K_I which was originally demonstrated in (4-4, 4-5) and reported in (4-3):

$$K_I = 1.122\, \sigma_{zz}\sqrt{\pi a}\ , \tag{4.2}$$

where a is the crack depth and σ_{zz} is the applied tensile stress. Table 4.3 summarizes the data input required for this model.

Like model 101, finite width and variable thickness effects are neglected. The input for body width, w, is used only to terminate the fatigue analysis (IFAT = 1) if $a \geq w$; otherwise, the crack will stop propagating when $K_I \geq$ XKIC. Nonuniform stress, finite width, and variable thickness effects for an edge cracked plate are accounted for when IFI = 204.

4.3 Two-Dimensional Flaw Model Library ($200 \leq$ IFI ≤ 299)

4.3.1 Center Cracked Plate for Modes I, II, or III (IFI = 201, 202, 203)

The general solution for a center-cracked finite width plate of uniform thickness,when the applied stress is symmetric about the crack

Table 4.3
IFI = 102 - EDGE-CRACKED SEMI-INFINITE PLATE IN TENSION

MODEL GEOMETRY

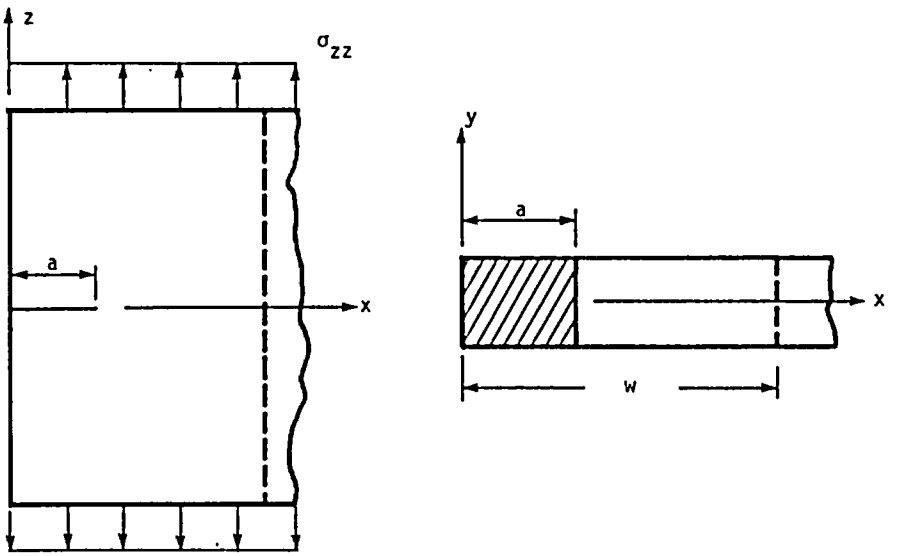

MODEL DESCRIPTION

MODEL FEATURES	PARAMETER	OPTION FEATURED
Model Index Number	IFI	102
Number of Degrees of Freedom	IDOF	1
Crack Front Shape	--	Straight
Crack Opening Mode	--	Mode I
Finite Width Effects	w	No
Variable Thickness Effects	NTH	No

DATA INPUT DESCRIPTION

INPUT DESCRIPTION	PARAMETER	INPUT FORMAT	CARD SERIES	REMARKS
Variable Thickness	NTH	Constant	B	Set NTH = 0 or leave blank
Initial Crack Size, a_i	AI(1)	Constant	C1	
Body Width, w	G(1)	Constant	C2	Only used to terminate analysis when $a \geq w$
Crack Coordinates, x_c	G(6)	Constant	C2	Leave blank ($x_c = 0$)
y_c	G(7)	Constant	C2	Leave blank ($y_c = 0$)
Crack Orientation, ϕ	G(8)	Constant	C2	Leave blank ($\phi = 0$)
Stress Input Option	IPLD	Constant	E2A	Set IPLD = 7
Stress Field, σ_{zz}	AGLD	Constant	E2A	σ_{zz} = AGLD

center (z axis) is given by Tada (4-6) for each of the three crack opening modes. The Mode III IF solution (IFI = 203) is an exact formulation whereas the Modes I and II IF solutions (IFI = 201, 202 respectively) are reported to give results to 1% accuracy. The flaw model geometry and data input are identical for each loading Mode with the only exception being the stress component used as the "uncracked" stress field. For the Mode I model, the normal crack face stress $\sigma_{zz}(x)$ is used; whereas for Modes II and III, the in-plane (σ_{xz}) and out-of-plane shear stress (σ_{yz}) are specified respectively. Tables 4.4 through 4.6 summarize the details for each model.

Since the model can only be used when the stress variation is symmetric, the input regarding the initial flaw size, stress data, and variable thickness data is only specified for $0 \leq x \leq w$. The model accounts for variable thickness effects in an approximate sense in that only the load distribution over the crack face area is considered as discussed in Section 2.5.

4.3.2 Edge Cracked Plate for Modes I, II or III (IFI = 204, 205, 206)

Library model indices 204, 205, and 206 have been assigned to the edge cracked finite width plate model for crack opening Modes I, II, and III respectively. Only Mode I can be used; the flaw models for Modes II and III are inactive but could be added easily. The Mode I model is based on Bueckner's (4-7) weight function solution. The flaw model geometry and data input for IFI = 204 is summarized in Table 4.7.

Table 4.4
IFI = 201 - CENTER-CRACKED PLATE IN MODE I

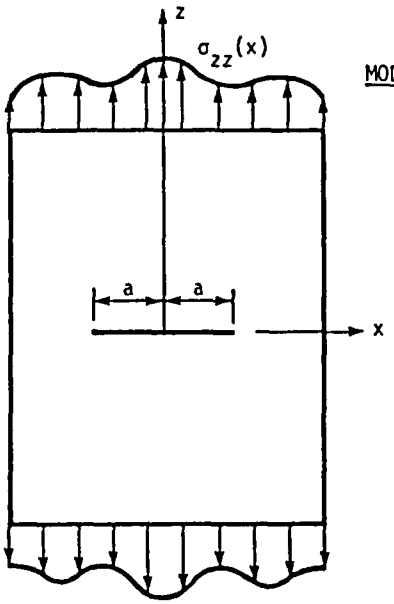

MODEL GEOMETRY

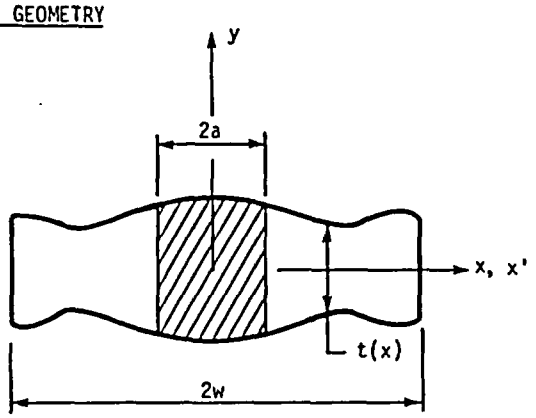

NOTE: Local crack (x') and global model (x) coordinate systems are shown as being coincident ($x_c = 0$)

MODEL DESCRIPTION

MODEL FEATURES	PARAMETER	OPTION FEATURED
Model Index Number	IFI	201
Number of Degrees of Freedom	IDOF	1
Crack Front Shape	--	Straight
Crack Opening Mode	--	Mode I
Finite Width Effects	W	Yes
Variable Thickness Effects	NTH	Yes

DATA INPUT DESCRIPTION

INPUT DESCRIPTION	PARAMETER	INPUT FORMAT	CARD SERIES	REMARKS
Variable Thickness	NTH	Constant	B	
Initial Crack Size, a_i	A1(1)	Constant	C1	
Body Width, w	G(1)	Constant	C2	
Crack Position, x_c	G(6)	Constant	C2	
y_c	G(7)	Constant	C2	Leave blank (y_c=0)
Crack Orientation, ϕ	G(8)	Constant	C2	Leave blank (ϕ = 0)
Thickness Variation, t(x)	XTH(N)	Tabular	C3B	Input required if NTH = 1
	THK(N)	Tabular	C3B	
Load Input Option	IPLD	Constant	E2A	
Stress Field, $\sigma_{zz}(x)$	σ(x)	Equational	E2B	$\sigma_{zz}(x)$ must be symmetric about z axis. Format depends on IPLD.
	CS(IX)	Tabular	E2C	

Table 4.5

IFI = 202 - CENTER-CRACKED PLATE IN MODE II

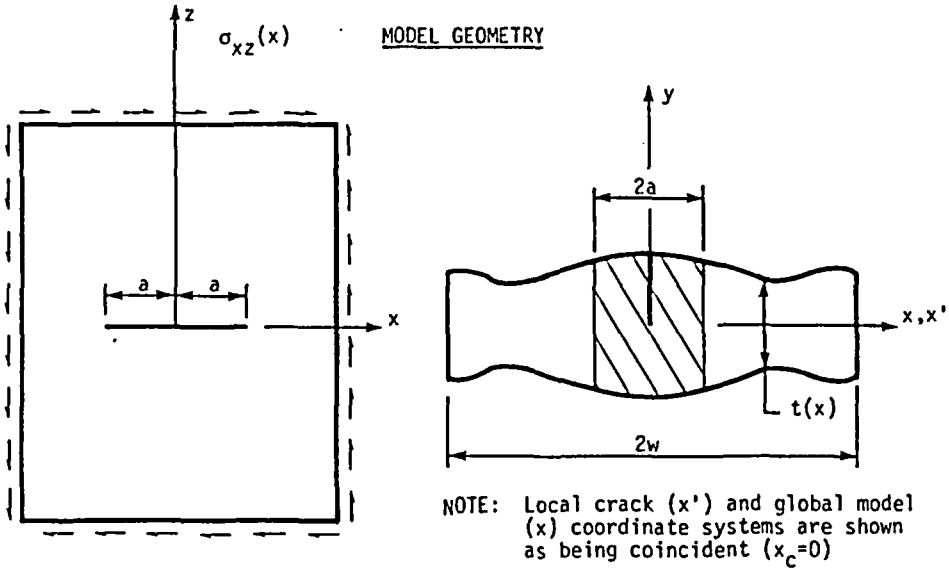

NOTE: Local crack (x') and global model (x) coordinate systems are shown as being coincident (x_c=0)

MODEL DESCRIPTION

MODEL FEATURES	PARAMETER	OPTION FEATURED
Model Index Number	IFI	202
Number of Degrees of Freedom	IDOF	1
Crack Front Shape	--	Straight
Crack Opening Mode	--	Mode II
Finite Width Effects	w	Yes
Variable Thickness Effects	NTH	Yes

DATA INPUT DESCRIPTION

INPUT DESCRIPTION	PARAMETER	INPUT FORMAT	CARD SERIES	REMARKS
Variable Thickness	NTH	Constant	B	
Initial Crack Size, a_i	AI(1)	Constant	C1	
Body Width, w	G(1)	Constant	C2	
Crack Position, x_c	G(6)	Constant	C2	
y_c	G(7)	Constant	C2	Leave blank (y_c=0)
Crack Orientation, ϕ	G(8)	Constant	C2	Leave blank (ϕ=0)
Thickness Variation, t(x)	XTH(N)	Tabular	C3B	Input required if NTH = 1
	THK(N)	Tabular	C3B	
Load Input Option	IPLD	Constant	E2A	
Stress Field, $\sigma_{xz}(x)$	$\sigma(x)$	Equational	E2B	$\sigma_{xz}(x)$ must be symmetric about z axis. Format depends on IPLD.
	CS(IX)	Tabular	E2C	

Table 4.6
IFI = 203 - CENTER-CRACKED PLATE IN MODE III

MODEL GEOMETRY

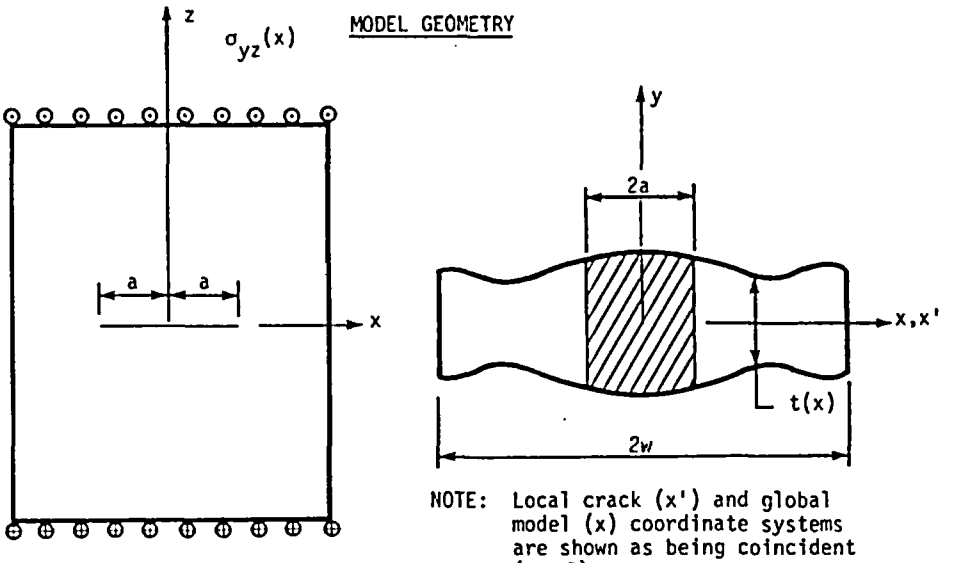

NOTE: Local crack (x') and global model (x) coordinate systems are shown as being coincident ($x_c = 0$)

MODEL DESCRIPTION

MODEL FEATURES	PARAMETER	OPTION FEATURED
Model Index Number	IFI	203
Number of Degrees of Freedom	IDOF	1
Crack Front Shape	--	Straight
Crack Opening Mode	--	Mode III
Finite Width Effects	w	Yes
Variable Thickness Effects	NTH	Yes

DATA INPUT DESCRIPTION

INPUT DESCRIPTION	PARAMETER	INPUT FORMAT	CARD SERIES	REMARKS
Variable Thickness	NTH	Constant	B	
Initial Crack Size, a_i	AI(1)	Constant	C1	
Body Width, w	G(1)	Constant	C2	
Crack Position, x_c	G(6)	Constant	C2	
y_c	G(7)	Constant	C2	Leave blank ($y_c = 0$)
Crack Orientation, ϕ	G(8)	Constant	C2	Leave blank ($\phi = 0$)
Thickness Variation, t(x)	XTH(N)	Tabular	C3B	Input required if NTH = 1
	THK(N)	Tabular	C3B	
Load Input Option	IPLD	Constant	E2A	
Stress Field, $\sigma_{yz}(x)$	$\sigma(x)$	Equational	E2B	$\sigma_{yz}(x)$ must be symmetric about z axis. Format depends on IPLD.
	CS(IX)	Tabular	E2C	

Table 4.7
IFI = 204 - EDGE-CRACKED PLATE IN MODE I

MODEL GEOMETRY

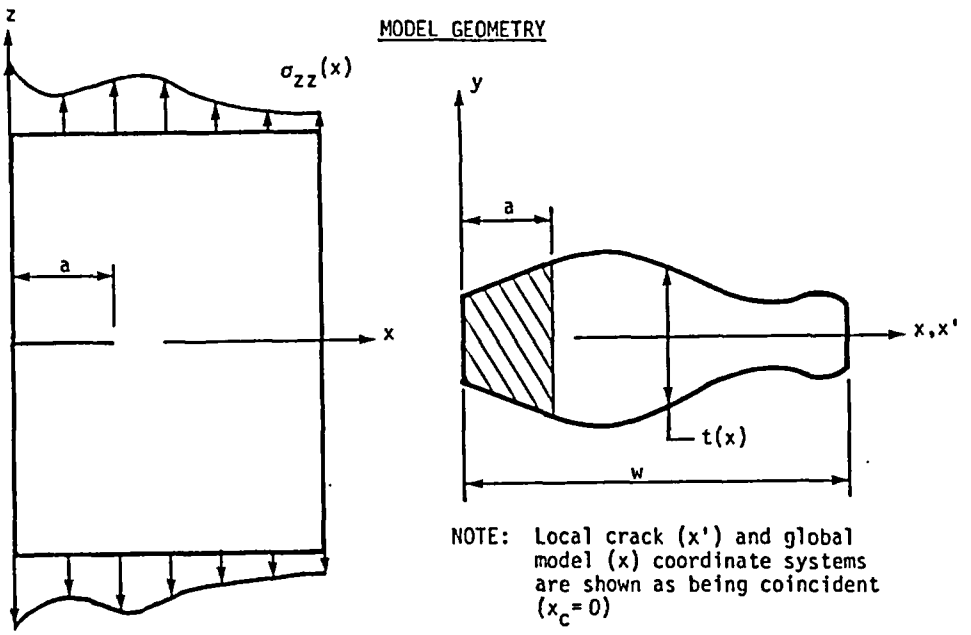

NOTE: Local crack (x') and global model (x) coordinate systems are shown as being coincident ($x_c = 0$)

MODEL DESCRIPTION

MODEL FEATURES	PARAMETER	OPTION FEATURED
Model Index Number	IFI	204
Number of Degrees of Freedom	IDOF	1
Crack Front Shape	--	Straight
Crack Opening Mode	--	Mode I
Finite Width Effects	w	Yes
Variable Thickness Effects	NTH	Yes

DATA INPUT DESCRIPTION

INPUT DESCRIPTION	PARAMETER	INPUT FORMAT	CARD SERIES	REMARKS
Variable Thickness	NTH	Constant	B	
Initial Crack Size, a_i	AI(1)	Constant	C1	
Body Width, w	G(1)	Constant	C2	
Crack Position, x_c	G(6)	Constant	C2	
y_c	G(7)	Constant	C2	Leave blank ($y_c = 0$)
Crack Orientation, ϕ	G(8)	Constant	C2	Leave blank ($\phi = 0$)
Thickness variation, t(x)	XTH(N)	Tabular	C3B	Input required if NTH = 1
	THK(N)	Tabular	C3B	
Load Input Option	IPLD	Constant	E2A	
Stress Field, $\sigma_{zz}(x)$	$\sigma(x)$	Equational	E2B	Format depends on IPLD.
	CS(IX)	Tabular	E2C	

The Mode I solution by Bueckner is based on a series solution which is reported in (4-7) to be accurate for values of a/w up to one-half. However, the authors have compared Bueckner's results to recent K solutions and found his solution to be accurate for $0 \leq a/w \leq 0.6$. It was also noted that stress intensity factor results for $a/w \geq 0.6$ will be significantly lower than correct solutions and should be ignored. The model accounts for variable thickness in the same approximate way as the center-cracked plate model (IFI = 201) using Eq. (2.6) for computing K.

4.4 Three-Dimensional Flaw Model Library ($300 \leq$ IFI ≤ 399)

4.4.1 Nozzle Blend Radius Corner Crack (IFI = 300)

The nozzle corner crack provided by this model is an approximate solution using the influence function of the one DOF semicircular surface flaw (IFI = 302). This model was developed as part of a three-dimensional feedwater nozzle study for a boiling water reactor (4-8) and was used to compute K for three different loadings involving pressure, thermal, and residual stresses. In the original study (4-8), two flaw models, a semicircular model and a quarter-circular model were used to bound the nozzle corner behavior. These two bounds were shown in (4-8) to give similar results. In fact, it was shown rigorously that for non-negative stress fields, the two one-degree-of-freedom models give $\bar{K}$ values that never differ by more than 10% and typically, the two models give $\bar{K}$ values that differ by less than 5%.

The important feature of this model which makes it different than IFI = 302 and suitable for nozzle applications is the stress mapping routine which allows the stresses to be input in the nozzle coordinate system (x,y) and the flaw model will map these stresses to the crack coordinates (x',y'). Figure 4.2 illustrates the technique used to map the uncracked stress field from the actual geometry to the model geometry of the semicircular crack model. The procedure illustrated in Fig. 4.2 gave optimum results compared with other methods tried earlier in the study (4-8) which involve overlaying the crack model geometries on the actual nozzle geometry.

The model geometry and data input details are provided in Table 4.8. The nozzle corner crack model is actually three models which allows the user to select the crack origin (i.e., center of the semi-circle) to be either on the nozzle side (x = 0), vessel side (y = 0) or anywhere on the nozzle blend corner arc segment. These model specifications are handled with G(3) through G(5) input parameters and these inputs are illustrated in Table 4.8. The crack position (x_c,y_c) and orientation (ϕ) parameters are not used in this model and input for these variables should be left blank. The origin of the global coordinate system is fixed at the intersection of the nozzle and vessel surface planes with the y axis parallel to the nozzle axis.

The nozzle corner model, like the surface crack solution it is based on, was formulated for a solid infinite body. The effect on influence functions and subsequent $\bar{K}$ values of the finite nozzle dimensions such as blend radius and (out-of-crack plane) nozzle curvature can be important. Recent results using the three-dimensional boundary integral equation model (4-9)

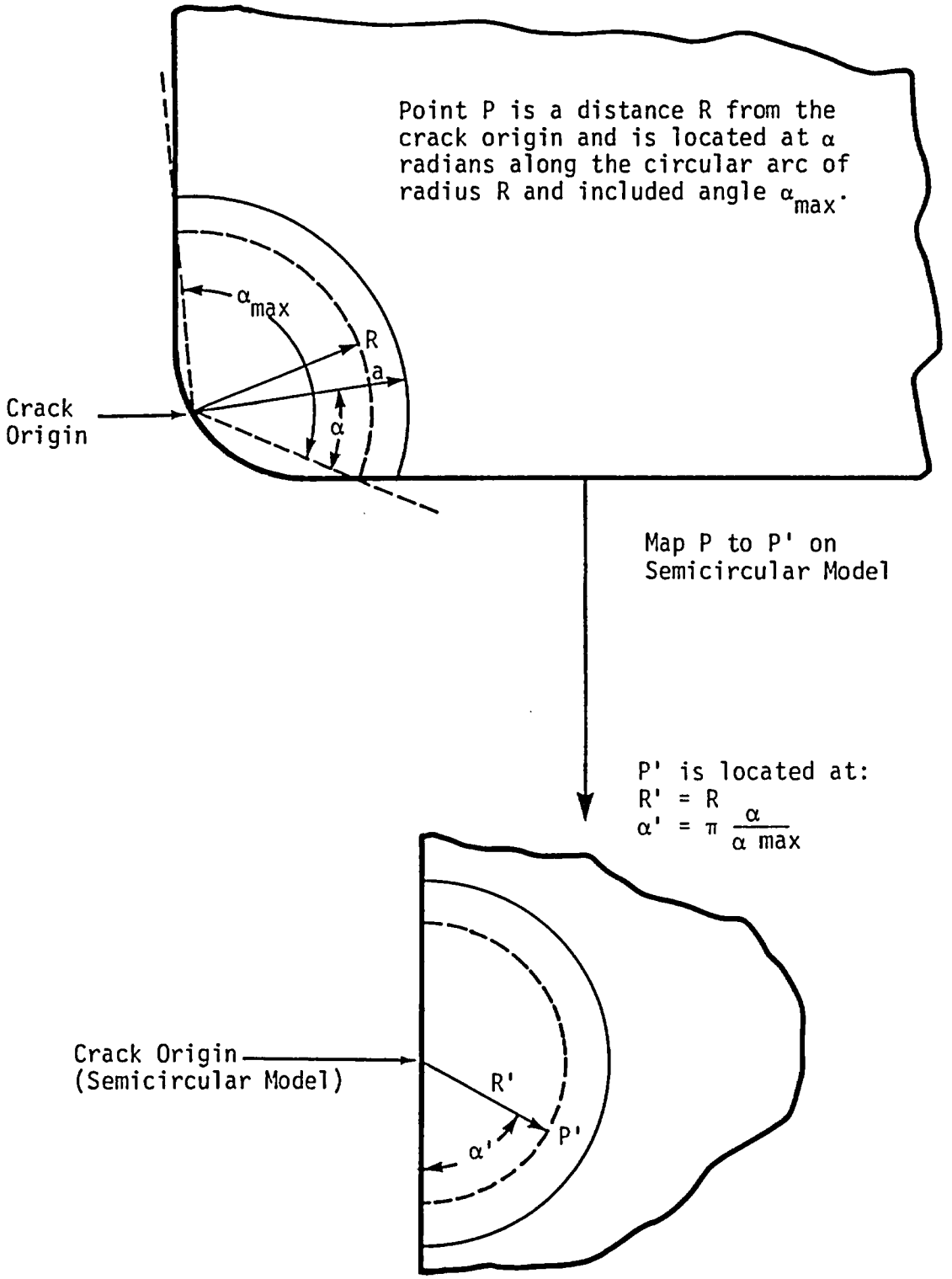

Figure 4.2 - Optimum Method for Mapping the Nozzle Uncracked Stress Field Onto the Semicircular Model Geometry.

Table 4.8
IFI = 300 - NOZZLE BLEND RADIUS CIRCULAR CORNER CRACK

MODEL GEOMETRY

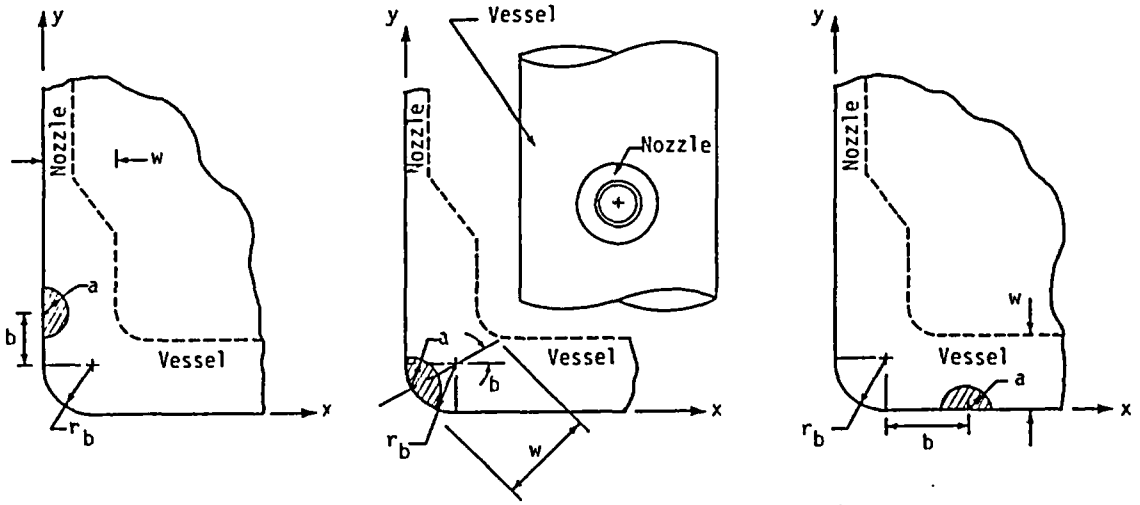

a) Nozzle Side Crack (G(4)=1.0)

b) Blend Corner Crack (G(4)=2.0)

c) Vessel Side Crack (G(4)=3.0)

MODEL DESCRIPTION

MODEL FEATURES	PARAMETER	OPTION FEATURED
Model Index Number	IFI	300
Number of Degrees of Freedom	IDOF	1
Crack Front Shape	--	Semi-Circular
Crack Opening Mode	--	Mode I
Finite Width Effects	w	No
Variable Thickness Effects	NTH	No

DATA INPUT DESCRIPTION

INPUT DESCRIPTION	PARAMETER	INPUT FORMAT	CARD SERIES	REMARKS
Variable Thickness	NTH	Constant	B	Set NTH = 0 or leave blank
Initial Crack Size, a_i	AI(1)	Constant	C1	
Body Width, w	G(1)	Constant	C2	Only used to terminate analysis when a ≥ w.
Nozzle Blend Radius, r_b	G(3)	Constant	C2	
Crack Origin Locator	G(4)	Constant	C2	Either on the nozzle side(G(4)=1.0), vessel side (G(4)=3.0) or on the blend corner arc (G(4)=2.0).
Crack Origin Position, b	G(5)	Constant	C2	Either linear distance or angular position (degrees) depending on G(4).
Crack Position, x_c	G(6)	Constant	C2	Leave blank (x_c=0)
y_c	G(7)	Constant	C2	Leave blank (y_c=0)
Crack Orientation, ϕ	G(8)	Constant	C2	Leave blank (ϕ=0)
Load Input Option	IPLD	Constant	E2A	
Stress Field, $\sigma_{zz}(x,y)$	$\sigma(x,y)$	Equational	E2B	Format depends on IPLD.
	CS(IX,IY)	Tabular	E2C	

have indicated that the nozzle corner model will give accurate results (errors less than 10%) for $a/w \leq 0.5$ for nozzle dimensions typical of a BWR feedwater nozzle. These error analysis results are summarized in Fig. 4.3 and are believed to include all significant effects of nozzle dimensions and curvatures on the IF for the circular crack.

4.4.2 Buried Circular Crack (IFI = 301)

The buried circular flaw model provides a one degree-of-freedom crack front behavior in an infinite body. The exact solution of the influence function for this model was derived from the buried elliptical crack solution of Green and Sneddon (4-10). Table 4.9 shows the crack geometry and input details for using this model.

Like all one-DOF flaw models, the crack will retain its original shape during the analysis, and crack growth is based on the (rms) average K or $\overline{K}$ along the crack front. This model is a special case of the general four-DOF buried ellipse (IFI = 304) and should be used when circular crack growth behavior is desired. The computation cost for this model is significantly less than for the elliptical model, IFI = 304.

4.4.3 Circular Surface and Corner Crack (IFI = 302, 303)

The semicircular surface (IFI = 302) or quarter-circular corner (IFI = 303) crack models are one DOF models that provide solutions for $\bar{K}$ when concentric circular crack growth behavior is wanted. The influence functions for these geometries were numerically determined using boundary integral

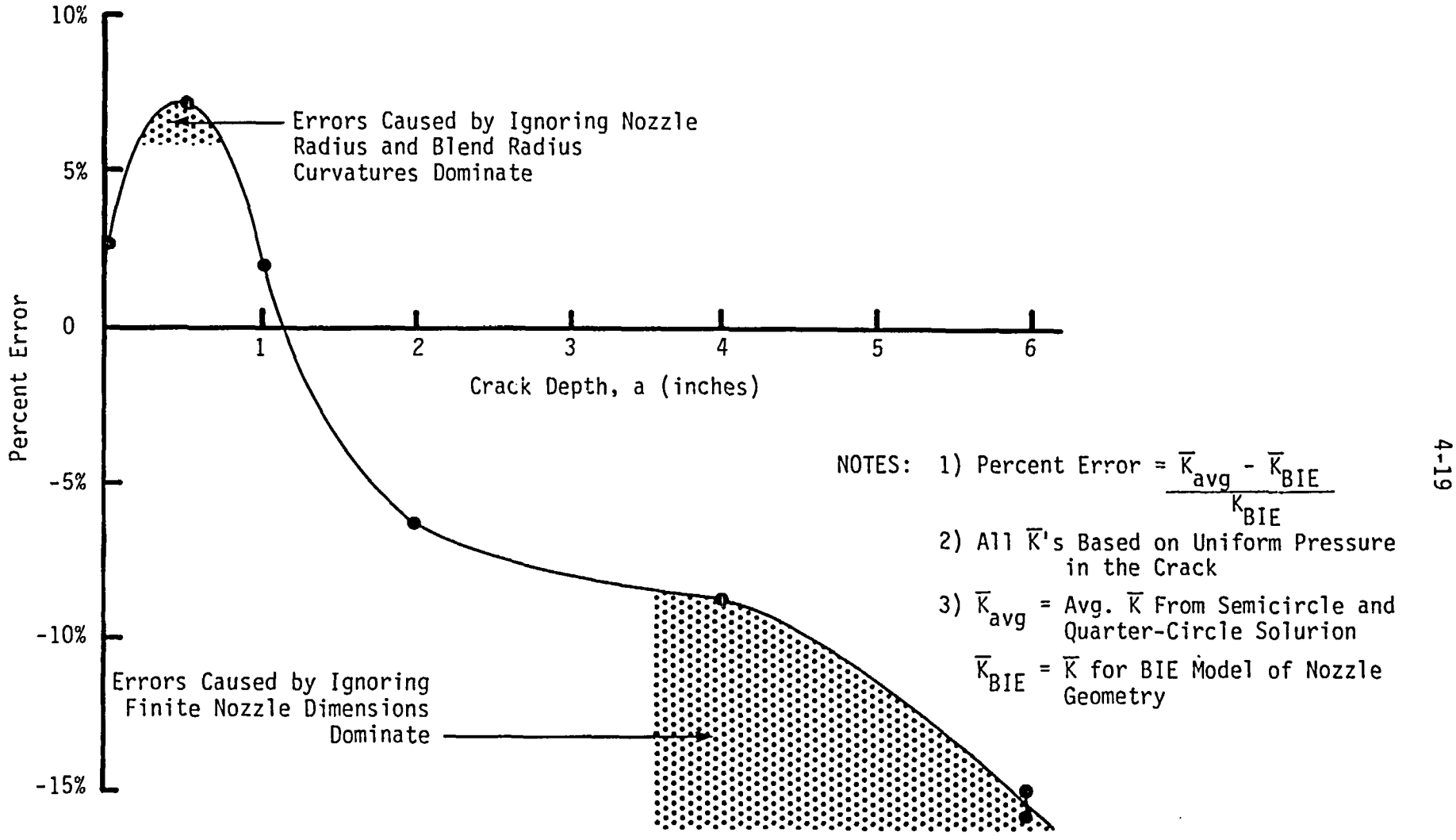

Figure 4.3 - Percent Errors of Stress Intensity Factor Estimates Caused by Ignoring Certain Details of the Nozzle Geometry in Calculation of Influence Functions.

Table 4.9
IFI = 301 - BURIED CIRCULAR CRACK

MODEL GEOMETRY

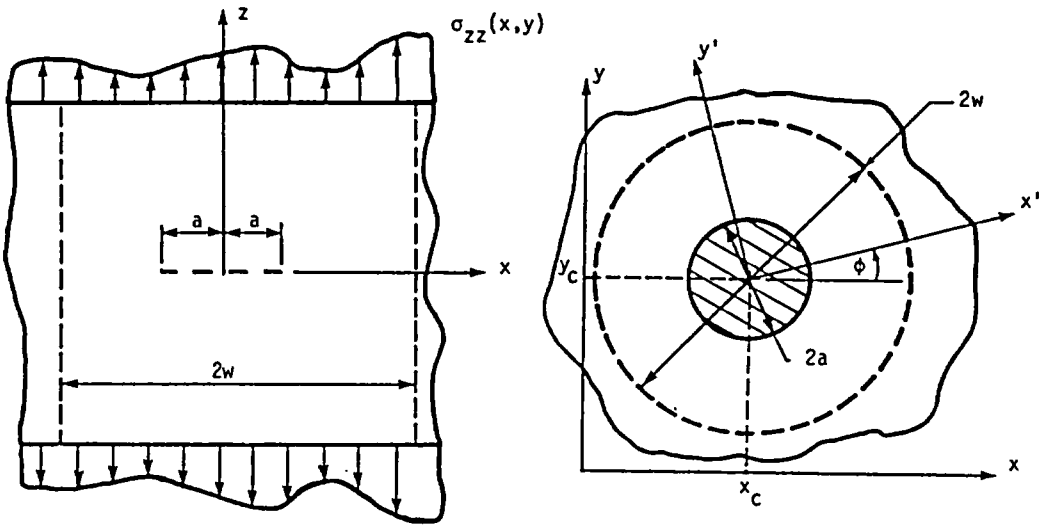

MODEL DESCRIPTION

MODEL FEATURES	PARAMETER	OPTION FEATURED
Model Index Number	IFI	301
Number of Degrees of Freedom	IDOF	1
Crack Front Shape	--	Circular
Crack Opening Mode	--	Mode I
Finite Width Effects	w	No
Variable Thickness Effects	NTH	No

DATA INPUT DESCRIPTION

INPUT DESCRIPTION	PARAMETER	INPUT FORMAT	CARD SERIES	REMARKS
Variable Thickness	NTH	Constant	B	Set NTH = 0 or leave blank
Initial Crack Size, a_i	AI(1)	Constant	C1	
Body Width, w	G(1)	Constant	C2	Only used to terminate analysis when $a \geq w$.
Crack Position, x_c	G(6)	Constant	C2	
y_c	G(7)	Constant	C2	
Crack Orientation, ϕ	G(8)	Constant	C2	Angle ϕ in degrees
Load Input Option	IPLD	Constant	E2A	
Stress Field, $\sigma_{zz}(x,y)$	$\sigma(x,y)$	Equational	E2B	Format depends on IPLD.
	CS(IX,IY)	Tabular	E2C	

equation analysis (4-11). The influence functions are believed to have errors smaller than 2% and maximum errors smaller than 5%. These error levels in the influence function lead to smaller than 2% errors in R for general stress behavior.

The crack geometry and required data input for these two flaw models are given in Tables 4.10 and 4.11. Both surface and corner crack models are valid for infinite bodies, i.e., crack depth is small relative to body size. The input for body width, w, is used only to terminate the analysis when $a \geq w$; otherwise, the crack analysis will stop when $\overline{K}_I \geq$ XKIC.

4.4.4 Buried Elliptical Crack (IFI = 304)

When IFI = 304, a buried elliptical crack model with four DOF is used to compute $\overline{K}_i$; i = 1, 4. The one DOF buried circular crack (IFI = 301) model already discussed is a special case of the 304 model. The buried elliptical model can grow in four directions simultaneously allowing its aspect ratio to change and translate in two different directions based on its local $\overline{K}$ and the da/dN behavior of the material. Although the initial crack can be rotated with respect to the global coordinate system used to specify the stress field, no crack rotation during crack growth is permitted. The exact influence functions for the buried ellipse were determined from the solution for the buried ellipse in tension by Green and Sneddon (4-10). The details of data input are given in Table 4.12.

The buried ellipse is valid for infinite bodies, i.e., major axis of the ellipse is small relative to body size. The body width, w, which

Table 4.10
IFI = 302 - CIRCULAR SURFACE CRACK

MODEL GEOMETRY

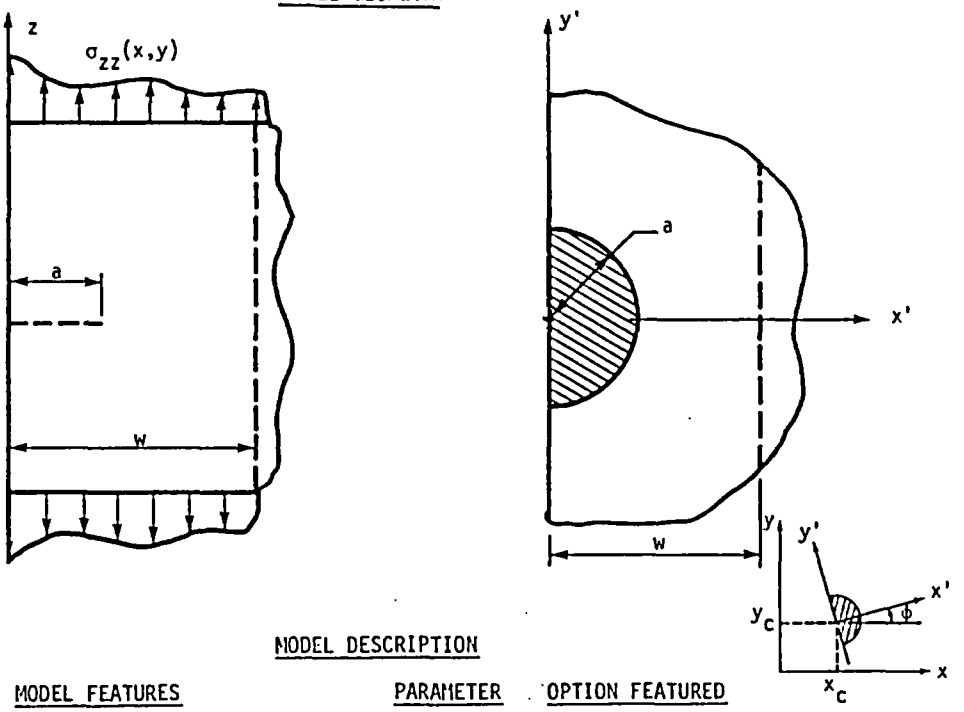

MODEL DESCRIPTION

MODEL FEATURES	PARAMETER	OPTION FEATURED
Model Index Number	IFI	302
Number of Degrees of Freedom	IDOF	1
Crack Front Shape	--	Semi-circular
Crack Opening Mode	--	Mode I
Finite Width Effects	w	No
Variable Thickness Effects	NTH	No

DATA INPUT DESCRIPTION

INPUT DESCRIPTION	PARAMETER	INPUT FORMAT	CARD SERIES	REMARKS
Variable Thickness	NTH	Constant	B	Set NTH = 0 or leave blank
Initial Crack Size, a_i	AI(1)	Constant	C1	
Body Width, w	G(1)	Constant	C2	Only used to terminate analysis when $a \geq w$.
Crack Position, x_c	G(6)	Constant	C2	
y_c	G(7)	Constant	C2	
Crack Orientation, ϕ	G(8)	Constant	C2	Angle ϕ in degrees
Load Input Option	IPLD	Constant	E2A	
Stress Input, $\sigma_{zz}(x,y)$	$\sigma(x,y)$	Equational	E2B	Format depends on IPLD.
	CS(IX,IY)	Tabular	E2C	

Table 4.11
IFI = 303 - CIRCULAR CORNER CRACK

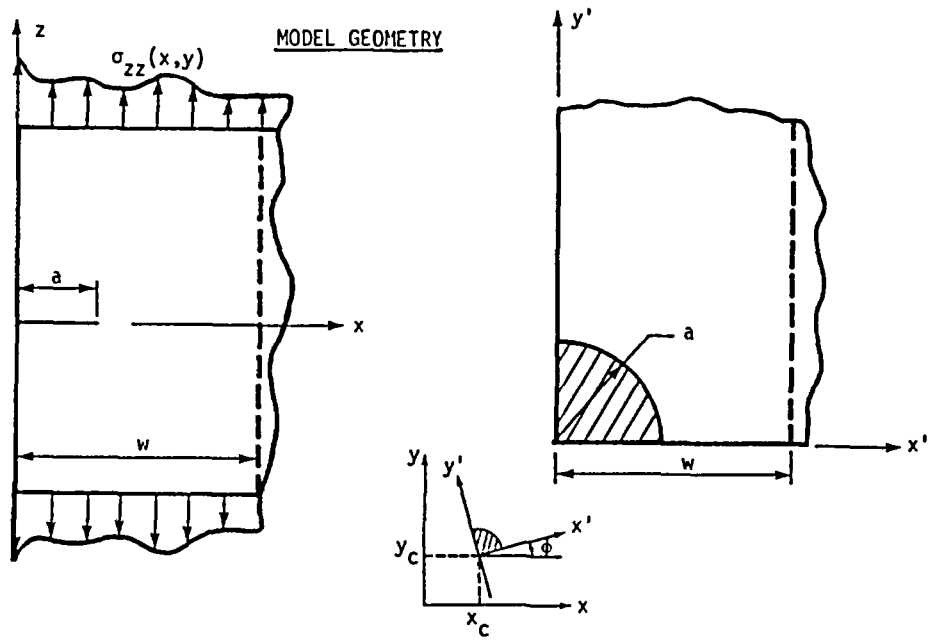

MODEL DESCRIPTION

MODEL FEATURES	PARAMETER	OPTION FEATURED
Model Index Number	IFI	303
Number of Degrees of Freedom	IDOF	1
Crack Front Shape	--	Quarter-Circular
Crack Opening Mode	--	Mode I
Finite Width Effects	w	No
Variable Thickness Effects	NTH	No

DATA INPUT DESCRIPTION

INPUT DESCRIPTION	PARAMETER	INPUT FORMAT	CARD SERIES	REMARKS
Variable Thickness	NTH	Constant	B	Set NTH = 0 or leave blank
Initial Crack Size, a_i	AI(1)	Constant	C1	
Body Width, w	G(1)	Constant	C2	Only used to terminate analysis when $a \geq w$.
Crack Position, x_c	G(6)	Constant	C2	
y_c	G(7)	Constant	C2	
Crack Orientation, ϕ	G(8)	Constant	C2	Angle ϕ in degrees
Load Input Option	IPLD	Constant	E2A	
Stress Field, $\sigma_{zz}(x,y)$	$\sigma(x,y)$	Equational	E2B	Format depends on IPLD.
	CS(IX,IY)	Tabular	E2C	

Table 4.12
IFI = 304 - BURIED ELLIPTICAL CRACK

MODEL GEOMETRY

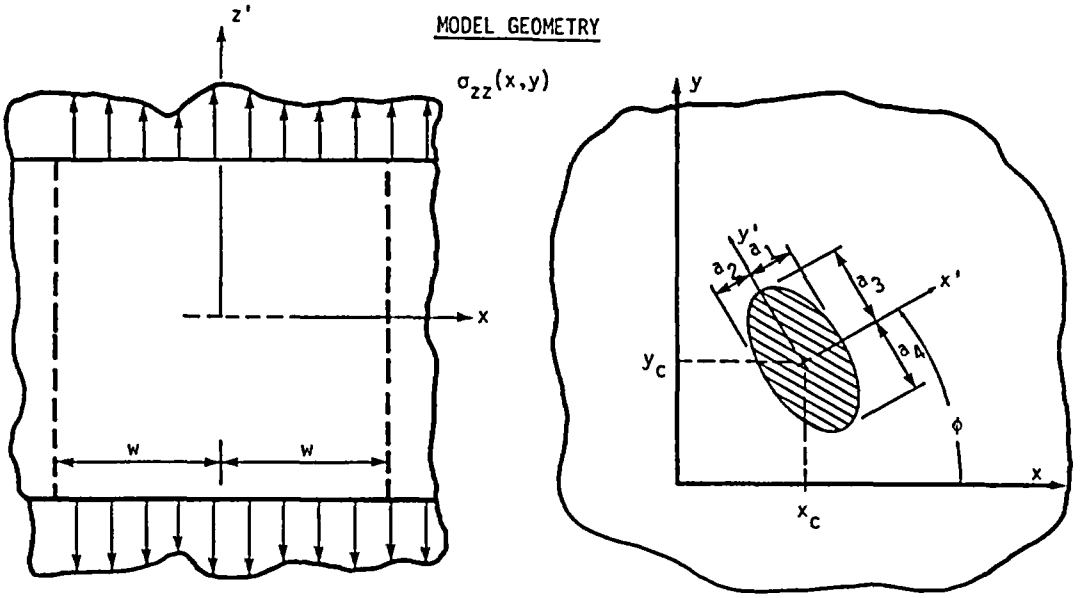

MODEL DESCRIPTION

MODEL FEATURES	PARAMETER	OPTION FEATURED
Model Index Number	IFI	304
Number of Degrees of Freedom	IDOF	4
Crack Front Shape	--	Elliptical
Crack Opening Mode	--	Mode I
Finite Width Effects	w	No
Variable Thickness Effects	NTH	No

DATA INPUT DESCRIPTION

INPUT DESCRIPTION	PARAMETER	INPUT FORMAT	CARD SERIES	REMARKS
Variable Thickness	NTH	Constant	B	Set NTH = 0 or leave blank
Initial Crack Size, a_1	AI(1)	Constant	C1	
a_2	AI(2)	Constant	C1	
a_3	AI(3)	Constant	C1	
a_4	AI(4)	Constant	C1	
Body Width, w	G(1)	Constant	C2	Used only to terminate analysis when maximum $a_1 \geq w$.
Crack Position, x_c	G(6)	Constant	C2	
y_c	G(7)	Constant	C2	
Crack Orientation, ϕ	G(8)	Constant	C2	Angle ϕ in degrees.
Load Input Option	IPLD	Constant	E2A	
Stress Field, $\sigma_{zz}(x,y)$	$\sigma(x,y)$	Equational	E2B	Format depends on IPLD.
	CS(IX,IY)	Tabular	E2C	

is specified on Card C2, is used only to stop the crack growth analysis (IFAT = 1) when first crack degree-of-freedom, a_1, breaks through the body ($a_1 \geq w$), otherwise the problem will terminate when $\bar{K}_I \geq$ XKIC.

4.4.5 Elliptical Surface and Corner Cracks (IFI = 305, 306)

The three DOF elliptical surface (IFI = 305) and two DOF corner (IFI = 306) crack models are more general cases of the circular surface models of IFI = 302 and 303. The elliptical surface crack has three DOF which allows the flaw to grow, change shape, and translate along the surface. The corner crack has two DOF which provides for both crack growth and change in shape. Both IFI = 305 and 306 influence functions were determined by numerical analysis using boundary integral equations (4-11). The influence functions are believed to have average errors of 1% to 3% and maximum errors smaller than 5%. These errors will typically lead to less than 2% errors in $\bar{K}$ for arbitrary stress fields. Tables 4.13 and 4.14 illustrate the crack models and required data input.

The surface and corner ellipses are valid for infinite bodies. The input for body width, w, on Card C2 allows the analysis to be terminated either when $a \geq w$ or $\bar{K}_I \geq$ XKIC. If the input for body width is left blank, then only the material toughness check will stop the analysis.

Table 4.13
IFI = 305 - ELLIPTICAL SURFACE CRACK

MODEL GEOMETRY

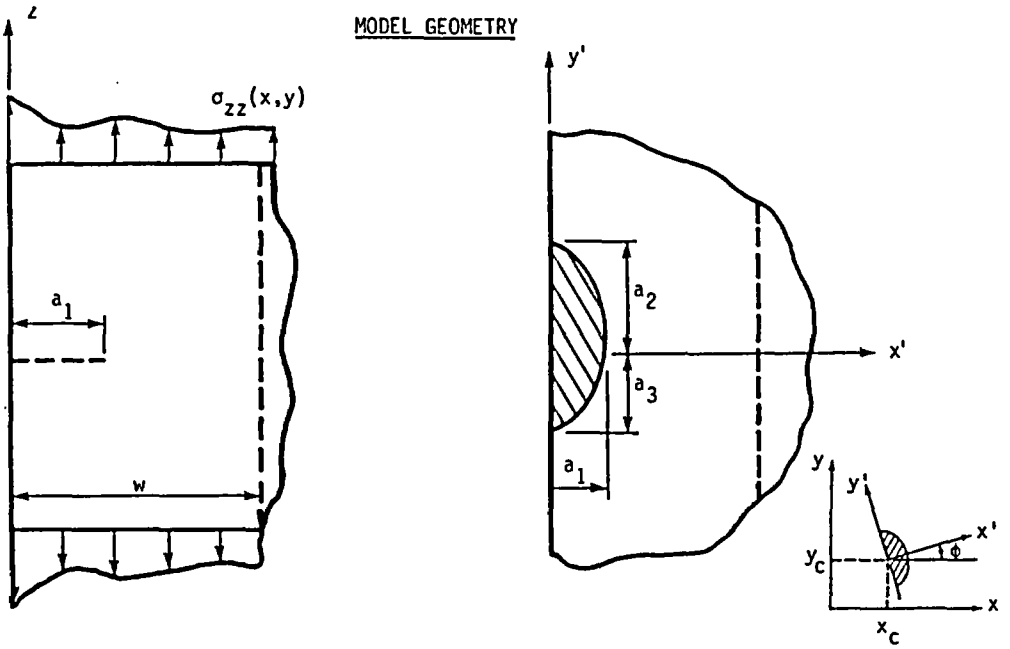

MODEL DESCRIPTION

MODEL FEATURES	PARAMETER	OPTION FEATURED
Model Index Number	IFI	305
Number of Degrees of Freedom	IDOF	3
Crack Front Shape	--	Semi-Elliptical
Crack Opening Mode	--	Mode I
Finite Width Effects	W	No
Variable Thickness Effects	NTH	No

DATA INPUT DESCRIPTION

INPUT DESCRIPTION	PARAMETER	INPUT FORMAT	CARD SERIES	REMARKS
Variable Thickness	NTH	Constant	B	Set NTH = 0 or leave blank
Initial Crack Size, a_1	AI(1)	Constant	C1	
a_2	AI(2)	Constant	C1	
a_3	AI(3)	Constant	C1	
Body Width, w	G(1)	Constant	C2	Used only to terminate analysis when $a_1 \geq w$.
Crack Position, x_c	G(6)	Constant	C2	
y_c	G(7)	Constant	C2	
Crack Orientation, ϕ	G(8)	Constant	C2	Angle ϕ in degrees
Load Input Option	IPLD	Constant	E2A	
Stress Input, $\sigma_{zz}(x,y)$	$\sigma(x,y)$	Equational	E2B	Format depends on IPLD.
	CS(IX,IY)	Tabular	E2C	

Table 4.14
IFI = 306 - ELLIPTICAL CORNER CRACK

MODEL GEOMETRY

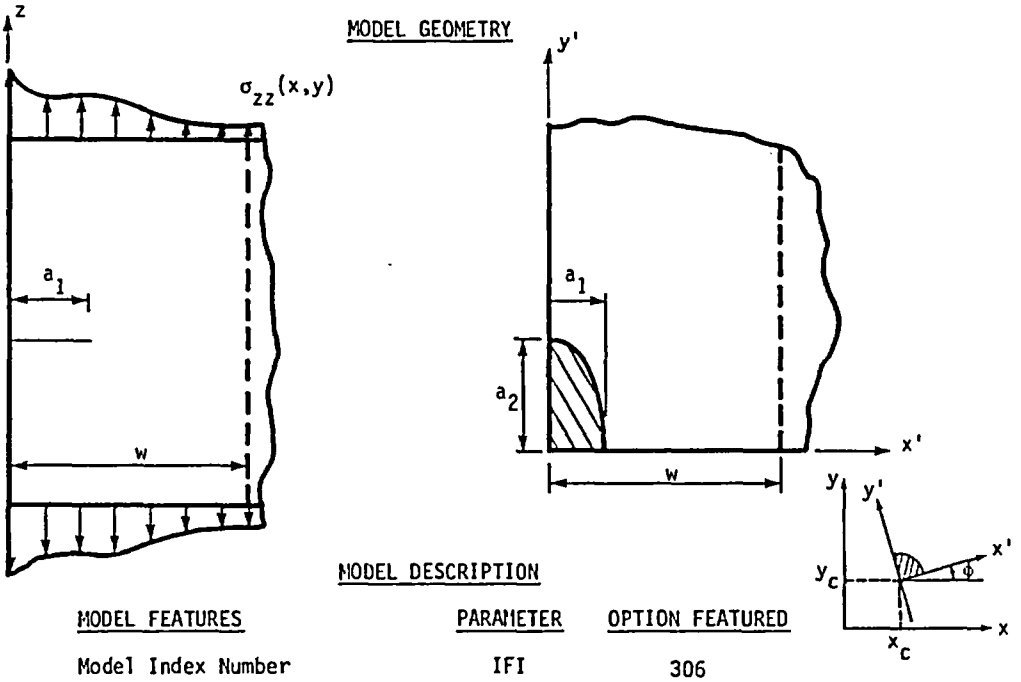

MODEL DESCRIPTION

MODEL FEATURES	PARAMETER	OPTION FEATURED
Model Index Number	IFI	306
Number of Degrees of Freedom	IDOF	2
Crack Front Shape	--	Quarter-Circular
Crack Opening Mode	--	Mode I
Finite Width Effects	w	No
Variable Thickness Effects	NTH	No

DATA INPUT DESCRIPTION

INPUT DESCRIPTION	PARAMETER	INPUT FORMAT	CARD SERIES	REMARKS
Variable Thickness	NTH	Constant	B	Set NTH = 0 or leave blank
Initial Crack Size, a_1	AI(1)	Constant	C1	
a_2	AI(2)	Constant	C2	
Body Width, w	G(1)	Constant	C2	Used only to terminate analysis when $a_1 \geq w$.
Crack Position, x_c	G(6)	Constant	C2	
y_c	G(7)	Constant	C2	
Crack Orientation, ϕ	G(8)	Constant	C2	Angle ϕ in degrees
Load Input Option	ILPD	Constant	E2A	
Stress Field, $\sigma_{zz}(x,y)$	$\sigma(x,y)$	Equational	E2B	Format depends on IPLD.
	CS(IX,IY)	Tabular	E2C	

REFERENCES

4-1 Irwin, G. R., "Analysis of Stresses and Strains near End of a Crack", J. Appl. Mech. 24, pp. 362-364, 1957.

4-2 Irwin, G. R., "Crack Extension Force for a Part-Through Crack in a Plate", J. Appl. Mech. 29, pp. 651-654, 1962.

4-3 Paris, P. C., and Sih, G. C., "Stress Analysis of Cracks", Fracture Toughness & Testing, ASTM 381, 1965.

4-4 Wigglesworth, L. A., "Stress Distribution in a Notched Plate", Mathematika 4, pp 76-96, 1957.

4-5 Irwin, G. R., "Analytical Aspects of Crack Stress Field Problems", Theo. and Appl. Mech. Dept., Rept. 13, University of Illinois, Urbana, 1962.

4-6 Tada, H., Paris, P., and Irwin, G, The Stress Analysis of Cracks Handbook, Del Research Corporation, 1973.

4-7 Bueckner, H. F., "Weight Functions for the Notched Bar", General Electric Report No. 69-LS-45, 1969.

4-8 Cohen, L. M., McLean, J. L., Moy, G., and Besuner, P. M., "Improve Evaluation of Nozzle Corner Cracking", EPRI NP-339, Final Report RP-700 and 498, March 1977.

4-9 Rau, C. A., et al, "Failure Analysis and Failure Prevention in Electric Power Systems", Interim Report RP-700-1, FAA-77-4-3, May 1977.

4-10 Green, A. E. and I. N. Sneddon, "The Stress Distribution in the Neighborhood of a Flat Elliptical Crack in an Elastic Solid", Proceedings, Cambridge, Phi., Soc., Vol 46, 1950.

4-11 Besuner, P. M., "Fracture Mechanics and Residual Fatigue Life Calculations for Complex Stress Fields", EPRI-217-1, Technical Report 2, July 1975.

5.0 GENERAL GUIDELINES FOR PROGRAM USAGE, INPUT, AND TROUBLESHOOTING

5.1 Guidelines for Problem Modeling

In past usage, the BIGIF program has been applied to two major classes of problems: failure analysis and failure prevention (e.g., design or repair analysis). The goals and the type and amount of available information differ significantly for these two problem classes which lead to the two different methods of approach discussed below.

5.1.1 Failure Analysis

In failure analysis, the analyst must "explain" a field or service failure and, under these circumstances, the analyst may be under high pressure to arrive quickly at a solution. Fortunately, the fact that there is a failure helps the analyst since physical evidence is available which may provide specific details regarding crack location, failure mode, crack shape as a function of crack depth, and any structural or metallurgical discontinuities which may have been present. If the failure cannot be explained by any immediate or obvious discrepancy in the design or severe abusive loads, an analysis must be performed using "best estimates" of actual field failure parameters for most inputs to the problem, including flaw geometry, material behavior and service stress. "Worst case" inputs for individual parameters may also be acceptable, but only as part of a sensitivity study or for statistical reasons. For example, if 1000 nominally identical rotor bores are subject to inclusions and one rotor fails due to

subcritical crack growth from an inclusion of unknown size, the analyst may be justified to input a largest-of-1000 inclusion size or crack growth rate into the BIGIF model. For more details regarding probabilistic fracture mechanics the reader is referred to (5-1).

All improvements in the data should be based upon tests performed on actual or exemplar materials. A refined stress analysis may be required to define accurately the uncracked stress behavior in the region of concern. Also the loads and loading frequency experienced in service may have to be determined from in-service measurements.

5.1.2 Failure Prevention Analysis

The second type of analysis which BIGIF can be used for is in the general class of failure prevention. There are actually two areas of application in failure prevention analysis. The first case is when a defect has been discovered in pre-service or in-service by planned or chance non-destructive inspection or flaw-caused changes in structural performance (e.g., rotor imbalance caused by large crack). The second is the situation of postulating a "realistically large" defect in the component at the design stage to assure expected design life. In performing failure prevention studies of either postulated or detected flaws, one must usually show that under "worst case" or conservative conditions the structural integrity of the component is not compromised by the assumed or detected flaw. Therefore, unlike the case of failure analysis, nominal or optimistic values of input parameters are usually not utilized for failure prevention and design.

5.2 Tips for Data Input

To formulate models and input for crack analysis, there is no substitute for the experience gained in performing and progressively improving fracture mechanics analysis of laboratory specimens and field structures. The user can develop his own techniques from successful experience as long as he can make good assessments of whether or not his success is due to (1) an adequate model or (2) luck (e.g., compensation of errors, fudging, etc.).

Fracture mechanics technology is new and complex enough that many errors still arise from fundamental mistakes such as misfitting data, improperly extrapolating da/dN versus ΔK curves, and failure to check units. The list of general rules are meant to reduce the frequency of fundamental user errors in running BIGIF. They can only supplement rather than replace the need for user skill and experience and the need for accurate and complete enough input data.

(1) Firmly establish the flaw model and options to be used before starting input. In the case of a failure analysis, use whatever data are available such as fractographic information to (1) establish the failure mode of concern and (2) select the flaw model to represent the actual service conditions.

(2) Decide immediately on the fundamental units (force, length, time) to be used for all input quantities. For the English system, the most popular units are stress in ksi, length in inches and time

in seconds. In the metric system, some popular units are stress in MN/m^2, length in meters and time in seconds. A conversion chart for units is given in Appendix D.

(3) Never alter any constants in the crack growth rate (da/dN) relation without carefully refitting the literature data or experimental observations.

(4) Always note when and how the da/dN relation is being extrapolated beyond the laboratory data.

(5) Never be afraid to input the initial crack size, (AI), smaller than, and/or fracture toughness (XKIC) larger than values inherent in the chosen model. This provides extra solution output that may give valuable information and reduce the number of required computer runs.

(6) The effect of R on da/dN must be accounted for directly in the input expression or data if the Paris rule (IDADN = 1 or 2) is selected.

5.3 Program Output and Diagnostics

During the input process, BIGIF reads the data, checks for gross input mistakes, and prints an input data summary sequentially for each card series. Since the input checks BIGIF performs are just for locating major errors, all input should be reviewed by the user for more subtle mistakes.

The type of solution output obtained is a function of the analysis type (IFAT). In general, only two types of solution output are printed.

The first solution output is a detailed breakdown of all fracture mechanics quantities for each transient and loading block, and for each crack DOF. The next type of output is a fatigue analysis summary listing the important fatigue quantities of the previous detailed printout. For a load block comprised of more than one transient, the summary output only prints out the DK solution for the first cycle of the first specified transient. When IFAT = 0, a single calculation for K is performed and printed under the detailed output format. When a fatigue analysis is specified (IFAT = 1), both the detailed output and the fatigue summary output are printed. The user is encouraged to review the solution output for the example problems given in Appendix C to obtain a better idea of the type of output BIGIF will print.

5.4 Common Errors and Troubleshooting

The following is a list of user mistakes which have occurred most frequently in usage of BIGIF and predecessor algorithms.

(1) General gross modeling errors resulting form the failure to understand the application and limitations of current models in the flaw library.

(2) Inconsistency in stress units, especially between the uncracked stress field $\sigma(x,y)$ and the da/dN relation. The most common error is when the stress is specified in psi while the coefficient C is in terms of ksi.

(3) While updating da/dN input, only one constant is changed in the da/dN relation without changing others to reflect a new data fit.

(4) Failure to define the stress, $\sigma(x,y)$, thickness variation, $t(x)$, or da/dN relationships over an adequate range or domain.

(5) Improper interpretation of load and stress parameters in terms of the transients (e.g., including residual stress as an alternating, rather than steady stress).

To aid in checking and troubleshooting actual problem output, a series of problem symptoms have been compiled. These symptoms, along with probable causes and suggested corrective actions, are listed in Table 5.1.

TABLE 5.1

PROBLEM DEBUGGING AND TROUBLESHOOTING AID

Symptom	Probable Cause	Corrective Action
1. Life predictions which do not correlate with experience and/or make no sense.	Could be due to variety of causes, anything from an input mistake to bad stress field estimates to possible inapplicability of da/dN data or even LEFM itself.	Check input, especially flaw model selection, stress and da/dN data.
2. Life of zero. Little or no solution output.	Specified toughness too low or initial crack size too large. Possible unit mix-up.	Check the units of stress and specified toughness. Also check initial crack size dimensions and flaw model selected.
3. Lack of smoothness in K(a) or $\Delta K(a)$ in solution output.	Lack of smoothness in $\sigma(x,y)$ and/or $t(x)$.	Check stress behavior and/or specified thickness variation over the crack face region where numerical oscillations are observed.
4. Lack of correlation between da/dN vs ΔK solution output and lab or literature data.	Most likely a data-fit error, or bad data input of C or n, or tabular data points.	Recheck C and n, or tabular data input in Card Series D. Recheck data-fitting analysis.
5. Negative K_{max} or ΔK values printed.	Negative stresses, $\sigma(x,y)$ acting over the crack face.	Check stress input for possible sign mistakes; otherwise, results indicate full crack closure and no crack growth will result.

REFERENCES

5-1 Besuner, P. M., Tetelman, A. S., "Probabilistic Fracture Mechanics", EPRI 217-1, Technical Report 4, NTIS No. PB-246225, July 1975.

6.0 ADVANCED PROBLEM MODELING TIPS AND TECHNIQUES

6.1 LEFM Background Information

Some applications of fracture mechanics are straightforward; there will be only one correct analytical approach, while other applications and techniques are learned only through trial and error. Modeling techniques, data interpretation, and even the interpretation of results may be subject to question. Additionally, there will always be some applications where residual life and strength of cracked parts are too unpredictable for deterministic analysis alone.*

Useful stress intensity factor solutions and modeling shortcuts can be obtained by reading LEFM solutions in the literature especially those references which are applied in nature. A list of several important works including papers as well as reference texts is provided at the end of this section (6-1 through 6-18). In addition to those references listed, leading fracture mechanics journals, such as International Journal of Fracture Mechanics, Engineering Fracture Mechanics, and the publications of the American Society for Testing and Materials, Special Technical Publications series (STP) and the fracture division of the American Society of Mechanical Engineers Pressure Vessels and Piping Division should be reviewed.

The following subsections provide specific modeling tips and techniques for some commonly encountered problems. In several cases, specific

*Refer to the work of Besuner, Tetelman, and Sorenson for formal probabilistic techniques to combine optimally the available field and laboratory data and engineering analysis for evaluating the significance of cracks in structures (e.g., 6-12 through 6-15).

details regarding how BIGIF should be utilized and the data input scheme are presented.

6.2 Through-Cracks in Unnotched and Notched Structures

After performing many fracture analyses, the analyst will realize that structural cracking initiates predominantly from regions of high local stress or stress concentration such as due to a surface notch. The regions of high stress may have been anticipated in the design stage (i.e., bolt holes or fillets), but the actual stress magnitude could be significantly larger than anticipated due to inadequate stress analysis or because dimensional tolerances were not assured. Alternatively, high local stresses in an unnotched component may be induced by some unanticipated circumstance which resulted in a surface defect such as a machining mark or a weld arc strike. What must be recognized is that although a structure may be designed with no notches, the design and fatigue analysis should contain margin for error.

The use of a two-dimensional through-crack flaw model ($a/2c = 0$) to represent the situation of a long part-through crack is conservative in that the computed K levels will be higher and the subsequent fatigue life shorter for a through-crack than for a part-through-crack under the same assumed loading. However, for "infinite" bodies, it takes a crack aspect ratio ($a/2c$) of only 1/10 for the K level associated with a part-through crack to be approximately equal to the through-crack level. Hence, a significant model simplification can be implemented although high aspect ratio cracks often tend to grow into nearly circular shapes ($a/2c = 1/2$). Furthermore, the selection of a through-crack model may be the best choice if the analyst suspects extremely high surface stresses so that cracks will grow fast in the through direction due to accelerated fatigue and possible multiple crack interaction and link-up.

As an example of how one would model the crack-in-notch problem, consider the idealized problem of a single edge-notched plate containing a crack under nominal tension as shown in Fig. 6.1. The BIGIF model library does not contain the exact representation of this geometry*; however, the closest approximation to Fig. 6.1 is the edge crack plate. If finite width effects are important, the IFI = 204 model could be used to solve the problem conservatively. Two possible approaches using IFI = 204 are shown in Fig. 6.2. Lacking any detailed stress distribution information regarding the magnitude of the stress concentration (K_t) effect, Fig. 6.2a illustrates a first cut at the problem using an initial flaw size $a_i = R + a$ in the uniform tension field. Any knowledge of local notch stress field behavior will allow the user to upgrade the model to Fig. 6.2b where $a_i = a$, the body width is w - R and $\sigma(x)$ is the local variation on the nominal tension stress. A special feature is then used by setting IPLD = 3 on Card E2A which allows the user to input the K_t for the particular problem of concern to match the surface stress exactly. The program will provide a distribution on the stress to the interior of the body, which will be computed based on the stress drop-off from a hole in a plate under uniaxial tension. For the model illustrated in Fig. 6.2b with IPLD = 3,

$$\sigma(x) = Q_1 \left\{ 1 + (Q_2 - 1) \left[\frac{1}{4} \left(\frac{Q_3}{Q_3 + x} \right)^2 + \frac{3}{4} \left(\frac{Q_3}{Q_3 + x} \right)^4 \right] \right\} \text{AGLD} \qquad (6.1)$$

where

$Q_1 = \sigma_o$

$Q_2 = K_t$

$Q_3 = R$

AGLD = 1

*It is anticipated that the next contemplated version of BIGIF will have IF solutions for the geometry in Fig. 6.1 and for many other two-dimensional edge crack configurations.

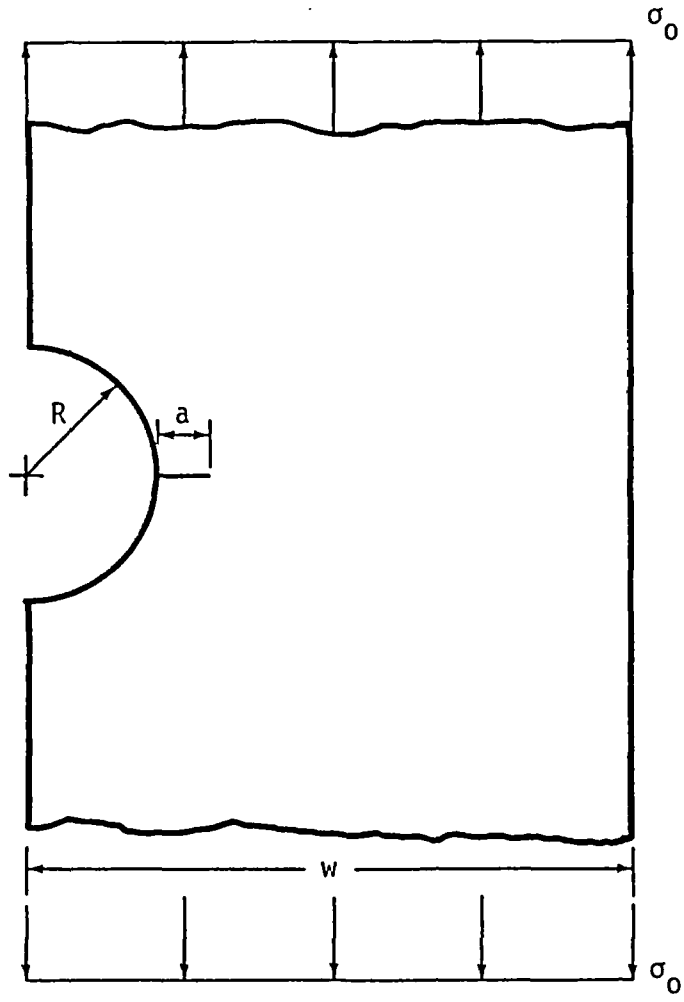

Figure 6.1 - Single Edge Notched Plate Containing a Crack Under Nominal Tension.

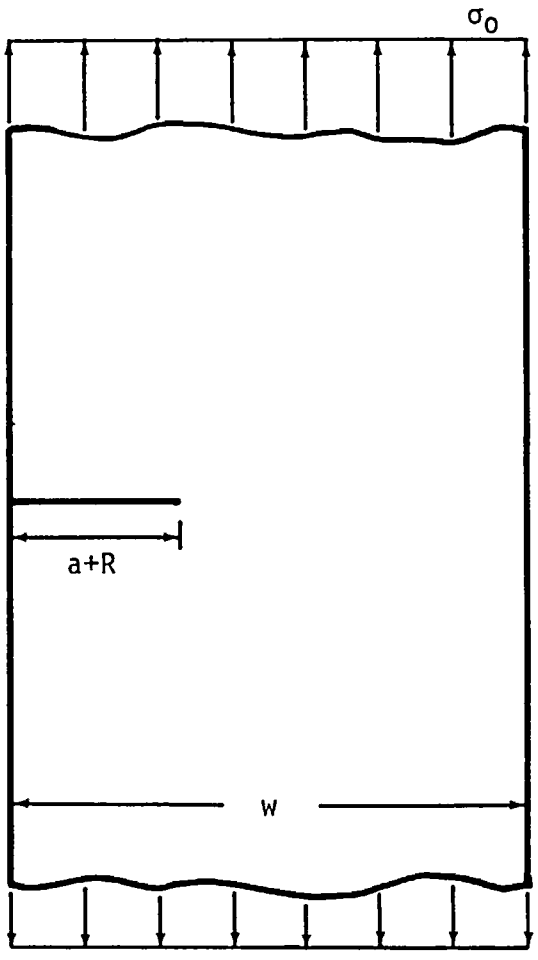

a) Flaw Model Based on Nominal (Unnotched) Stress

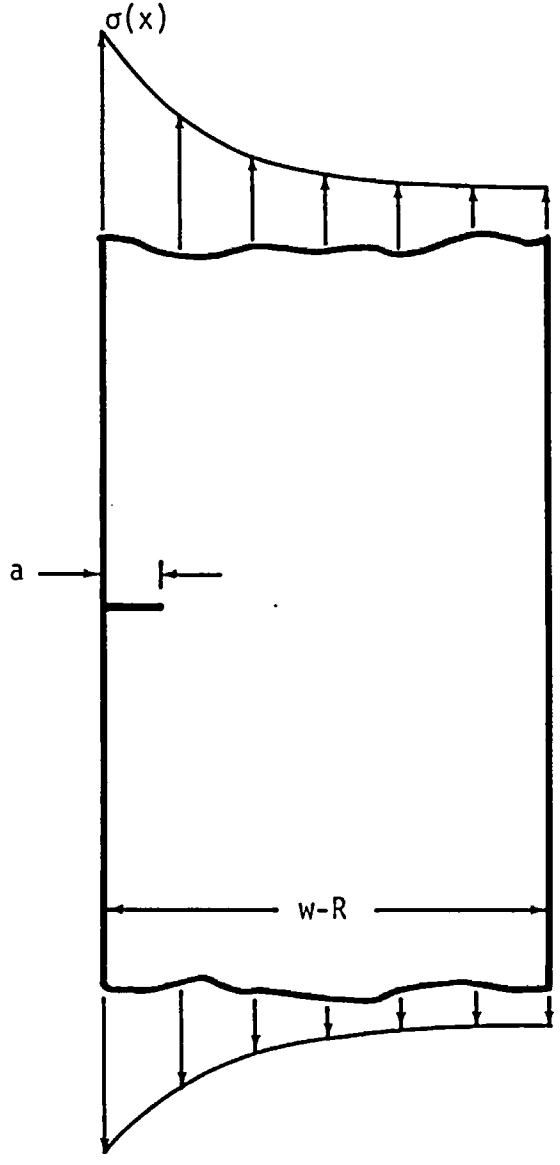

b) Flaw Model Based on Notched Stress

Figure 6.2 - Two Possible Flaw Model Representations of an Edge-Notched Plate Containing a Crack.

A solved example of an edge crack model for unnotched (nominal) conditions using IFI = 204 is presented in Section 7.2.

6.3 Part-Through Cracks and Leak-Before-Break

The potential problems associated with detecting part-through cracks in structures place additional constraints on the analyst to limit the alternating stresses of the component in terms of number of service cycles, stress amplitude, or both. When applying LEFM to the design of pressure retaining components such as pressure vessels, piping, or pump or valve housings, an additional safeguard is to provide sufficient material toughness so that a fatigue failure would initially result only in leaking which could be easily detected, as opposed to a catastrophic fracture or breaking of the component with the potential of causing significant damage. The problem of assuring leak-before-break is one of determining the minimum critical crack size under all expected service conditions. A schematic showing an incipient leak condition is shown in Fig. 6.3. The following steps would outline the general procedure:

(1) Compute the critical flaw size, a_c, for the part-through crack accounting for initial crack shape and the change in shape during stable crack growth. In general, if $a_c < 0.5w$, it is unlikely that leak-before-break could be assured.

(2) Postulate the part-through crack shape which would exist just at crack breakthrough. For vessels that experience only pressure cycling with little or no thermal or discontinuity stresses (i. e., are

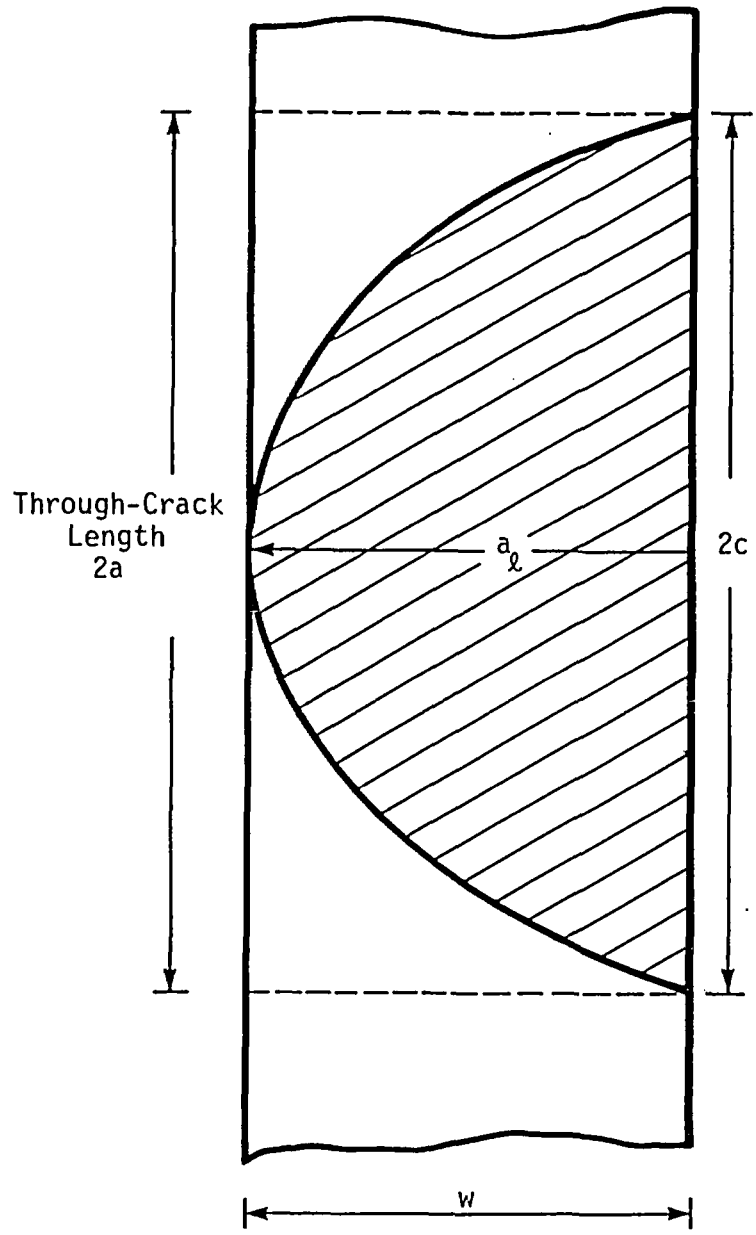

Figure 6.3 - Schematic Showing Analytical Conditions at Incipent Leaking for Assessing Leak-Before-Break.

uniformly stressed), the final flaw shape at incipient leak would be approximately semicircular with $a_\ell/2c = w/2w$. For vessels with thermal or bending stresses such as thermal shock loading or cyclic bending loads in piping, the flaw length at breakthrough may be greater than 2w.

(3) Determine the minimum critical flaw size, a_c, of the through-crack taking into account dynamic or strain rate effects on K_c.

(4) Compare a_c with c for the part-through flaw at incipient leak; if $a_c > c$, leak-before-break, and $a_c < c$ break-before-leak.

Because of uncertainties in the probably abnormal stress levels that may occur during the fracture process and as a generally conservative approach, the leak-before-break criterion can also be established using the yield stress as the operating stress for (3) above.

6.4 Effect of Welding on Residual Life

In analyzing welded structures, it is necessary to recognize several facts which are important when computing the fatigue life:

(1) The weldments consist of three distinct regions in the structure where the material behavior, strength, toughness and crack growth may vary significantly. These regions are (a) the base or original parent material; (b) the weld metal; and (c) the heat affected zone between base and weld metal.

(2) Inherent planar or two-dimensional defects such as intrusions or lack of penetration, which behave like cracks at the start of service, may be present. Thus, the crack initiation life associated with welds may be zero. Many three-dimensional weld defects such as porosity of reasonable levels and solid inclusions are not crack-like and have negligible effect on residual life.

(3) In as-welded structures, residual stresses which can be as high as the yield strength will be present in the direction of subsequent stressing. These residual stresses will elevate the applied steady service stresses which must be accounted for in determining crack growth rate for a given ΔK (where ΔK arises only from applied cyclic loads and is independent of residual stress).

6.5 Fatigue Analysis Involving Once-in-a-Lifetime Maximum Stress Condition

In performing certain types of analyses where the failure mode of fatigue is of primary concern, the analyst may also like to check, say, at the end of each considered increment of crack growth, a static fracture event consisting of a once-in-a-lifetime loading condition. An example of this would be a component such as a pressure vessel where the fatigue damage is due to normal operating conditions but there exists a stress condition with a low probability of occurrence such as a loss-of-coolant accident, which also must be accounted for in the design. A schematic showing of how BIGIF could be used to solve this problem is given in Fig. 6.4. Here the cyclic loading encompassing one month of service of a component is represented by a loading block composed of two transient conditions. The maximum stress condition postulated to occur once in a forty-year service life is specified as the third transient with a

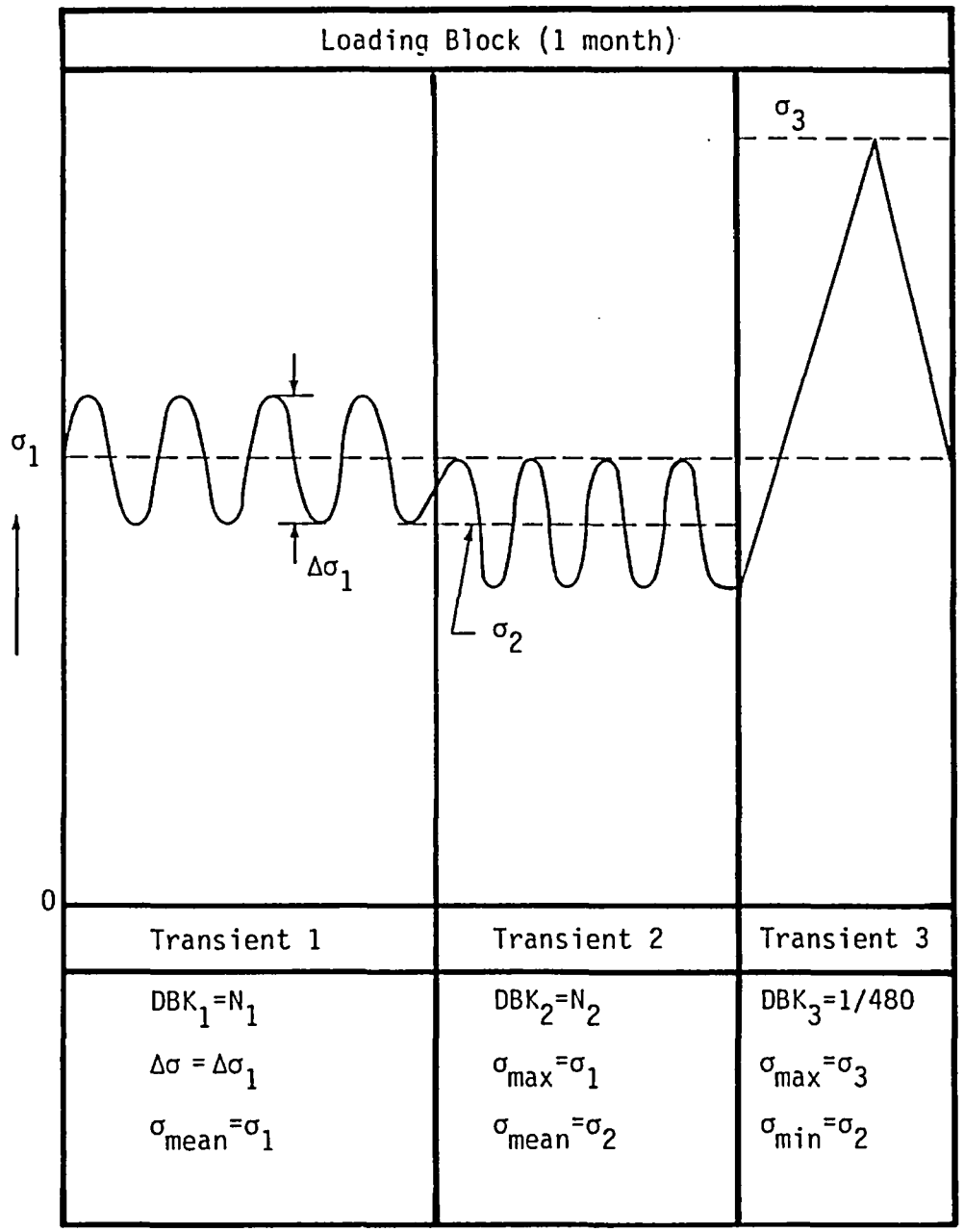

Figure 6.4 - Schematic Illustrating BIGIF Input for Fatigue Analysis with Once-in-a-Lifetime Loading Condition for a Component with a Forty-Year Service Life.

total number of cycles for each block of loading to be 1/480. In this way, K_{max} for the maximum stress condition will be checked against K_{IC}, while at the end of forty years, only one complete cycle has been accumulated in the fatigue crack growth. Actually, if the user wanted to completely eliminate the once-in-a-lifetime transient from the fatigue damage, DBK(3) = 0 is acceptable.

6.6 Flaw Evaluations According to ASME Code Section XI, Appendix A

The purpose of Section XI of the ASME Code (6-16) is to assure the mechanical integrity of the pressure boundary of a nuclear plant as part of a failure prevention assurance for imperfections found during service. Flaws that exceed the ASME Code inspection standards during the in-service examination can be analytically evaluated using the procedures outlined in Appendix A of Section XI (6-16) to determine if the detected flaw could become of critical size in the remaining service life of the component. Upon satisfying the flaw acceptability criterion (subject to approval by the regulatory authority) a component may be returned to service without repair.

The flaw evaluation procedures of the Code have been computerized (6-17) and the program called FACET, which performs the calculations, is generally available to the industry. Certain analytical techniques of the procedure are only Code recommendations rather than requirements and these techniques may be inadequate in some cases. Alternative methods are allowed by the Code so long as these techniques are well documented. The BIGIF program provides analytical refinements which can be utilized when the Code procedure cannot

be applied. There are three areas where the Code procedure is prohibitive and where the BIGIF program could be applied with substantial improvements:

(1) There are only two flaw models in the code: a semielliptical surface flaw and an elliptical subsurface flaw.

(2) The procedure for determining K involves only tension and bending (linear) stress fields. All general varying stress behavior would be linearized by a procedure which is usually, but not always, conservative. A comparison of calculated K's from BIGIF and the Code has been performed in (6-18) for the case of the Pilgrim 1 nozzle weld inspection indications.

(3) The Code presents only a single degree-of-freedom fatigue crack growth procedure that cannot account for three-dimensional complications such as crack shape change during growth and K or $\overline{K}$ variation around the crack front.

For the analyses required to be performed to meet the Code acceptability criterion, BIGIF could be used in two areas:

(1) Performing the fatigue analysis for computing the final flaw size, a_f.

(2) Performing a K analysis which would be used in a hand evaluation for calculating the critical flaw sizes.

Some difficulty will be experienced in applying BIGIF to a Code analysis because the Code requires* a fatigue analysis to be performed over

*Actually, this cycle-by-cycle Code requirement is unnecessary in that the BIGIF life integration algorithm will certainly converge for NDUB greater than 5 to 10.

all expected service cycles (i.e., a cycle-by-cycle approach) while the BIGIF algorithm increments on crack size, a, and not N. To circumvent this problem a large value for the crack increment parameter NDUB (NDUB ≈ 10 to 40) could be specified to produce a large amount of output for crack depth versus N. The analyst could then interpolate on N_{total} where N_{total} is the total number of expected loading blocks in the remaining service life to obtain a_f.

6.7 Effect of the Crack on Structural Stiffness

A question which is often asked about a structural defect, especially when vibratory loads are significant, is what effect does the presence of the crack have on the overall stiffness and natural frequency of the structure. The change in stiffness is related to the crack depth or crack area through the computation of total energy released by cracking, U_c. For a given load, the total strain energy $U_u + U_c$ (where U_u is the strain energy of the appropriate part of the uncracked structure) is directly proportional to part flexibility. Since the energy release rate can be calculated from K, the life integration portion of BIGIF can be converted to compute $U_c(a)$ directly. From (6-4), the energy release rate can be written as

$$\frac{dU_c}{da} = \frac{t\,K^2(a)}{E^*} \tag{6.4}$$

where t is the body thickness, which must be constant, and

$$E^* = \begin{cases} E & \text{(plane stress)} \\ E/(1-\nu^2) & \text{(plane strain)} \end{cases}$$

In the above expression, E is the modulus of elasticity and ν is Poisson's ratio. By simple analogy of life N to energy U_c and by use of a Paris expression (IDADN = 1), the total energy $U_c(a)$ can be determined from Eq. (6.4) by setting

$$C = E^*/t$$

$$n = -2$$

$$a_i << a$$

$$K_{IC} = \text{large}$$

in the life integration analysis (IFAT = 1) of BIGIF.

6.8 Relative Estimates in Fracture Mechanics

Once a detailed analysis has been performed and now the user would like to know what effect changing one or two of the input variables such as stress magnitude or the constant C in the da/dN rule would have on life, a reanalysis using the program may not be necessary. In many cases, a good feel of how the input variables affect the total life can be obtained using a simple dimensional analysis fracture mechanics approach. As a simple example, consider the following problem involving two different input conditions A and B:

(1) The material behavior for both conditions is modeled by Paris' rule with the same exponent, n, but with different coefficients, C_A and C_B where $S_c = C_B/C_A$.

(2) The model geometry, including initial and final crack sizes, scales to a characteristic dimension such as the width, w, so that a scaling factor on size can be defined for the geometrically similar structures as $S_w = w_B/w_A$.

(3) The generic shape* of the stress distribution for each case is the same but the magnitude scales as $S_\sigma = \sigma_B/\sigma_A$.

From these assumptions, the following relations can be constructed

$$\begin{aligned} C_B &= S_C C_A \\ n_B &= n_A = n \\ \sigma_B &= S_\sigma \sigma_A \\ w_B &= S_w w_A \\ a_B/w_B &= a_A/w_A \\ \Delta K &= F\Delta\sigma\, a^{\frac{1}{2}} \quad \text{(from dimensional analysis)} \end{aligned} \tag{6.2}$$

where F is the shape function for the arbitrary model geometry and loading and $F_A = F_B = F$ from (2) and (3) above. By substituting the relations of Eq. (6.2) into Eq. (2.5), which is the life integral, and taking the ratio of N_B/N_A, the following relative relation for life can be obtained.

$$\frac{N_B}{N_A} = \left(\frac{C_A}{C_B}\right)\left(\frac{\sigma_B}{\sigma_A}\right)^{-n}\left(\frac{w_B}{w_A}\right)^{(1-n/2)} \tag{6.3}$$

---

*i.e., $\sigma^{(A)}\ (x/w_A,\ y/w_A)\ /\ \sigma^{(B)}\ (x/w_B,\ y/w_B) = \text{Constant} = 1/S_\sigma$

or

$$N_B = S_c^{-1} S_\sigma^{-n} S_w^{(1-n/2)} N_A$$

As indicated by Eq. (6.3), if an analysis for N_A has been performed, and the input changes are such that the assumptions of Eq. (6.2) are valid, then the new life N_B can be determined without the need of the computer. Equation (6.3) also indicates which input parameters have the greatest sensitivity to the fatigue life. The life is only inversely proportional to the coefficient C in the da/dN equation. Stress changes will have the most dramatic effect on life since life scales to the stress ratio to the -n power where n is typically between 2.5 and 4 for fatigue.

REFERENCES

6-1 Paris, P. C., Gomez, M. P., and Anderson, W. E., "A Rational Analytical Theory of Fatigue", The Trend in Engineering, Vol 13, No. 1, University of Washington (January 1961).

6-2 Paris, P. C. and Sih, G. C., "Stress Analysis of Cracks", Fracture Toughness Testing, ASTM 381 (1965).

6-3 Sih, G. C., Handbook of Stress Intensity Factors for Researchers and Engineers, Vol. 1, Lehigh University (1973).

6-4 Tada, H., et al, The Stress Analysis of Cracks Handbook, Del. Research Co. (1973).

6-5 Saal, H., "Fatigue Crack Growth in Notched Parts with Compressive Mean Load", Journal of Basic Engineering, pp. 243-247 (March 1972).

6-6 Barsom, J. M., Rolfe, S. T., Fracture and Fatigue Control in Structures, Applications of Fracture Mechanics, Prentice Hall (1977).

6-7 Knott, J. F., Fundamentals of Fracture Mechanics, Wiley & Sons (1973).

6-8 Broek, D., Elementary Engineering Fracture Mechanics, Noordhoff Publishing (1974).

6-9 McClintock, F. A. and Argon, A. S., Mechanical Behavior of Materials, Addison-Wesley Co. (1966).

6-10 Tetelman, A. S. and McEvily, A. J., Fracture of Structural Materials, Wiley & Sons (1967).

6-11 Hertzberg, R. W., Deformation and Fracture Mechanics of Engineering Materials, Wiley & Sons (1976).

6-12 Besuner, P. M., Tetelman, A. S., Egan, G. R. and Rau, C. A., "The Combined Use of Engineering and Reliability Analysis in Risk Assessment of Mechanical and Structural Systems", Proceedings of Risk-Benefit Methodology and Application Conference, Asilomar, CA, UCLA-ENG-7598, ed. by David Okrent (December 1975).

6-13 Egan, G. R., Besuner, P. M., Cipolla, R. C., Johnson, D. P., and Tetelman, A. S, "An Engineering Analysis of the Risk of Brittle Fracture of the Carquinez West Bridge", Failure Analysis Associates Report 75-7-02-1 (January 1976).

6-14 Tetelman, A. S. and Besuner, P. M., "The Application of Risk Analysis to the Brittle Fracture and Fatigue of Steel Structures", presented at the Fourth International Conference on Fracture, Waterloo, Canada (June 1977).

6-15 Besuner, P. M., Sorenson, K. G., and Johnson, D. P., "A Workable Approach for Extending the Life of Turbine Rotors", presented at the ASME Gas Turbine Division Annual Meeting, Philadelphia, PA (March 1977). Published in the ASME Volume Fatigue Life Technologies ed. by T. Cruse and J. Gallagher.

6-16 ASME Boiler and Pressure Vessel Code, Section XI, "Rules for In-Service Inspection of Nuclear Power Plant Components", 1977 Edition, Summer 1977 Addenda.

6-17 Cipolla, R. C., "Computerized Method to Perform the Flaw Evaluation Procedure as Specified in the ASME Code, Section XI, Appendix A, Part I: General Description and Background Manual", EPRI RP 700-1, Technical Report (January 1978).

6-18 Besuner, P. M., "Analysis of the Pilgrim 1 Nozzle-to-Pressure Vessel Weld Discontinuities", EPRI 217-1, Technical Report 6 (October 1975).

7.0 EXAMPLE PROBLEMS

7.1 Introduction

Modeling structural crack problems are often difficult but many good basic approximations and assumptions are available. This Section presents a few of these approximations and also points out some pitfalls. Four general problems (with variations) are presented in increasing order of difficulty. The first example involves a through-thickness edge crack in a large body and, although the problem is straightforward, it contains valuable lessons. The second general example introduces a residual stress due to welding and subsequent fatigue analysis to compute residual life. A third example points out the significance of notch radius size in crack propagation problems. The fourth example presents and discusses an analysis of a nozzle corner crack in a pressure vessel feedwater nozzle under pressure and thermal loadings. The total direct computer cost for the four example problems including printing charges is less than three dollars. The BIGIF output to these problems is listed in Appendix C.

7.2 Example 1 - Simple Edge Crack In An Unnotched Infinite Plate Under Tension

7.2.1 Problem Scope

The design and fatigue analysis of highly stressed structural details without geometric stress concentrators (e.g., turbine rotor bore) contains much room for serious error. This is because fatigue analysts are anxious

to take credit for the absence of holes and other mechanical stress raisers. This is reasonable but how much credit should be taken? The old approach was to test small unnotched (K_t = 1) specimens in fatigue which, taken together, will sample less than one-millionth of the highly stressed volume of material to be exposed by the fleet. The point of the volume comparison is that the probability of encountering material defects (which may occur occasionally in a fleet of disks) in small specimens is vanishingly small. Therefore, reason (and experience) tells us that taking full credit for the lack of notches* is dangerous.

Some debit must be taken if crack-like defects are present. Fracture mechanics (with some elementary probabilistic order statistics to account for volume effect) is the discipline to quantify this debit. A simplified example follows.

7.2.2 Problem Statement

Consider the bore of a turbine rotor with a very long 10 mil deep crack-like inclusion or axial surface scratch (Fig. 7.1). The stress field is essentially uniform at the crack locus and the stress cycle is between 0 and 70 ksi. The rotor is a steel with medium material crack growth performance characterized by

$$da/dN = C\Delta K^n \quad \text{(in/cycle)} \tag{7.1}$$

*A similar argument may be applied to possible material defects near notched details, but to a lesser extent. This is because the volume of material subject to concentrated stress is not terribly large, even in a fleet of rotors. Fatigue or corrosion induced cracks are typically more troublesome than material defects near notches, although important exceptions occasionally occur.

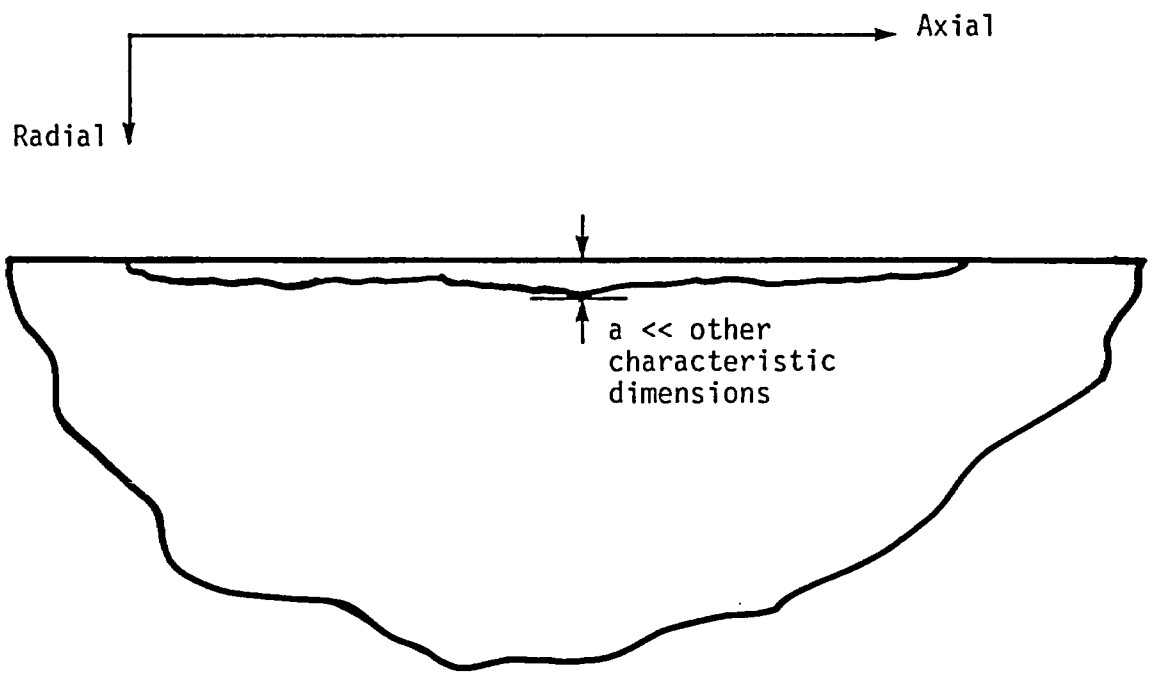

Figure 7.1 - Schematic Representation of Example 1a, a Long Axial Surface Crack in the Bore of a Rotor.

where $C = 4.5 \times 10^{-10}, \quad n = 2.8$

for $10 \text{ ksi } \sqrt{\text{in}} < \Delta K < K_{IC}$ (7.2)

The median fracture toughness is $K_{IC} = 85 \text{ ksi } \sqrt{\text{in}}$.

Recall that the stress intensity factor for the very long shallow edge crack can be approximated by the formula

$$K = 1.122 \, \Delta\sigma \sqrt{\pi a} \, . \tag{7.3}$$

Combining Eq. (7.1) and Eq. (7.3) and integrating we obtain an explicit formula for the life N required to produce failure, N_f, as a function of initial a_i and final a_f crack depths. The formula is

$$N_f = (1/mC) \, (1.122 \, \Delta\sigma \sqrt{\pi})^{-n} \left[a_i^{-m} - a_f^{-m} \right] \tag{7.4}$$

where $m = n/2 - 1, \quad (n \neq 2)$

$$K(a_f) = K_{IC}$$

We now have enough information to solve problems such as:

(1) What is the critical crack depth?

(2) Compute the number of cycles required to grow a through-thickness edge crack with an initial depth of 10 mils ($a_i = 0.010"$) to failure ($\Delta K = K_{IC} = 85 \text{ ksi } \sqrt{\text{in}}$.).

(3) What are the lives and critical lengths if

(a) K_{IC} = 30 ksi $\sqrt{in}$?

(b) K_{IC} = 300 ksi $\sqrt{in}$?

(4) Assume K_{IC} = 85 ksi $\sqrt{in}$. and the initial defect is 40 mils deep. What is the life?

(5) If there was no crack, what would Eq. (7.4) predict? Can this form of fracture mechanics be used to predict the life of a structure with no crack?

The solution for problems (1) and (2) are provided below. Answers to questions (3) through (5) are not provided, and the reader is encouraged to work these problems for himself. By checking the answers using BIGIF, the reader will gain faster insight into the program and LEFM itself.

7.2.3 Problem Solution and Answers to (1) and (2) Above

Our static failure criterion is

$$K_{max} = \Delta K \geq K_{IC} \qquad (R = 0)$$

so that the critical crack depth, a_c, is determined from

$$K_{IC} = 1.122\ \Delta\sigma\ \sqrt{\pi a_c}$$

or

$$a_c = \frac{1}{\pi}\left(\frac{K_{IC}}{1.122\ \Delta\sigma}\right)^2 = \frac{1}{\pi}\left(\frac{85}{1.122 \times 70}\right)^2 = 0.373" \ .$$

Therefore,

$$a_c = 0.373" \equiv a_f \quad \text{(final crack length)}$$

Substituting known quantities into Eq. (7.4), where n = 2.8, m = 0.4, the life is

$$N_f = \Delta N = \frac{1}{(0.4)(4.5 \times 10^{-10})} (1.122\ (70)\ \sqrt{\pi})^{-2.8} \left[(0.010^{-0.4}) - (0.373^{-0.4})\right]$$

$$N_f = 5530\ [6.31 - 1.48] = 26700$$

N_f = 26700 cycles (the predicted median cycle life).

The above problem was also analyzed with BIGIF using two different flaw models for comparison of results. Example 1a uses the non-IF simple case solution (IFI = 102). The second model (Example 1b) is the general stress IF model (IFI = 204) described in Section 4.3.2. A listing of the data input is given in Table 7.1. The 26700 cyclic life is in agreement with the output BIGIF results in Appendix C.1 using both the 102 model stress (N_f = 37200 - 11100 = 26100 cycles) and the 204 model with a standard integration grid (N_f = 35820 - 10670 = 25200 cycles). Deviations from the 26700 value are caused by small numerical integration errors. BIGIF has been designed such that, in most cases, numerical errors will tend to lower the calculated life, as observed above.

7.3 Example 2 - Through-Cracks in Notched Structures

7.3.1 Problem Statement

Figure 7.2 shows two examples of through-cracks originating from a notch. Problems involving through-cracks in notched and unnotched structures

TABLE 7.1

DATA INPUT LISTING FOR EXAMPLE 1

```
                                        **** CARD COLUMNS ****
         1    1    2    2    3    3    4    4    5    5    6    6    7    7    8
1   5    0    5    0    5    0    5    0    5    0    5    0    5    0    5    0
V   V    V    V    V    V    V    V    V    V    V    V    V    V    V    V    V


EXAMPLE 1A - EDGE CRACK UNDER UNIFORM STRESS (NON-IF,IFI=102)          PMB10JAN78
    1    1  102    1    0    1    0    2    0    0
0.005     0.0       0.0       0.0
1000.     0.0       0.0       0.0       0.0       0.0       0.0       0.0
85.       4.5   E-10 2.8
ONLY TRANSIENT                 1.
70.            0    7    0    0    0    0
0.             1    7    0    0    0    0
FINIS
EXAMPLE 1B - EDGE CRACK UNDER UNIFORM STRESS (IF SOLUTION,IFI=204)     PMB10JAN78
    1    1  204    1    0    1    0    2    0    0
0.005
1000.
85.       4.5   E-10 2.8
ONLY TRANSIENT                 1.
70.            0    1    0    0    0    0
1.0       0.0       0.0       0.0
0.             3    0    0    0    0    0
FINIS
```

```
A   A    A    A    A    A    A    A    A    A    A    A    A    A    A    A    A
1   5    1    1    2    2    3    3    4    4    5    5    6    6    7    7    8
         0    5    0    5    0    5    0    5    0    5    0    5    0    5    0
```

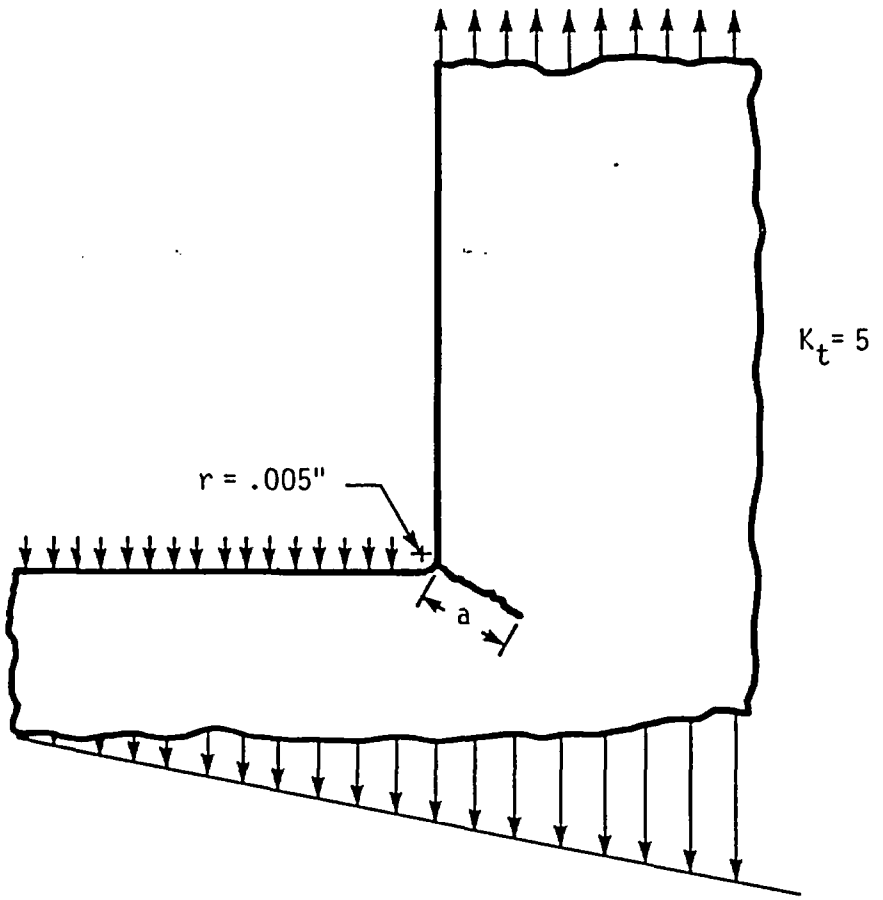

a) Example 2a - High K_t, Small Radius Notch with Crack.

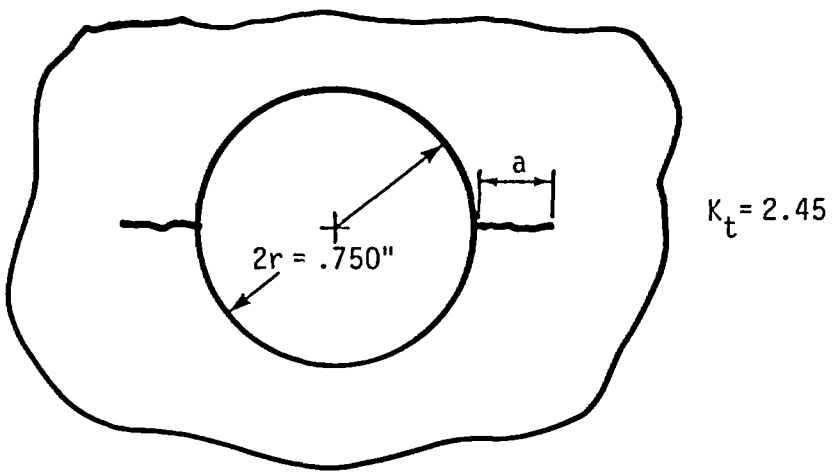

b) Example 2b - Moderate K_t, Large Radius Notch with Crack.

Figure 7.2 - Two Examples of Through Cracks in Notches.

are discussed in Section 6.2. Both examples are fabrications that represent typical field problems in rotating structures. The first case (Example 2a) is a severe notch with a 5 mil radius and an assumed elastic stress concentration factor (K_t) equal to 5. This situation might represent a poor shaft shoulder or snap fillet design or an outright machining hack or mark. It is also assumed that this defect is crack-like with no initiation life to a 10 mil deep crack. The edge crack (IFI = 204) flaw model is used to analyze the severe notch geometry.

The second example (Example 2b) is a disk bolt hole of radius 0.375" with a more typical K_t of 2.45. Assume that field experience indicates that as few as 2000 cycles are required to initiate a 10 mil deep crack on both sides of the hole. Furthermore, the initial crack is a part-through crack with an aspect ratio (a/2c) of 1/4. As part of Example 2b it is also desired to use the same edge crack flaw model (IFI = 204). Since K is directly proportional to stress, a multiplying factor will be applied to the stress field for the bolt hole to account for the fact that the crack is not a through-crack and as the crack grows away from the influence of the hole, the value for K for the bolt hole will approach the center-cracked infinite plate solution (Eq. (4.1)). By simply comparing Eqs. (4.1) and (4.2), and using (7-1) to determine the effect of crack shape (a/2c = 1/4 rather than a/2c = ∞), this multiplying factor which will be applied to the stress input, is computed to be

$$K_{actual}/K_{model} = 1/1.122\ E_k = 0.735$$

where E_k is the elliptical integral of the second kind of modulus K and $k^2 = 1-4(a/2c)^2$. This stress correction factor will tend to favor (i.e.,

increase the calculated life of) the bolt hole problem. For the sake of comparison, assume all other factors (e.g., nominal stress, material, environment) are identical as given in Table 7.2. The problem is to compute the crack propagation time (N_p) in cycles for each set of conditions.

7.3.2 Problem Solution

As mentioned above the two problems were analyzed using the edge crack plate flaw model (IFI = 204) for approximating the crack geometries shown in Fig. 7.2*. The input stream is shown in Table 7.3, and the output is listed in Appendix C.2. Excluding the difference in radii, every comparison between snap fillet and bolt hole either favors the bolt hole or favors neither. Table 7.4 shows the residual life computations using a standard integration breakup for both cases. Note the dramatic result. The predicted bolt hole minimum residual life (N_p = 8500 cycles) is inadequate (less than the required 10,000 cycles). The much more highly concentrated stress snap fillet (N_p = 13,300 cycles) is adequate. Qualitative explanation of this extremely important effect of notch size on subcritical crack growth, which has been verified in both test and field, is left to the reader.

*It is anticipated that better models will be available in contemplated future versions of BIGIF to compute K for the bolt hole problem. However, the 204 model is adequate to solve the particular problem illustrated in Fig. 7.2.

TABLE 7.2

COMPARISON OF INPUT PARAMETERS IN EXAMPLE 2

INPUT PARAMETERS	SNAP FILLET PROBLEM (2a)	BOLT-HOLE PROBLEM (2b)
σ_{nom} (ksi)	50.0	50.0
K_t (elastic)	5.0	2.45
"Min Life" FCGR Relation (in./cycle)	$\frac{da}{dN} = 15 \times 10^{-10} \Delta K^{2.8}$	$\frac{da}{dN} = 15 \times 10^{-10} \Delta K^{2.8}$
Fracture Toughness (ksi $\sqrt{in.}$)	85.0	85.0
Notch Radius (in.)	0.005	0.375
Nominal Stress Correction Factor*	1.00	0.735
Initiation Cycles (N_i)	0	2,000
Initiation Crack Depth (a_i) after N_i Cycles (in.)	0.010	0.010
Required Cyclic Life	12,000	12,000
Effective Width (w) of Structure	∞	∞

*The non unity multiplicative stress correction factor for the bolt-hole accounts for the beneficial effect of the expected partial thickness crack of aspect ratio a/2c = 1/4 combined with the elimination of the free surface correction factor as a/(R+a) approaches unity (see text). Note that this correction "favors" the bolt-hole.

TABLE 7.3

DATA INPUT LISTING FOR EXAMPLE 2

```
                                  **** CARD COLUMNS ****
         1    1    2    2    3    3    4    4    5    5    6    6    7    7    8
1   5    0    5    0    5    0    5    0    5    0    5    0    5    0    5    0
V   V    V    V    V    V    V    V    V    V    V    V    V    V    V    V    V

EXAMPLE 2A - CRACK IN SMALL RADIUS NOTCH WITH HIGH KT (KT=5)          PMB10JAN78
    1    1  204    1    0    1    0    2    0    0
0.010     0.0       0.0       0.0
1000.     0.0       0.0       0.0       0.0       0.0       0.0       0.0
85.       15.   E-10 2.8
ONE TRANSIENT                 1.
1.0            0    3    0    0    0    0
50.       5.        0.005     0.0       0.0       0.0       0.0
0.             3    0    0    0    0    0
FINIS
EXAMPLE 2B - CRACK IN LARGE RADIUS NOTCH WITH LOW KT (KT=2.45)        PMB10JAN78
    1    1  204    1    0    1    0    2    0    0
0.010     0.0       0.0       0.0
1000.     0.0       0.0       0.0       0.0       0.0       0.0       0.0
85.       15.   E-10 2.8
ONE TRANSIENT                 1.
0.735          0    3    0    0    0    0
50.       2.45      0.375     0.0       0.0       0.0       0.0
0.             3    0    0    0    0    0
FINIS

A   A    A    A    A    A    A    A    A    A    A    A    A    A    A    A    A
1   5    1    1    2    2    3    3    4    4    5    5    6    6    7    7    8
         0    5    0    5    0    5    0    5    0    5    0    5    0    5    0
```

TABLE 7.4

Example 2 - NUMERICAL RESULTS

Crack Depth (Inches)	CALCULATED CYCLIC LIFE			
	Snap Fillet (2a)		Bolt-Hole (2b)	
	N_p (1)	N_r (1)	N_p	N_r
0.010	0	12,000	0	10,000 (5)
0.020	2,100	9,900	1,400	8,600
0.040	4,700	7,300	2,500	7,500
0.080	7,300	4,700	3,600	6,400
0.160	9,700	2,300	4,800	5,200
0.320	11,700	300	6,100	3,900
0.364 (2)	12,000	0	6,400	3,600
0.640	13,200	-1,200	7,700	2,300
0.700 (3)	13,300	-1,300	7,900	2,100
0.940 (4)	-	-	8,500	1,500
		(Snap is Adequate by 1,300 Cycles)		(Bolt-Hole is Not Adequate by 1,500 Cycles)

NOTES:

(1) N_p is the number of cycles to propagate the crack and N_r is the remaining required service life for the component.

(2) Final flaw size (a_f = 0.36") for snap fillet defect at end-of-life (N_f = 12,000 cycles).

(3) Critical flaw size (a_c = 0.70") for snap fillet problem ($K_{max}(a_c)$ = 85 ksi $\sqrt{in}$).

(4) Critical flaw size (a_c = 0.94") for bolt-hole problem ($K_{max}(a_c)$ = 85 ksi $\sqrt{in}$).

(5) The remaining propagation cycles at a_i = 0.010" is 10,000 which is determined from the required 12,000 service cycles minus the 2,000 cycles to initiate the 10 mil crack.

7.4 Example 3 - Fatigue Analysis of a Weld Crack

7.4.1 Problem Statement

A weld seam under longitudinal (y-direction) load symmetric about the y-axis, with a transverse through-thickness crack of length 2a is illustrated in Fig. 7.3. This section describes the analysis of fatigue growth of a center-cracked laboratory specimen of width 2b = 10". The applied uniform longitudinal stress cycle in the test includes an alternating component $\Delta\sigma$, and a mean component, σ_m. A complex residual stress field, $\sigma_{res}(x)$, is also present as illustrated in Fig. 7.3. The residual stress distribution was estimated from measurements in (7-2).

For simplicity, a crack growth relation (Eq. (2.9)) suggested by Forman for positive values of R, has been selected to compute da/dN for all values of R, and, as presented in (7-3), the relation overpredicts da/dN for negative R. The applied crack growth relationship is based on the weld region material data in (7-4) and is given by

$$\frac{da}{dN} = 1.4 \times 10^{-7} \Delta K^{2.74} \left\{K_{IC}(1-R) - \Delta K\right\}^{-1}, \quad K_{max} > 0 \qquad (7.5)$$

$$\frac{da}{dN} = 0, \quad K_{max} < 0$$

where the force, length and time units are kilopounds, inches, and constant amplitude fatigue cycles, and $K_{max} = \Delta K/(1-R)$. The initial crack length is

assumed to be $2a_i$ = 0.25" and the final crack length, $2a_f$, is defined by the fracture toughness

$$K_{max}\ (a_f) = K_{IC} = 150\ \text{ksi}\ (\text{in.})^{\frac{1}{2}}. \tag{7.6}$$

7.4.2 Problem Solution

The center-cracked plate model (IFI = 201) in BIGIF with a refined integration grid was selected and the corresponding data input is reproduced in Table 7.5. The interesting residual stress K(a) output of BIGIF is given in Appendix C.3 and these results are plotted in Fig. 7.3. Note that $\sigma(2") = 0$ but K(2") is nearly at its maximum value. Clearly the frequently used "back-of-the-envelope" solution which uses the "crack-tip" stress, i.e. $K(a) = \sigma(a)\sqrt{\pi a}$, is in gross error for the complex residual stress field of Fig. 7.3. This example clearly points out the need for advanced solution techniques, such as IF, for complex stress problems.

Two load cases are analyzed for the center-cracked panel. For both cases the cyclic stress component $\Delta\sigma = 2\sigma_m$ = 25 ksi. The first case (Example 3a) includes the residual stress field which elevates the applied mean stress of the test. The second case (Example 3b) excludes residuals. The half-crack length (a) versus N computed by BIGIF is plotted in Fig. 7.4, which indicates that the residual stress significantly increases the crack growth rate in the early stage and substantially reduces overall fatigue life. Several other load cases in this problem are discussed in an earlier report (7-5). The other cases show that, even for the case of applied cyclic compression, corresponding to σ_m = 17.5 ksi, the positive residual stresses

TABLE 7.5

DATA INPUT LISTING FOR EXAMPLE 3

```
                                        **** CARD COLUMNS ****
         1    1    2    2    3    3    4    4    5    5    6    6    7    7    8
1   5    0    5    0    5    0    5    0    5    0    5    0    5    0    5    0
V   V    V    V    V    V    V    V    V    V    V    V    V    V    V    V    V


EXAMPLE 3A - CENTER-CRACKED FINITE WIDTH PLATE (CYCLIC + RESIDUALS)   PMB01DEC76
    1    1  201    1    0    3    0    3    0    0
0.125     0.0       0.0       0.0
5.0       0.0       0.0       0.0       0.0       0.0       0.0       0.0
150.0     1.4   E-07 2.74
CYCLIC STRESS + RESIDUALS     1.
1.0           1    4    0    0   11    0
0.        52.5
0.4       48.5
0.8       38.
1.2       20.
1.6       7.5
1.8       3.7
2.4       -9.
3.        -17.
3.6       -22.
4.5       -35.5
5.0       -37.5
25.0          2    4    0    0    2    0
0.        1.
5.0       1.
FINIS
EXAMPLE 3B - CENTER-CRACKED FINITE WIDTH PLATE (CYCLIC STRESS ONLY)   PMB01DEC76
    1    1  201    1    0    3    0    3    0    0
0.125     0.0       0.0       0.0
5.0       0.0       0.0       0.0       0.0       0.0       0.0       0.0
150.0     1.4   E-07 2.74
CYCLIC STRESS ONLY            1.
0.0           3    0    0    0    0    0
25.0          2    4    0    0    2    0
0.        1.
5.0       1.
FINIS



A   A    A    A    A    A    A    A    A    A    A    A    A    A    A    A    A
1   5    1    1    2    2    3    3    4    4    5    5    6    6    7    7    8
         0    5    0    5    0    5    0    5    0    5    0    5    0    5    0
```

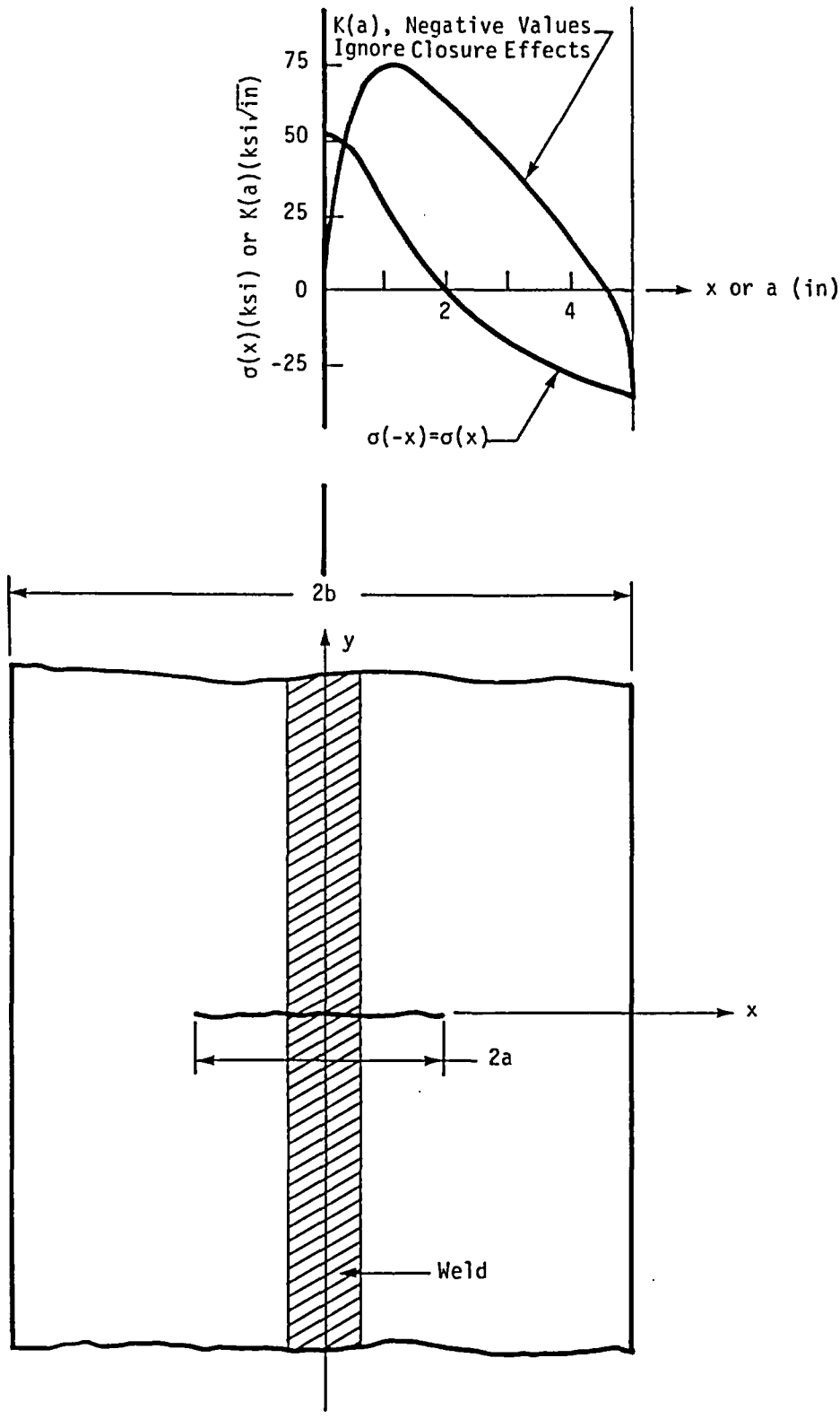

Figure 7.3 - Weld-Induced Symmetric Residual Stress, σ(x), in an Uncracked Specimen and Resulting Stress Intensity Factor K(a) When a Center-Crack of Length, 2a is Introduced.

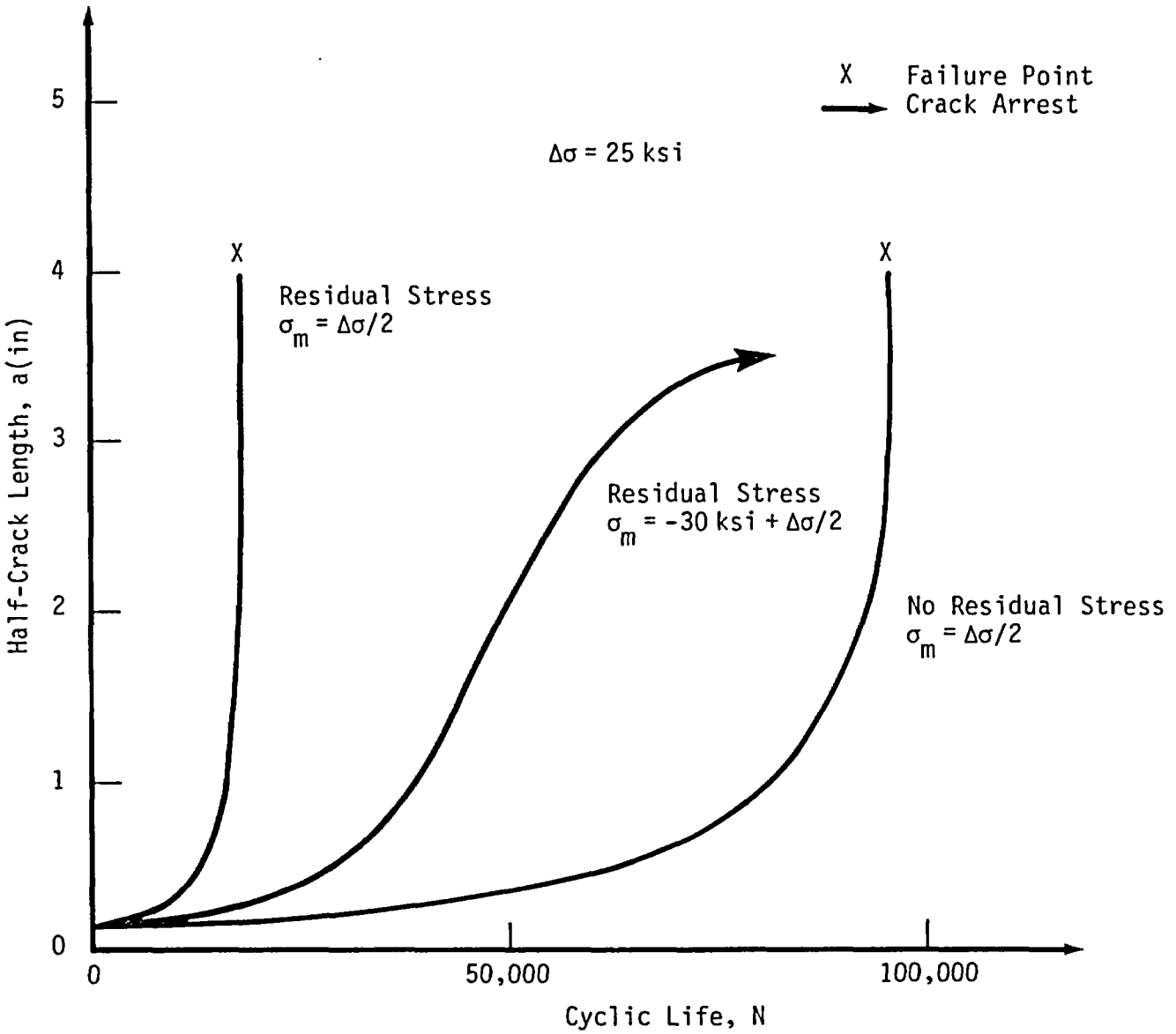

Figure 7.4 - Weld Crack Propagation in a 10 Inch Wide Specimen for Three Mean Stress Distributions.

permit some initial growth of the crack (followed by subsequent crack arrest at $K_{max} < 0$).

7.5 Example 4 - Pressure Vessel Nozzle Corner Crack Under Two Loading Transients

7.5.1 Problem Statement

This example is a simplified version of an example given in BIGIF introductory manual (7-6) and is meant to illustrate the ease with which the user may simultaneously account for several complex and distinct load cycles. Figures 7.5 and 7.6 show the nozzle crack geometry and pressure and thermal loading cycles, respectively. Both the thermal and pressure loads lead to high gradient, bivariate stress fields, $\sigma(x,y)$. (The reader should refer to (7-7) for a full description of the nozzle stress analysis.) These stress fields were previously input to BIGIF using the bivariate table option (IPLD = 5). However, for the example given, the already computed K values as a function of crack depth for pressure and thermal cycles given in (7-7) are used as input (IPLD = 6) to run the fatigue analysis in Appendix C.4. Also, for the purpose of this example, the high frequency fatigue (HFF) depicted in Fig. 7.6 was excluded from the analysis. A complete analysis of all fatigue components including HFF was already conducted and discussed in (7-8) and will be presented later for comparative purposes.

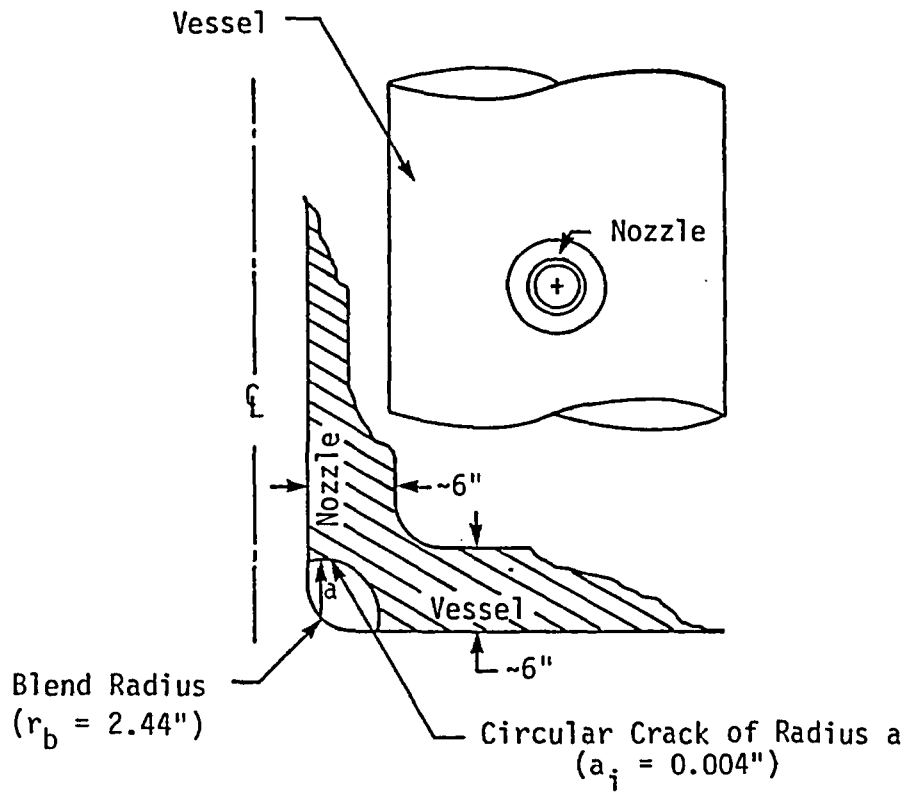

Figure 7.5 - Idealization of Crack in Blend Radius of a Nuclear Reactor Pressure Vessel Nozzle (IFI = 300)

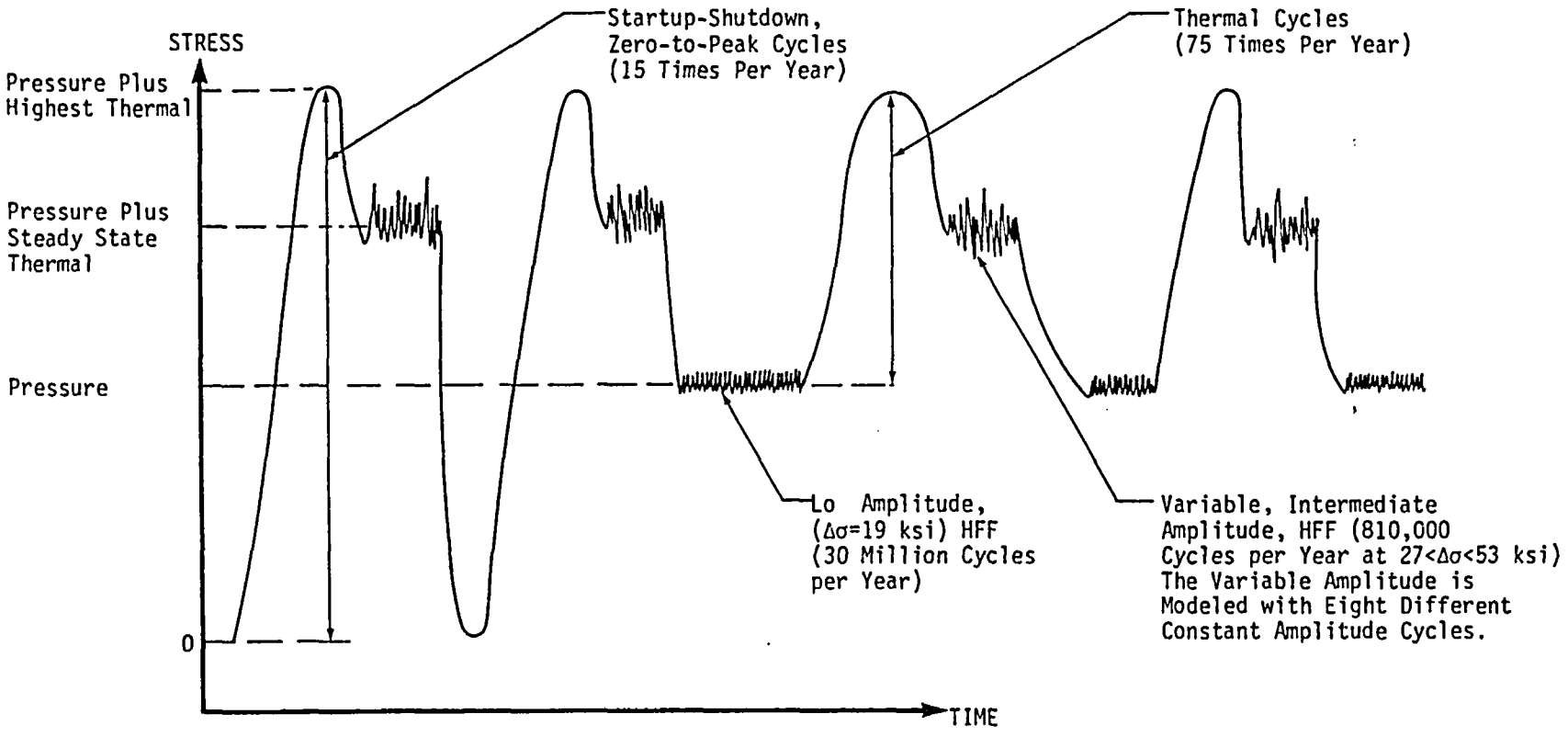

Figure 7.6 - A Schematic Representation of the Multiple-Load Inner Surface Stress Transient of a Pressure Vessel Feedwater Nozzle.

7.5.2 Problem Solution

This solution demonstrates the capabilities of the nozzle corner crack model (IFI = 300) as described in Section 4.4.1. The input description is provided in Table 7.6, and the program output is reproduced in Appendix C.4. The start-up/shutdown cyclic spectrum shown in Fig. 7.6 but excluding the low and variable amplitude HFF cycles was described in BIGIF by two constant amplitude transients. The first transient specifies the pressure plus one cycle of thermal fatigue occurring 15 times per year. The remaining low cycle thermal fatigue cycles occurring 60 times a year (75 minus 15) is described by the second transient specification. The loading block size, N, is therefore one year. As shown in Table 7.6 the "KAME" option is used to set the maximum K(a) function for the thermal cycle in the second transient. The body width w, which in this IF algorithm is used only to terminate the analysis when $a \geq w$, was set to a large value to allow computations beyond the body width. For computational purposes K_{IC} = 300 ksi $\sqrt{in}$, and two separate analyses, one with a coarse breakup and the other a standard scheme was specified (INCL = 1).

The crack depth versus N results for the standard breakup are plotted in Fig. 7.7 along with results based on the more complex loading transients given in (7-8). Note the dramatic effect the relatively low-stress but frequently occurring thermal HFF cycles in Fig. 7.7 have on subcritical crack growth residual life, when compared to low frequency fatigue results calculated herein. A comparison between coarse and standard integration schemes indicates a 2% difference in final flaw size at 40 year life. Since K(a) is

TABLE 7.6

DATA INPUT LISTING FOR EXAMPLE 4

```
                                  **** CARD COLUMNS ****
          1    1    2    2    3    3    4    4    5    5    6    6    7    7    8
1    5    0    5    0    5    0    5    0    5    0    5    0    5    0    5    0
V    V    V    V    V    V    V    V    V    V    V    V    V    V    V    V    V

EXAMPLE 4 - NOZZLE CORNER CRACK UNDER PRESSURE + THERMAL STRESS       PMB01DEC76
    1    2  300    1    0    6    4    2    1    0
0.004     0.0        0.0        0.0
1000.     0.0        2.44*      3.0*       15.0*      0.0        0.0        0.0
300.0
0.0            6
0.5        1.0    E-28
5.2        1.0    E-08
5.5        2.0    E-08
6.5        7.0    E-08
7.5        1.3    E-07
83.0       1.0    E-03
0.5            6
0.353      1.0    E-28
3.68       1.0    E-08
3.89       2.0    E-08
4.6        7.0    E-08
5.3        1.3    E-07
58.7       1.0    E-03
0.9            6
0.1581     1.0    E-28
1.644      1.0    E-08
1.739      2.0    E-08
2.06       7.0    E-08
2.37       1.3    E-07
26.2       1.0    E-03
0.99           6
0.05       1.0    E-28
0.52       1.0    E-08
0.55       2.0    E-08
0.65       7.0    E-08
0.75       1.3    E-07
8.3        1.0    E-03
```

*NOTE: The nozzle dimensions do not affect the result since K(a) is to be specified rather than calculated.

```
A    A    A    A    A    A    A    A    A    A    A    A    A    A    A    A    A
1    5    1    1    2    2    3    3    4    4    5    5    6    6    7    7    8
          0    5    0    5    0    5    0    5    0    5    0    5    0    5    0
```

TABLE 7.6

DATA INPUT LISTING FOR EXAMPLE 4 (CONT'D)

```
                                        **** CARD COLUMNS ****
          1   1   2   2   3   3   4   4   5   5   6   6   7   7   8
1   5     0   5   0   5   0   5   0   5   0   5   0   5   0   5   0
V   V     V   V   V   V   V   V   V   V   V   V   V   V   V   V   V


PRES + THERM WITH R=0          15.
0.0             3   0   0   0   0   0
1.0             2   6   0   0   9   0
0.0       0.0
0.125     59.2
0.25      81.4
0.50      108.3
1.0       135.8
2.0       149.5
4.0       138.8
6.0       200.0
9.0       1000.
THERMALS ONLY                  60.
1.0             1   6   0   0   9   0
0.0       0.0
0.125     16.0
0.25      22.6
0.50      31.6
1.0       43.6
2.0       57.7
4.0       69.8
6.0       100.0
9.0       500.0
1.0             0   6   1   2   0   0
FINIS
```

```
A   A   A   A   A   A   A   A   A   A   A   A   A   A   A   A   A
1   5   1   1   2   2   3   3   4   4   5   5   6   6   7   7   8
        0   5   0   5   0   5   0   5   0   5   0   5   0   5   0
```

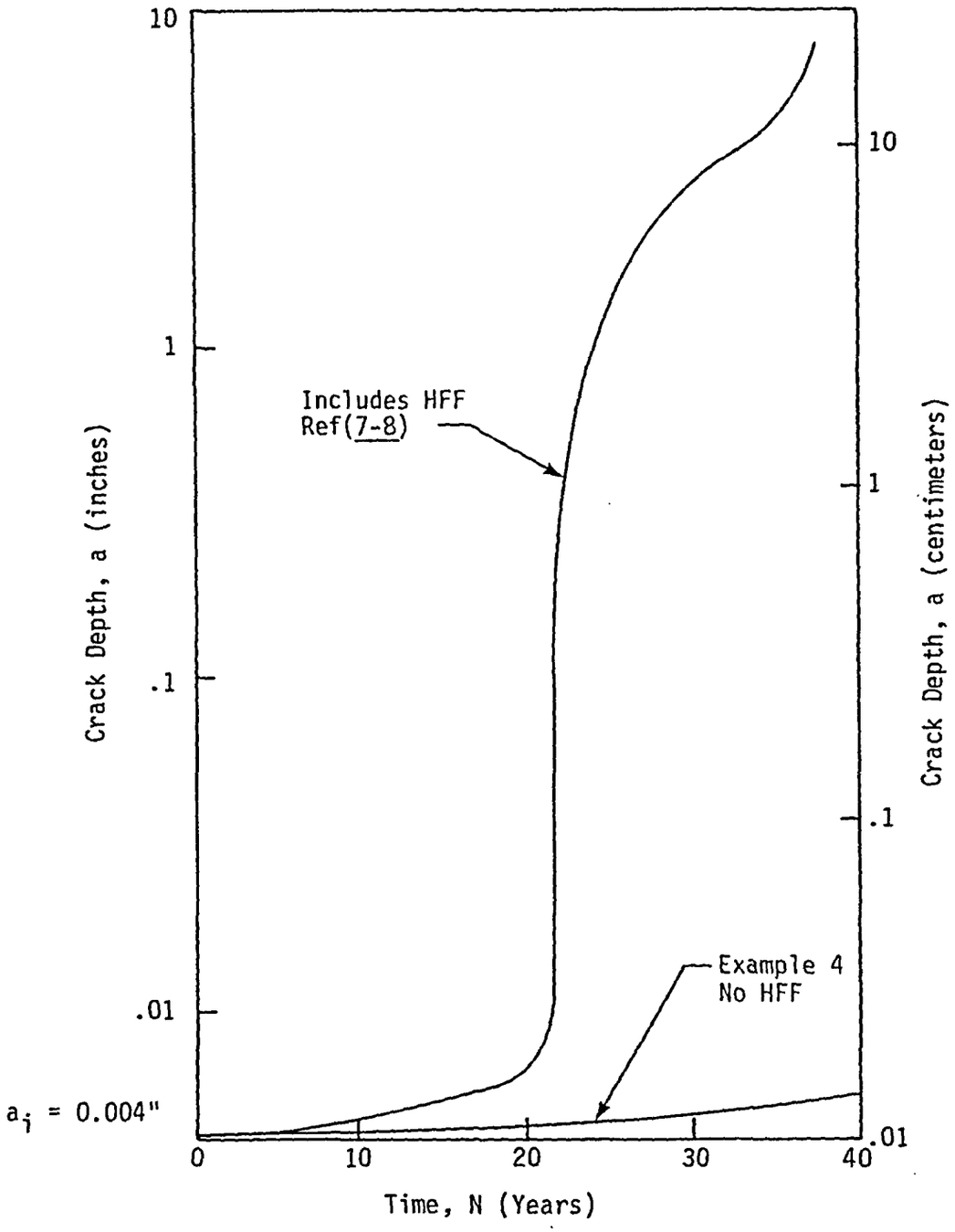

Figure 7.7 - Comparison of Results of a Worst-Case Fracture Mechanics-Based Fatigue Analysis Showing Crack Depth "a" as a Function of Usage Time (Years). Note the Rapid Crack Growth for 0.01" ≤ a ≤ 0.50" Due to High Frequency Loading Above the Threshold (ΔK_{th}).

directly input into BIGIF, this difference is due solely to the different values for the crack incrementor NDUB in the life integration for coarse (NDUB = 2) and standard (NDUB = 4) schemes.

REFERENCES

7-1 Tada, H., Paris, P., and Irwin, G., The Stress Analysis of Cracks Handbook, Del Research Corporation, (1973), pgs. 19.1, 19.13 and 26.1.

7-2 Wells, A. A., "The Brittle Fracture Strengths of Welded Steel Plates", Paper No. 6, Meetings of the Institution of Naval Architects, London (1956).

7-3 Yuen, A., Hopkins, S. W., Leverant, G.R., and Rau, C. A., "Correlations between Fracture Surface Appearance and Fracture Mechanics Parameters for Stage II Fatigue Crack Propagation in Ti-6Al-4V", Metallurgical Trans. 5 (August 1974).

7-4 Gurney, T. R., "An Investigation of the Rate of Propagation of Fatigue Cracks in a Range of Steels", The Welding Institute Members' Report No. E18/12/68.

7-5 Besuner, P. M., "Fracture Mechanics and Residual Fatigue Life Analysis for Complex Stress Fields", EPRI 217-1, Technical Report 2, (July 1975).

7-6 Besuner, P. M., Peters, D. C., and Cipolla, R. C., "BIGIF: A Computer Program Which Performs Engineering Fracture Mechanics Computations for Structures Under Complex Stress Gradients and Cyclic Load Spectra; Introduction and Theoretical Background, Manual 1 of 3", EPRI RP 700-1, FAA 78-1-3(1) (January 1978).

7-7 Cohen, L. M., McLean, J. L., Moy, G., and Besuner, P. M., "Improved Evaluation of Nozzle Corner Cracking", EPRI RP-700 and 498 Final Report NP-339 (March 1977).

7-8 Besuner, P. M., Peters, D. C., and Cipolla, R. C., "BIGIF: A Computer Program which Performs Engineering Fracture Mechanics Computations for Structures under Complex Stress Gradients and Cyclic Load Spectra, Introduction and Theoretical Background (Manual 1 of 3)", Technical Report FAA-78-1-3(1), EPRI RP-700-1, (December 1977).

Attachment 3

to

SOUTHERN CALIFORNIA EDISON
RESPONSE TO NRC STAFF
REQUEST FOR ADDITIONAL INFORMATION
SUPPORTING RELIEF REQUESTS ISI-3-11 AND ISI-3-12
PRESSURIZER HEATER SLEEVE REPAIR
SAN ONOFRE NUCLEAR GENERATING STATION UNITS 2 AND 3

Pages 12, 13, and 27 of SCE Calculation M-DSC-360
(Aptech Engineering Services Calculation No. AES-C-3227-1)

2.3 Borated Water Corrosion Evaluation

The potential BWC of the low alloy steel head/shell material was conservatively evaluated. Local corrosion was modeled as a circumferential planar groove within the hole penetration. The postulated corrosion damage is shown in Figure 4-2. The integrity of the nozzle attachment was determined as a function of location of BWC within the hole, and depth and length of the corrosion groove. A limit load-based evaluation (including fatigue crack growth) was completed following the general approach of ASME Section XI, Appendix H, for flaws in ferritic piping. The allowable corrosion depths and lengths were established based on maintaining a minimum safety factor of 2.77 for normal and upset service conditions and 1.39 for accident conditions.

The allowable corrosion depths were computed at two hole penetration locations: (1) at the gap region between the new nozzle and the remaining nozzle stub and (2) in the crevice region at the nozzle-to-pad weld. The allowable corrosion depths for a 360° circumferential groove are summarized below:

Location	Allowable Corrosion Size	
	Depth	Length
Gap Region	> 0.50 inch	360°
Crevice Region	0.42 inch	360°

The computed corrosion growth rates and maximum flaw growth by fatigue (FCG) for a 40-year design life are as follows:

Location	Flaw Depths (inches)		
	BWC	FCG	Total
Gap Region	0.144	0.0007	0.15
Crevice Region	0.064	0.002	0.07

The total corrosion depths (including fatigue), after 40 years of service, are computed to be less than the allowable corrosion depths. Therefore, the safety margin requirements of ASME Section XI will be satisfied for the half-nozzle attachment weld design.

2.4 Allowable Flaw Depths

The allowable flaw depths for nozzle stub flaws and BWC degradations for use as inspection standards are developed in Section 8.3. The computed results are given in Figures 8-3 and 8-4.

Calculation No.: AES-C-3247-1	Made by: [illegible]	Date: 5/8/98	Client: SCE
	Checked by: [illegible]	Date: 8 MAY 98	Project No.: AES 97123247-IQ
Title: Evaluation of Half-Nozzle Repair for Pressurizer and Steam Generator Instrumentation Nozzles Under Long-Term Service Conditions — SONGS 2 and 3	Revision No.: 0	Document Control No.: I-2	Sheet No.: 27 of 69

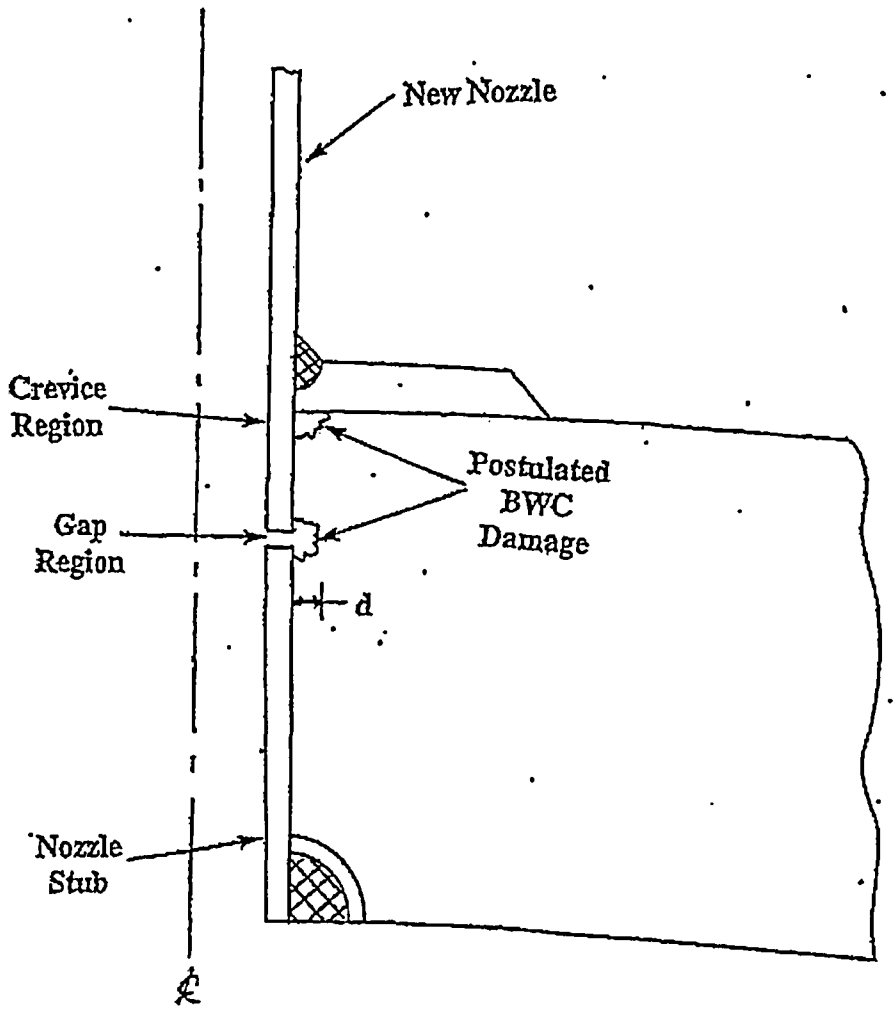

Figure 4-2 — Postulated BWC in Nozzle Repair Region.